INVESTIGATIONS ON FULLY SEPARATED FLOWS PAST AIRFOIL SECTIONS

A Thesis Submitted
In Partial Fulfilment of the Requirements
for the Degree of

MASTER OF TECHNOLOGY

BY

SQUADRON LEADER I. S. GUPTA

to the

DEPARTMENT OF AERONAUTICAL ENGINEERING
INDIAN INSTITUTE OF TECHNOLOGY KANPUR

MAY, 1970

CERTIFICATE

Certified that this work "Investigations on the Fully Separated Flows" has been carried out under my supervision and the same has not been submitted elsewhere for a degree.

V. Vasanta Ram

V. Vasanta Ram
Assistant Professor
Department of Aeronautical Engineering
Indian Institute of Technology, Kanpur

ACKNOWLEDGEMENTS

It has been a privilege for the author to work under Dr. V. Vasanta Ram. The author is thankful to him for the guidance and the interest taken during the investigations.

The author is thankful to Sqn. Ldr. I.S. Ahuja of Air Force Station, Kanpur who helped in the fabrication of the flat plate model. Messers S.C.M. Yadav and K.S. Muddappa of Wind Tunnel Laboratory assisted the author during the experimentation programme and Mr. R. Krishnamurthy photographed the set up. The author acknowledges their help with thanks.

TABLE OF CONTENTS

TABLE OF CONTENTS

SUMMARY

The pressure distribution on bodies with the separated flows can b determined by the "modified free streamline theories". However, applicatio of these theories requires a knowledge of the base pressure. Investigation were carried out in regions of the separated flows on an airfoil (NACA 6601 and a flat plate with a view to understand the criteria governing the base pressure of bodies in the separated flows. Effects of a splitter plate on the base pressure of bodies in separated flows were also investigated. A correlation for quantities $\frac{2}{C_{DS}}$ Vs. R_{eS} in the fully separated flow past airfoil like bodies with no periodic vortex shedding and a flat plate (body with periodic vortex shedding) has been verified for R_{e_∞} 4.8 x 10^5 and 4.0 x 10^5.

LIST OF NOTATIONS

Geometric quantities

L	Model chord
b	Model span
X	Distance downstream measured from centre of the end disc
Y	Coordinate normal to x
Z	Coordinate normal to both x and y
$\hat{X}$	Distance along airfoil or flat plate chord line measured from the leading edge.
$\hat{Y}$	Distance from $\hat{X}$ measured normal to $\hat{X}$.
α	Geometric angle of attack.

Flow quantities

ρ	Mass density
ν	Kinematic viscosity
u	Local velocity
U_∞	Velocity of undisturbed flow
U_s or kU_∞	Velocity on free streamline on separation
p	Static pressure on surface
p_∞	Static pressure of the undisturbed flow
$\mathcal{J}_\infty = p_\infty + \frac{1}{2}\rho U_\infty^2$	Total pressure of the undisturbed flow
p_s	Base pressure
$\mathcal{J}$	Total pressure
D	Drag
n	Shedding frequency
$\delta_{2\infty}$	Momentum thickness

$R_{e\infty} = \frac{U_\infty L}{\nu}$ Reynolds number based on undisturbed flow velocity U_∞ and model chord L

$C_p = \frac{p - p_\infty}{\frac{1}{2}\rho U_\infty^2}$ Pressure coefficient

$C_{ps} = \frac{p_s - p_\infty}{\frac{1}{2}\rho U_\infty^2}$ Base pressure coefficient

$C_{D_\infty} = \frac{D}{\frac{1}{2}\rho U_\infty^2 L b}$ Drag coefficient, based on undisturbed flow velocity U_∞ and model chord L

$K = \frac{U_s}{U_\infty} = \sqrt{1 - C_{ps}}$ Base pressure parameter

Base region quantities

$R_{es} = \frac{U_s \delta_{2\infty}}{\nu}$ Reynolds number based on momentum thickness and velocity on free streamline at separation.

$C_{Ds} = \frac{D}{\frac{1}{2}\rho U_s^2 \delta_{2\infty} b}$ Drag coefficient based on momentum thickness and separation velocity

Subscripts

∞	Free stream
s	Base region
2	Measuring station in the wake
P	Flat plate
a	airfoil

LIST OF FIGURES

LIST OF TABLES

CHAPTER 1

Introduction

The flow of a real fluid past a body on which the flow separates is one of the major problems in fluid mechanics. Flow separation is often considered as a scourge to may technical devices which depend upon the dynamics of fluid flow for successful operation, in as much as, separation often limits the usefulness of the device. For example, the maximum lift of an airfoil and the maximum compression ratio of a compressor are limited by the occurrence of separation. Separated regions can also occur near a deflected flap, around a spoiler control, in an over expanded rocket nozzle, behind a blunt base and near the impingement of a shock wave from one body upon the boundary layer of another.

The characteristics of the device e.g. a wing or a compressor are amenable to theoretical analysis in the narrow working regions of attached flows. At points far off design, the analysis is elusive due to the predominance of the separated flows.

1.2 Theoretical Observations

In inviscid and incompressible flow past a cylindrical body in a fluid of infinite extent theory leads to the conclusion that there can be no drag (D'Alemberts Paradox). The actual pressure distribution on the body can be calculated in the high Reynolds number range when the flow is not separated. In these cases, the drag which is mostly viscous is small. However, outside the viscous layer the real flow is significantly different from the ideal one when there is separation of the boundary layer. In the cases of the blunt bodies or the airfoils at high angles of attack the drag arises mostly from the pressure forces. Early attempts at a theoretical treatment of the flow past bluff bodies were due to Helmoltz and Krichhoff [1] . Helmoltz and Kirchhoff [1] proposed a

"free streamline theory" to determine the pressure distribution on bodies with the separated flows. Their theory yields values for the drag coefficients which are too low in comparison with the experiment. This discrepancy has been explained by A. Roshko [2] as a consequence of a basic assumption in Kirchhoff's theory [1] being far off from reality. Kirchhoff's theory postulates that the velocity U_s on the free streamlines at separation is equal to the undisturbed stream velocity U_∞. Also the speed along the free streamline is considered constant ($= U_\infty$) every where. The pressure at the separation point and on the base of the body in the separated region is supposed to be equal to the undisturbed stream pressure ($= p_\infty$), whereas the observed pressures in this region are below p_∞. Attempts to improve the Helmoltz Kirchhoff "free streamline theory" have been made by Roshko [2], Eppler [3] and Wu [4]. These "modified free streamline theories" allow for arbitrary base pressures. The value of the surface speed at separation is assumed to be different from the undisturbed flow velocity U_∞. Roshko [2] introduced a parameter K which defines the separation velocity by the relation $U_s = K U_\infty$ and gives a base pressure coefficient $C_{p_s} = 1 - K^2$. The significant feature of the modified free streamline theories [2], [3], [4] is that the base pressure p_s is a <u>free parameter.</u> In the case when $p_s = p_\infty$, all these theories [2], [3], [4] degenerate into that of Helmoltz Kirchhoff theory [1]. Applications of the modified free streamline theories for the prediction of the pressure distribution requires a knowledge of the base pressure, for which upto now no satisfactory method of prediction has been developed.

V. Vasanta Ram [5] suggested correlation for the quantities in the fully separated flows past airfoil like bodies with no periodic vortex shedding, which could serve as a criterion for determining the base pressure. The

correlation is analogous to that of Roshko's hypothesis for vortex shedding [2] viz. that for vortex shedding bodies, the fully separated flows are similar to each other and are independent of the bodies themselves.

1.3 Aim and Scope of present Investigations

The aim of the present study is the examination of the correlation of V. Vasanta Ram [5] under a variety of conditions. In particular it is proposed to examine the separated flow past a flat plate and an airfoil (NACA 66010) section with a view to either substantiating or refuting the proposal of [5]. This, it is believed, will represent a contribution to our understanding of the separated flows.

The contents of the report are divided into six chapters. In Chapter 2 the experimental arrangement and procedure are given. Chapter 3 gives the results of the experiment. Reduction of Data is given in Chapter 4. Chapter 5 is a discussion of the results. Chapter 6 concludes the work and contains some suggestions for further work.

CHAPTER 2

Experimental Arrangement and Procedure

The coordinate systemsfor the airfoil section (NACA 66010) and the flat plate are given in Figure 1 and Figure 2 respectively.

Models

An airfoil (NACA 66010) and a flat plate were the models for the investigation. The coordinates for the airfoil (NACA 66010) are given in Figure 3 (taken from reference [6]). The dimensions of the model were chord L_{ac} = 406.4 mm and the span b = 304.8 mm. The airfoil was constructed of laminated compressed seasoned hard wood. 31 flush copper tubes of 3 mm diameter were imbedded in the surface. The location of the pressure taps is shown in Figure 3. Three spanwise rows of 1/64" diameter pressure taps were drilled at mid span and at 76.2 mm on each side of the mid span row of taps. The surfaces of the model were finished with sandpaper and were left unpainted, unlacquered. Contour was checked visually for truth all along the chord with the help of a template. The model spanned the working section (4' x 1') of the wind tunnel.

The dimensions of the flat plate were L_p = 152.4 mm, thickness t = 6.4 mm and span b = 304.8 mm. The ends of the flat plate were chamfered to 30° angle as shown in Figure 4 . The flat plate was made of mild steel. 11 flush copper tubes were imbedded with Araldite after milling square slots in the surface. After fixing of the copper tubes, the surfaces were ground on a surface grinder to obtain a fine smooth finish. Five spanwise rows of 1/64" diamter pressure taps were drilled on each tube. The location of the pressure taps is shown in Figure 4.

A splitter plate (Figure 5) was fabricated to study its effects on the base pressures on the airfoil and on the flat plate. The splitter plate was made by joining two aluminium plates. Three rows of 17 flush pressure taps were attached on the top and bottom surfaces of the splitter plate. The splitter plate could be moved along X-axis and could be fixed in the desired position. Figure 6 shows the photographs of the models with the splitter plate in position in the working section of the wind tunnel.

Equipment

Wind Tunnel: The experiment was conducted in (4' x 1') working section of the low speed, close circuit wind tunnel of I.I.T. Kanpur.

Wake Survey Rake: Wake surveys were made using a total head - static head rake. The rake consisted of 35 total head tubes and 5 static head tubes. The spacing between the tubes was 19 mm. Details of the rake are given in Figure 7. The rake could be fixed in any streamwise position.

Manometer: Two multi-tube manometers of 100 limbs and 15 limbs respectively, filled with distilled water were used for reading pressures.

2.2 Experimental Procedure

Undisturbed Flow Total Head Measurement: The undisturbed flow total head (q_∞) was measured as the average of several total head tubes placed in the settling chamber.

Undisturbed Flow Static Pressure Measurement: The undisturbed static pressure was measured through a flush wall tap fitted a short distance after the entry to the working section.

The following configurations were studied:

1. With the airfoil as model (see Figure 1).
   a). Without splitter plate
   b). With splitter plate close to the model in position 1 (Figure 1)
   c). With splitter plate some distance downstream in position 2 (Figure 1)
2. With the flat plate as model (see Figure 2)
   a). Without the splitter plate
   b). With splitter plate close to the model in position 1 (Figure 2)
   c). With the splitter plate some distance downstream in position 2 (Figure 2)

With each of the above configurations, the following measurements were taken:-

a). Pressure distribution on the model (and on the splitter plate in cases 1b, 1c and 2b, 2c above).

b). Velocity (and static pressure) distribution in the wake.

The Reynolds numbers for the tests were:-

a). For the airfoil,

$$R_{e_\infty} = \frac{U_\infty L_a}{\nu} = 4.0 \times 10^5,\ 4.8 \times 10^5,\ 5.83 \times 10^5 \text{ and } 9.2 \times 10^5$$

b). For the flat plate,

$$R_{e_\infty} = \frac{U_\infty L_p}{\nu} = 2.75 \times 10^5,\ 4.0 \times 10^5 \text{ and } 4.8 \times 10^5$$

Higher Reynolds numbers could not be achieved due to the limitations on the power available in the wind tunnel.

The angles of attack covered in the experiment were:-

a). For the airfoil α = 20°, 25°,30°,35°, 40°,45°.

b). For the flat plate α = 30°,45°,60°,90°.

Wake surveys were carried out at two streamwise positions, at $\frac{x}{l_a}$ = 1.475 and 2.1 for the airfoil (Figure 1) and at $\frac{x}{l_p}$ =3.94 and 5.6 for the flat plate (Figure 2). In both cases at values of x closer to the model than the lower values above it was found that the rake was in the region of reverse flow and hence its readings were unreliable.

Checks on the two dimensionality of the flow were conducted on both models by reading surface pressures on the model at locations away from the mid-span position (see models at Figures 8,9,10, and 11). These checks were conducted at the following Reynolds numbers and angles of attack:-

a). For the airfoil angles R_{e_∞} No.

45° 9.0 x 10^5, 5.83 x 10^5,
4.8 x 10^5, 4.0 x 10^5

30° 5.83 x 10^5, 4.8 x 10^5, 4.0 x 10^5

20° 4.0 x 10^5

b). For the flat plate Angle R_{e_∞} No.

90° 4.8 x 10^5, 4.0 x 10^5

45° 2.75 x 10^5

The complete experimental programme took 96 hours of actual wind tunnel operation.

CHAPTER 3

Results of the Experiment

Pressure Distrubution: The pressure distribution on the model surfaces were recorded and non-dimensional pressure coefficients based on upstream dynamic pressure ($\frac{1}{2} \rho U_\infty^2$) were calculated. From the pressure distribution force coefficients normal to the airfoil (C_{N_∞}) and parallel to the chord of the airfoil (C_{c_∞}) and the drag coefficient (C_{D_∞}) obtained by the relation

$$C_{D_\infty} = C_{N_\infty} \sin\alpha + C_{c_\infty} \cos\alpha \qquad (1)$$

where C_{N_∞} is the integrated normal force coefficient and C_{c_∞} is the integrated chordwise force coefficient. The expression is taken from reference ([8] , page No.169-70).

Two Dimensionality of Data: Before presenting results of the experiment, the question of whether the flow phenomena are uniform across the span of the model for different angles of attack and at different Reynolds numbers should be considered. Comparisons for the different angles of attack of the pressure distributions measured at different spanwise locations on the airfoil and on the flat plate are given in Figures 8, 9, 10 and 11. An inspection of the data of Figures 8, 9, 10 and 11 indicates that there are some variations in the pressure distributions as measured at different spanwise sections. The variations are more pronounced on the airfoil than on the flat plate. The spanwise variations do not indicate to form any consistent pattern with either angle of attack or with the Reynolds numbers. Figure 12 gives a typical C_L vs. α curve for the airfoil. Curves for the measured

pressure distribution on the airfoil and on the flat plate without the splitter plate in the wake of the models are plotted in Figures 13 to 18 and Figures 19 to 22 respectively. The pressure distribution measured on the models with the splitter plate in the wake are given in Figures 23 to 42.

The velocity profiles in the wake of the airfoil and of the flat plate without the splitter plate in the wake are given in Figures 43 to 51. The velocity profiles in the wake of the models with the splitter plate are plotted in Figures 52 to 61. The pressure distribution on the splitter plate in the wake of the airfoil or flat plate are given in Figures 66 to 69.

CHAPTER 4

Reduction of Data

Wake Survey: The wake velocity profiles and the drag coefficient were evaluated with the aid of formula due to Jones [9] because of its comparative simplicity over the method due to Betz. Jones formula, taken from reference ([9], page 711-12) is given below for ready reference

$$\frac{C_{D\infty}}{2} = \int_{-\infty}^{+\infty} \sqrt{\frac{p_2 - p_2}{q_\infty}} \left(1 - \sqrt{\frac{p_2 - p_\infty}{q_\infty}}\right) d\left(\frac{y}{L}\right) \quad (2)$$

where $q_\infty = p_\infty - p_\infty$

The values of $C_{D\infty}$ thus calculated are given in Tables 1 and 5 for airfoil and flat plate respectively.

Base Pressures Coefficient and Calculation of Re_s: The base pressure coefficient ($= C_{p_s}$) is taken as that value of pressure coefficient ($= C_p$) which is almost constant on the base of the model behind the separation points. This is observed to be always a negative quantity. The data was reduced in the following manner:-

a). Calculation of Velocity at Separation: Knowing the base pressure p_s from the experiment, U_s the characteristic separation flow velocity was determined by the relation

$$p_s + \frac{1}{2}\rho U_s^2 = p_\infty + \frac{1}{2}\rho U_\infty^2 \quad (3)$$

b). The characteristic length dimension for the wake is obtained from the measured drag (wake survey) by the relation

$$D = \rho U_\infty^2 \, b \, \delta_{2\infty} \tag{4}$$

where $\delta_{2\infty}$ is the momentum thickness of the wake far down-stream.

c). The plots are of the form $\frac{2}{C_{DS}}$ vs. R_{eS} where

$$C_{DS} = \frac{D}{\frac{1}{2}\rho U_S^2 \, b \, \delta_{2\infty}} \tag{5}$$

and hence

$$\frac{2}{C_{DS}} = \frac{\rho U_S^2 \, b \delta_{2\infty}}{D} = \frac{\rho U_S^2 \, b \, \delta_{2\infty}}{\rho U_\infty^2 \, b \, \delta_{2\infty}} = \left(\frac{U_S}{U_\infty}\right)^2 \tag{6}$$

$$R_{eS} = \frac{\rho U_S \delta_{2\infty}}{\mu} = R_{e\infty}\left(\frac{C_{D\infty}}{2}\right)\left(\frac{U_S}{U_\infty}\right) \tag{7}$$

4.2 Wind Tunnel Blockage Correction :

The $C_{D\infty}$ obtained from pressure distribution has been corrected by the method given in reference [8]. The corrected values of $C_{D\infty}$ have been included in Tables 1 and 5 . The other results of the experiment and the calculations of R_{eS} for the models without and with splitter plate are tabulated in Tables 1 to 8 .

CHAPTER 5

Discussion of Results

Pressure Distribution: A study of pressure distribution plots for the airfoil and the flat plate reveals the following;

The value of pressure coefficients on the separated side viz. the base pressure, is almost constant ($= C_{p_s}$). Figures 62 and 63 respectively give the variation of the base pressure coefficient ($= C_{p_s}$) with the angle of attack for different Reynolds numbers. It is seen that in both cases decrease of angle of attack increases the base pressure coefficient. In both cases increase of Reynolds numbers increases the base pressure. The variation of base pressure with Reynolds numbers are more pronounced than in the case of the flat plate. From Figure 63 it is seen that for the flat plate at $\alpha = 90°$, the dependence of base pressure coefficient on Reynolds numbers is negligible. At angles of attack lower than 90°, C_{p_s} dependence on angle of attack and Reynolds numbers is similar to those of the airfoil.

Splitter Plate Effects: Figures 64 and 65 show the effect of introducing a splitter plate in the wake of the model. The base pressure coefficient is plotted against the angle of attack for the airfoil at $R_{e_\infty} = 9.2 \times 10^5$ and the flat plate at $R_{e_\infty} = 4.0 \times 10^5$. The following conclusions may be drawn from the curves:

a). In the case of the airfoil, the base pressure increases when the splitter plate is placed close to the airfoil. The increase in base pressure causes lower drag coefficient. It is also found that the x-wise position of the splitter plate has considerable effect on the base pressure on the model (Figure 64). In the rearmost position of the splitter plate

corresponding to $\frac{x}{L_{cr}} = 1.75$, the base pressure is lower than its value with the splitter plate placed foremost.

b). In the case of the flat plate, the base pressure increases considerably when the splitter plate is placed close to the model. (Figure 65). In this case the base pressure on the model is not appreciably affected by the X-wise position of the splitter plate. This is probably due to the size of the splitter plate being big in relation to the flat plate model. This finding is contrary to that of Roshko [7] because the size of the splitter plate in the later case was small. It is seen from Figures 64 and 65 that even in the rearmost position of the splitter plate the base pressure does not fall as low as when the splitter plate is absent. These observations agree qualitatively with those of Roshko [7] on a cylinder.

Pressure Distribution on the Splitter Plate: Figures 66, 67, 68 and 69 give the pressure distribution on the splitter plate placed in the wake of the models. It is seen that the pressures on both sides of the splitter plate is fairly constant when placed in wake of the airfoil. Moving the splitter plate closer to the model increases the pressures on both surfaces. However in the case of the splitter plate in the wake of the flat plate at $\alpha = 90°$ the pressure increases appreciably in the downstream direction when the splitter plate is in rearmost position (Figure 69). In the foremost position the pressures are almost constant.

Wake Survey: The values of C_{D_∞} calculated from wake survey data is given in Table 1 for the airfoil and Table 5 for the flat plate. It is observed that generally the value of C_{D_∞} obtained from wake survey are higher than those obtained from the integration of the pressure distribution.

$\frac{2}{C_{Ds}}$ Vs R_{e_s} PLOT : The calculate values of R_{e_s} have been tabulated in Tables 2 and 3 and 4 for airfoil and Tables 6, 7 and 8 for the flat plate. The reduced $\frac{2}{C_{Ds}}$ vs. R_{e_s} are plotted in Figures 70 and 71 for airfoil and the flat plate at $R_{e\infty} = \left(\frac{U_\infty L_a}{\nu} = \frac{U_\infty L_p}{\nu}\right) = 4.8 \times 10^5$ and $R_{e\infty} = \left(\frac{U_\infty L_a}{\nu} = \frac{U_\infty L_p}{\nu}\right) = 4.0 \times 10^5$. A curve has been drawn which passes through various points for the airfoil and those for the flat plate. It is observed that the curves for different $R_{e\infty}$ are not parallel. Thus for a common $R_{e\infty}$, on the $(2/C_{Ds})$ vs. R_{es}, plot the points for the airfoil and those for the flat plate lie on the same curve. Hence the validity of V. Vasanta Ram's correlation appears plausible. In the case of the splitter plate in the wake of the models there is a wide scatter of points for both models. (Figure 72).

CHAPTER 6

Conclusions

An experimental investigations of the base pressure on an airfoil and a flat plate in the separated flow region to examine the validity of the correlation of V. Vasanta Ram [5] shows the following:

1). The stated correlation seems to hold good for $R_{e\infty} = 4.8 \times 10^5$ and $R_{e\infty} = 4.0 \times 10^5$ i.e. the $\frac{2}{C_{DS}}$ vs. R_{eS} points for the airfoil and for the flat plate lie on the same curves.

2). The curves for $R_{e\infty} = 4.8 \times 10^5$ and 4.0×10^5 are not parallel. This indicates that the slope of the straight line is probably a function of the free stream Reynolds numbers. This point can only be settled by extending the experiment to a larger number of free stream Reyhdlds numbers.

3). The splitter plate, in general, increases the base pressure and the drag coefficient is reduced. This result holds only when the splitter plate is nearest to the model. As the splitter plate is moved downstream, beyond a certain $\frac{x}{L}$ location base pressure starts decreasing again. At certain $\frac{x}{L}$ position the base pressure is likely to return to the base pressure value on model without the splitter plate. This point could not be verified due to the limitations of the working section of the wind tunnel.

Suggestion for Future Investigation

The relationship $\frac{2}{C_{DS}}$ vs. R_{eS} is by far not final and satisfactory. It needs further investigation on various other models. While fabricating the models the limited Reynolds numbers range available in the wind tunnel should be kept in mind. A large number of $\frac{2}{C_{DS}}$ vs. R_{eS} curves for a large number of $R_{e\infty}$ will finally settle the problem and probably give the trend of variations with varying $R_{e\infty}$.

Shedding frequency should also be determined by hot wire Anemometer and compared.

LIST OF REFERENCES

[1] B. Thwaites: Incompressible Aerodynamics, Oxford Univ. Press., 1960.

[2] A. Roshko: A New Hodograph for Free Streamline Theory, NACA TN3168, 1954

[3] R. Eppler: Journal of Rational Mechanics & Analysis, Vol.3, pp 591-644, 1954

[4] T.Y. Wu: Wake Model for Free Streamline Theory, Journal of Fluid Mechanics, Vol.13, 1962

[5] V. Vasanta Ram: Separated Flows Past Airfoil Section, Internal Report, Fluid Dynamics Lab., Brown Boveri, Switzerland, 1968

[6] Abbot & Doenhoff: Theory of Wing Section, Dover Edn.

[7] A. Roshko: On the Drag and Shedding Frequency of 2 Dimensional Bluff Bodies, NACA TN3169, 1954

[8] A Pope: Wind Tunnel Technique, John Wiley, 1964.

[9] H. Schlichting: Boundary Layer Theory, McGraw Hill Book Co., 1968

TABLE 1

Airfoil NACA 66010 Drag Coefficient

Angle α	Re_∞	Airfoil				Airfoil-splitter Plate Foremost			Airfoil Splitter Plate Rearmost		
		Pressure Distribution		Wake Survey		Pressure Distribution		Wake Survey	Pressure Distribution		Wake Survey
		$C_{D\infty}$ (Uncorr.)	$C_{D\infty}$ (Corr.)	$\frac{x}{La}=1.475$	$\frac{x}{La}=2.1$	$C_{D\infty}$ (Uncorr.)	$C_{D\infty}$ (Corr.)	$\frac{x}{La}=2.1$	$C_{D\infty}$ (Uncorr.)	$C_{D\infty}$ (Corr.)	$\frac{x}{La}=2.1$
45°	9.0×10^5	1.335	0.77	0.81	0.965	1.14	0.665	0.53	1.31	0.765	0.712
	5.83×10^5	1.35	0.845	0.82	0.98	1.05	0.614	0.494	–	–	0.712
	4.8×10^5	1.265	0.737	0.80	0.995	1.02	0.592	0.73	1.21	0.705	0.668
	4.06×10^5	1.361	0.795	0.80	0.935	1.07	0.624	0.455	1.215	0.71	0.635
40°	9.2×10^5	0.9262	0.5963	0.715	1.162	0.9283	0.55	0.532	1.0383	0.61	0.603
	5.9×10^5	1.125	0.6635	0.544	1.12	0.9835	0.58	0.528	0.9847	0.58	0.614
	4.8×10^5	0.905	0.5329	0.596	1.05	–	–	0.475	0.908	0.535	0.515
	4.0×10^5	0.925	0.5454	0.512	0.986	1.0743	0.5964	0.565	1.0234	0.602	0.515
35°	9.0×10^5	0.8349	0.5431	0.655	1.154	0.7935	0.5182	0.645	0.7728	0.505	0.633
	5.83×10^5	0.8088	0.6479	0.600	1.17	0.7946	0.5220	0.62	0.7682	0.502	0.615
	4.8×10^5	0.775	0.5034	0.895	1.162	0.7920	0.5202	0.657	0.7573	0.496	0.606
	4.0×10^5	0.7642	0.5022	0.565	1.00	0.8552	0.56	0.576	0.8076	0.530	0.570
30°	9.2×10^5	0.6236	0.4298	0.562	0.95	0.602	0.284	0.542	0.603	0.4160	0.78
	5.83×10^5	0.5492	0.3780	0.512	1.045	0.6303	0.3017	0.526	0.5982	0.4120	0.67
	4.8×10^5	0.5426	0.3153	0.53	0.96	–	–	0.588	0.4630	0.3268	0.624
	4.0×10^5	0.50	0.2242	0.62	0.706	0.6350	0.2988	0.608	0.5728	0.3974	0.67
25°	9.1×10^5	0.4392	0.2918	0.497	0.544	0.456	0.306	0.515	0.4355	0.292	0.494
	5.9×10^5	0.4284	0.2867	0.470	0.527	0.4558	0.304	0.49	0.4122	0.276	0.485
	5.12×10^5	0.4210	0.2818	0.466	0.497	0.4802	0.322	0.464	0.4059	0.27	0.480
	4.0×10^5	0.3820	0.2570	0.51	–	–	–	0.62	0.4544	0.304	0.494
	9.0×10^5	0.2850	0.223	0.428	0.318	0.3235	0.254	0.26	0.2918	0.2297	0.254
20°	5.83×10^5	0.2816	0.222	0.432	0.39	0.3444	0.272	0.294	0.23	0.1668	0.238
	4.8×10^5	0.2746	0.216	0.504	0.405	0.36	0.261	0.34	0.3815	0.30	0.20
	4.0×10^5	0.262	0.206	0.418	0.3562	0.3327	0.262	0.344	0.2995	0.236	0.292

TABLE 2

Airfoil NACA 66010 R_{es} Calculations

Angle α	$R_{e\infty}$ No.	$C_{N\infty}$	$C_{C\infty}$	$\frac{C_{D\infty}}{2}$	$C_{P_S} = 1-\left(\frac{U_S}{U_\infty}\right)^2$	$R_{es} = R_{e\infty}\left(\frac{C_{D\infty}}{2}\right)\left(\frac{U_S}{U_\infty}\right)$	$\frac{2}{C_{DS}} = \left(\frac{U_S}{U_\infty}\right)^2$	$\frac{U_S}{U_\infty}$
45°	9.2×10^5	1.8290	0.05294	0.6675	-1.70	10.08×10^5	2.70	1.6432
	5.83×10^5	1.8664	0.05242	0.675	-1.675	6.44×10^5	2.675	1.6355
	4.8×10^5	1.731	0.05366	0.6325	-1.43	4.70×10^5	2.43	1.5588
	4.0×10^5	1.8790	0.05856	0.6805	-1.54	4.35×10^5	2.54	1.5937
40°	9.2×10^5	1.3700	0.06270	0.4631	-1.47	6.7×10^5	2.470	1.5716
	5.85×10^5	1.6942	0.04990	0.5625	-1.49	5.16×10^5	2.49	1.5780
	4.8×10^5	1.3374	0.05952	0.4525	-1.00	3.07×10^5	2.00	1.414
	4.0×10^5	1.5854	0.04540	0.4625	-1.26	2.78×10^5	2.26	1.5033
35°	9.2×10^5	1.3750	0.05494	0.41745	-1.250	5.76×10^5	2.250	1.5000
	5.83×10^5	1.3312	0.05482	0.4044	-1.15	3.45×10^5	2.15	1.4663
	4.8×10^5	1.2746	0.05086	0.3875	-1.075	2.68×10^5	2.075	1.4405
	4.0×10^5	1.2638	0.04932	0.3821	-1.00	2.162×10^5	2.00	1.4142
30°	9.2×10^5	1.1548	0.05320	0.3118	-0.99	4.06×10^5	1.930	1.4100
	5.83×10^5	1.0202	0.04530	0.2746	-0.875	2.19×10^5	1.875	1.3693
	4.5×10^5	0.9962	0.05144	0.2713	-0.875	1.665×10^5	1.875	1.3693
	4.06×10^5	0.8546	0.05118	0.250	-0.742	1.34×10^5	1.742	1.3199
25°	9.2×10^5	0.9260	0.05100	0.2196	-0.776	2.68×10^5	1.776	1.33
	5.83×10^5	0.8958	0.0556	0.2142	-0.78	1.685×10^5	1.78	1.3342
	5.12×10^5	0.8844	0.05260	0.2105	-0.74	1.43×10^5	1.74	1.3191
	4.0×10^5	0.8000	0.04844	0.1910	-0.715	1.00×10^5	1.715	1.3096
20°	9.2×10^5	0.8256	0.05240	0.1415	-0.73	1.715×10^5	1.73	1.3153
	5.83×10^5	0.8212	–	0.1408	-0.744	1.08×10^5	1.744	1.3191
	4.8×10^5	0.8036	–	0.1373	-0.715	0.86×10^5	1.715	1.3096
	4.0×10^5	0.7608	–	0.131	-0.68	0.68×10^5	1.68	1.2961

TABLE 3

Airfoil NACA 66010 with Splitter Plate Foremost (Position 1) R_{es} Calculations

Angle α	$R_{e\infty}$ No.	$C_{N\infty}$	$C_{c\infty}$	$\frac{C_{D\infty}}{2}$	$C_{p_S} = 1-\left(\frac{U_s}{U_\infty}\right)^2$	$R_{es} = R_{e\infty}\left(\frac{C_{D\infty}}{2}\right)\left(\frac{U_s}{U_\infty}\right)$	$\frac{2}{C_{DS}} = \left(\frac{U_s}{U_\infty}\right)^2$	$\frac{U_s}{U_\infty}$
45°	9.2 x 10^5	1.5594	0.05180	0.570	-1.33	8.13 x 10^5	2.33	1.5264
	5.83 x 10^5	1.4292	0.06270	0.525	-1.25	4.58 x 10^5	2.25	1.5000
	4.80 x 10^5	1.3980	0.04760	0.510	-1.21	3.64 x 10^5	2.21	1.4866
	4.06 x 10^5	1.4760	0.04394	0.535	-1.175	3.20 x 10^5	2.175	1.4748
40°	9.10 x 10^5	1.3888	0.05002	0.46415	-1.16	6.24 x 10^5	2.16	1.4697
	6.15 x 10^5	1.4764	0.04966	0.49175	-1.34	4.61 x 10^5	2.34	1.5297
	4.80 x 10^5	-	-	-	-1.22	-	2.22	1.4900
	4.0 x 10^5	1.5190	0.04756	0.5371	-1.261	3.24 x 10^5	2.261	1.5034
35°	9.2 x 10^5	1.3110	0.05302	0.39675	-1.14	5.35 x 10^5	2.14	1.4629
	5.83 x 10^5	1.3112	0.05450	0.3973	-1.16	3.39 x 10^5	2.16	1.4697
	4.80 x 10^5	1.3102	0.04894	0.3960	-1.115	2.77 x 10^5	2.115	1.4543
	4.0 x 10^5	1.4286	0.04668	0.4276	-1.20	2.54 x 10^5	2.20	1.4832
30°	9.1 x 10^5	1.1098	0.05054	0.301	-0.928	3.78 x 10^5	1.928	1.3874
	5.83 x 10^5	1.1844	0.04656	0.31515	-0.895	2.52 x 10^5	1.895	1.3764
	4.06 x 10^5	1.1770	0.04558	0.3125	-1.00	1.79 x 10^5	2.00	1.4142
25°	9.1 x 10^5	0.9700	0.05068	0.2280	-0.795	2.77 x 10^5	1.795	1.3398
	5.33 x 10^5	0.9780	0.04730	0.2279	-0.815	1.785 x 10^5	1.815	1.3472
	4.3 x 10^5	1.0602	0.04976	0.2401	-0.80	1.55 x 10^5	1.80	1.3416
	3.21 x 10^5	-	-	-	-0.835	-	1.835	1.3543
20°	9.0 x 10^5	0.8136	0.04852	0.16175	-0.74	1.92 x 10^5	1.74	1.3191
	5.83 x 10^5	0.8622	0.05264	0.1722	-0.736	1.32 x 10^5	1.736	1.3176
	4.80 x 10^5	0.8122	0.05848	0.18	-0.75	1.142 x 10^5	1.75	1.3229
	4.0 x 10^5	0.8430	0.04770	0.1663	-0.78	8.88 x 10^4	1.78	1.3342

TABLE 4

Airfoil NACA 66010 with Splitter Plate Rearmost (Position 2) R_{es} Calculations

Angle α	$R_{e\infty}$ No	$C_{N\infty}$	$C_{c\infty}$	$\frac{C_{D\infty}}{2}$	$C_{pS} = 1-\left(\frac{U_S}{U_\infty}\right)^2$	$R_{es} = R_{e\infty}\left(\frac{C_{D\infty}}{2}\right)\left(\frac{U_S}{U_\infty}\right)$	$\frac{2}{C_{DS}} = \left(\frac{U_S}{U_\infty}\right)^2$	$\frac{U_S}{U_\infty}$
45°	9.2×10^5	1.P174	0.04224	0.655	-1.495	9.5×10^5	2.495	1.5796
	4.83×10^5	1.6680	0.04770	0.605	-1.42	4.55×10^5	2.42	1.5556
	4.06×10^5	1.6324	0.04400	0.6075	-1.47	3.88×10^5	2.47	1.5716
40°	9.2×10^5	1.5510	0.0527	0.5191	-1.35	7.3×10^5	2.35	1.5330
	5.83×10^5	1.4750	0.048	0.4923	-1.22	4.28×10^5	2.22	1.4900
	4.8×10^5	1.2614	0.04304	0.454	-1.11	3.17×10^5	2.11	1.4526
	4.0×10^5	1.5302	0.0540	0.5117	-1.33	3.12×10^5	2.33	1.5264
35°	9.2×10^5	1.2750	0.05228	0.3864	-1.11	5.17×10^5	2.11	1.4526
	5.83×10^5	1.2690	0.05280	0.3841	-1.07	3.26×10^5	2.07	1.4387
	4.80×10^5	1.2236	0.07006	0.37865	-1.00	2.57×10^5	2.00	1.4142
	4.0×10^5	1.3364	0.05224	0.40385	-1.045	2.30×10^5	2.045	1.4301
30°	9.2×10^5	1.1130	0.05430	0.3015	-0.96	3.88×10^5	1.96	1.4000
	5.83×10^5	1.1034	0.05336	0.2941	-0.95	2.40×10^5	1.95	1.3964
	4.8×10^5	1.0684	0.04480	0.2315	-0.707	1.45×10^5	1.707	1.3065
	4.0×10^5	1.0632	0.04834	0.2864	-0.865	1.57×10^5	1.865	1.3729
25°	9.2×10^5	0.9220	0.0513	0.2178	-0.825	2.70×10^5	1.825	1.3509
	5.83×10^5	0.9364	0.05320	0.2061	-0.762	1.60×10^5	1.762	1.3274
	4.8×10^5	0.9634	0.04626	0.2029	-0.704	1.27×10^5	1.704	1.3053
	4.0×10^5	0.9754	0.04688	0.2272	-0.865	1.24×10^5	1.865	1.3729
20°	9.20×10^5	0.7190	0.04988	0.1459	-0.715	1.76×10^5	1.715	1.3096
	5.83×10^5	0.1958	0.0459	0.1065	-0.615	7.9×10^4	1.615	1.2708
	4.8×10^5	0.7200	0.04212	0.1907	-0.63	1.17×10^5	1.63	1.2767
	4.0×10^5	0.7234	0.04526	0.1498	-0.635	7.65×10^4	1.635	1.2786

TABLE 5

Flat Plate Drag Coefficient

Angle α	Re_∞ No	Flat Plate				Flat Plate with Splitter Plate Foremost			Flat Plate with Splitter Plate Rearmost		
		Pressure Distribution		Wake Survey		Pressure Distribution		Wake Survey	Pressure Distribution		Wake Survey
		$C_{D\infty}$ (uncorr)	$C_{D\infty}$ (Corr)	$C_{D\infty}$ $\frac{x}{L_p}=3.94$	$C_{D\infty}$ $\frac{x}{L_p}=5.6$	$C_{D\infty}$ (uncorr)	$C_{D\infty}$ (corr)	$C_{D\infty}$ $\frac{x}{L_p}=5.6$	$C_{D\infty}$ (uncorr)	$C_{D\infty}$ (corr)	$C_{D\infty}$ $\frac{x}{L_p}=5.6$
90°	4.8×10^5	2.56	1.97	2.79	2.82	2.0412	1.575	1.78	2.0812	1.60	1.965
	4.0×10^5	2.56	1.97	2.70	2.80	2.056	1.58	1.738	1.9938	1.535	1.942
	2.76×10^5	2.56	1.97	2.56	2.780	–	–	–	–	–	–
60°	4.8×10^5	1.92	1.530	–	–	1.46	1.165	1.71	1.450	1.16	1.535
	4.0×10^5	1.950	1.550	–	–	1.48	1.18	1.682	1.490	1.19	1.595
	2.75×10^5	1.980	1.580	–	–	–	–	–	–	–	–
45°	2.8×10^5	1.414	1.18	2.01	1.625	0.95	0.794	1.04	0.94	0.784	0.945
	4.0×10^5	1.490	1.25	2.20	1.36	1.02	0.85	1.08	1.062	0.886	0.977
	2.75×10^5	1.610	1.34	2.40	1.50	–	–	–	–	–	–
30°	4.8×10^5	0.5472	0.483	0.628	0.612	0;476	0.421	0.472	0.535	0.471	0.465
	4.0×10^5	0.5666	0.50	0.79	0.596	0.492	0.435	0.475	0.522	0.463	0.453
	2.75×10^5	–	–	0.97	0.571	–	–	–	–	–	–
40°	4.0×10^5	1.13	0.97	–	1.262	–	–	–	–	–	–
35°	4.0×10^5	0.91	0.785	–	0.92	–	–	–	–	–	–
25°	4.0×10^5	0.451	0.406	–	0.386	–	–	–	–	–	–
20°	4.0×10^5	0.35	0.32	–	0.370	–	–	–	–	–	–

TABLE 6

Flat Plate R_{es} Calculations

Angle α	Re_∞	$C_{N\infty}$	$\frac{C_{D\infty}}{2}$	$C_{Ps} = 1-\left(\frac{U_s}{U_\infty}\right)^2$	$Re_s = Re_\infty\left(\frac{C_{D\infty}}{2}\right)\left(\frac{U_s}{U_\infty}\right)$	$\frac{2}{C_{Ds}} = \left(\frac{U_s}{U_\infty}\right)^2$	$\frac{U_s}{U_\infty}$
90°	4.8×10^5	2.56	1.28	-1.78	10.3×10^5	2.78	1.6673
	4.0×10^5	2.56	1.28	-1.80	8.56×10^5	2.80	1.6733
	2.75×10^5	2.56	1.28	-1.78	5.90×10^5	2.78	1.6673
60°	4.8×10^5	2.218	0.96	-1.54	7.33×10^5	2.54	1.5937
	4.0×10^5	2.260	0.975	-1.57	6.25×10^5	2.57	1.6031
	2.75×10^5	2.290	0.99	-1.615	4.40×10^5	2.615	1.6170
45°	4.8×10^5	2.000	0.707	-1.53	5.40×10^5	2.53	1.5906
	4.0×10^5	2.11	0.745	-1.65	4.85×10^5	2.65	1.6279
	2.75×10^5	2.28	0.805	-1.825	3.72×10^5	2.825	1.6808
30°	4.8×10^5	1.0944	0.2736	-0.84	1.78×10^5	1.84	1.3565
	4.0×10^5	1.1334	0.2833	-0.88	1.55×10^5	1.88	1.3711
75°	4.0×10^5	2.43	1.17	-1.69	7.67×10^5	2.69	1.6401
70°	4.0×10^5	2.241	1.05	-1.65	6.85×10^5	2.65	1.6279
50°	4.0×10^5	2.02	0.765	-1.48	4.83×10^5	2.48	1.5748
40°	4.0×10^5	1.7658	0.565	-1.35	3.47×10^5	2.35	1.5330
35°	4.0×10^5	1.5636	0.455	-1.22	2.71×10^5	2.22	1.4900
25°	4.0×10^5	1.0704	0.2255	-0.762	1.2×10^5	1.762	1.3274
20°	4.0×10^5	1.0284	0.175	-0.77	9.3×10^4	1.77	1.3304

TABLE 7

Flat Plate with Splitter Plate Foremost (Position 1) R_{es} Calculations

Angle α	$R_{e\infty}$ NO	$C_{N\infty}$	$\frac{C_{D\infty}}{2}$	$C_{PS} = 1-\left(\frac{U_s}{U_\infty}\right)^2$	$R_{es} = R_{e\infty}\left(\frac{C_{D\infty}}{2}\right)\left(\frac{U_s}{U_\infty}\right)$	$\frac{2}{C_{DS}} = \left(\frac{U_s}{U_\infty}\right)^2$	$\left(\frac{U_s}{U_\infty}\right)$
90°	4.8 x 10^5	2.0412	1.0206	-1.245	7.35 x 10^5	2.245	1.4983
	4.0 x 10^5	2.056	1.028	-1.21	6.14 x 10^5	2.21	1.4866
60°	4.8 x 10^5	1.6852	0.73	-1.045	5.01 x 10^5	2.045	1.4301
	4.0 x 10^5	1.7128	0.74	-1.07	4.26 x 10^5	2.07	1.4387
45°	4.8 x 10^5	1.3482	0.475	-0.86	3.14 x 10^5	1.86	1.3638
	4.0 x 10^5	1.4434	0.51	-0.965	2.86 x 10^5	1.965	1.4018
30°	4.8 x 10^5	0.9516	0.2379	-0.73	1.50 x 10^5	1.73	1.3153
	4.0 x 10^5	0.9844	9.2461	-0.73	1.295 x 10^5	1.73	1.3153

TABLE 8

Flate Plate with Splitter Plate Rearmost (Position 2) R_{es} Calculations

Angle α	$R_{e\infty}$ NO.	$C_{N\infty}$	$\frac{C_{D\infty}}{2}$	$C_{PS} = 1-\left(\frac{U_S}{U_\infty}\right)^2$	$R_{es} = R_{e\infty}\left(\frac{C_{D\infty}}{2}\right)\left(\frac{U_S}{U_\infty}\right)$	$\frac{2}{C_{DS}} = \left(\frac{U_S}{U_\infty}\right)^2$	$\frac{U_S}{U_\infty}$
90°	4.8×10^5	2.0812	1.0406	-1.285	7.58×10^5	2.285	1.5117
	4.0×10^5	1.9938	0.9979	-1.215	5.95×10^5	2.215	1.4883
60°	4.8×10^5	1.6866	0.729	-1.015	4.95×10^5	2.015	1.4195
	4.0×10^5	1.7250	0.745	-1.06	4.28×10^5	2.06	1.4353
45°	4.8×10^5	1.338	0.47	-0.90	3.13×10^5	1.90	1.3784
	4.0×10^5	1.5096	0.531	-1.06	3.07×10^5	2.06	1.4353
30°	4.8×10^5	1.0634	0.266	-0.755	1.69×10^5	1.755	1.3248
	4.0×10^5	1.0428	0.261	-0.73	1.37×10^5	1.73	1.3153

AIRFOIL CO-ORDINATE SYSTEM

FIG.1

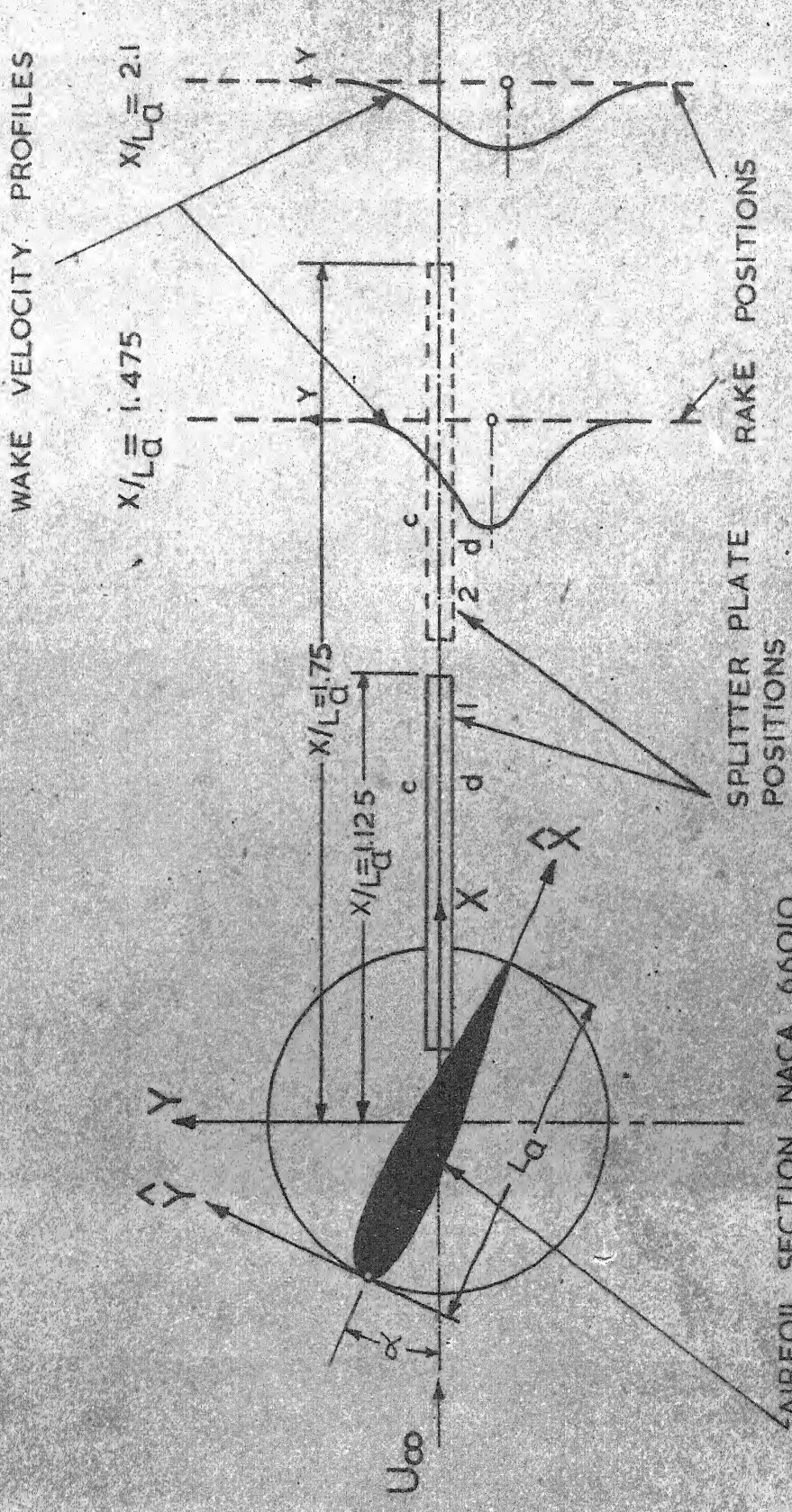

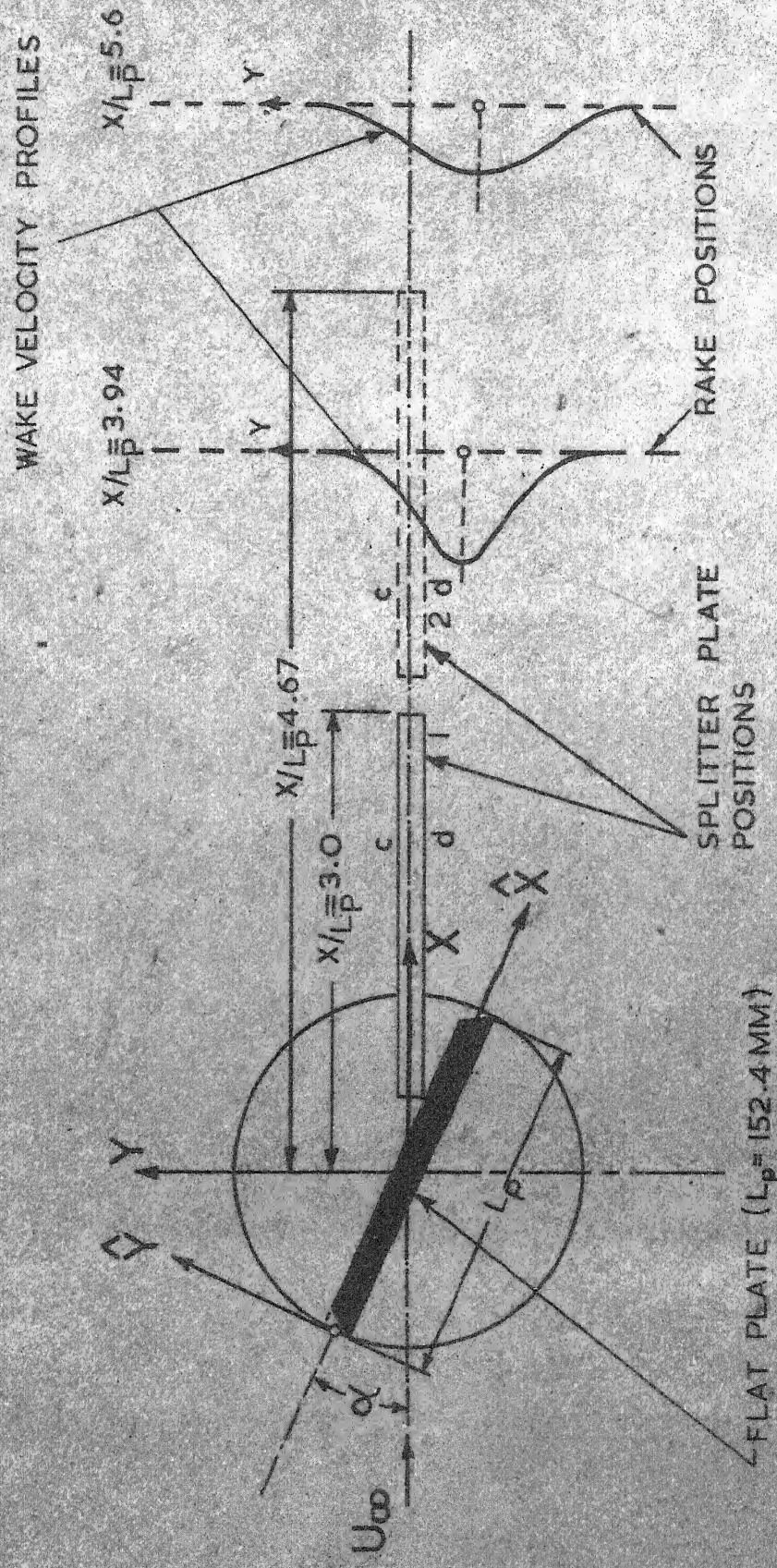
WAKE VELOCITY PROFILES
X/Lp=5.6
Y
X/Lp=3.94
Y
RAKE POSITIONS
c
2 d
X/Lp=4.67
X/Lp=3.0
c
d
SPLITTER PLATE POSITIONS
X
X
Y
Y
Lp
FLAT PLATE (Lp= 152.4 MM)
α
U∞

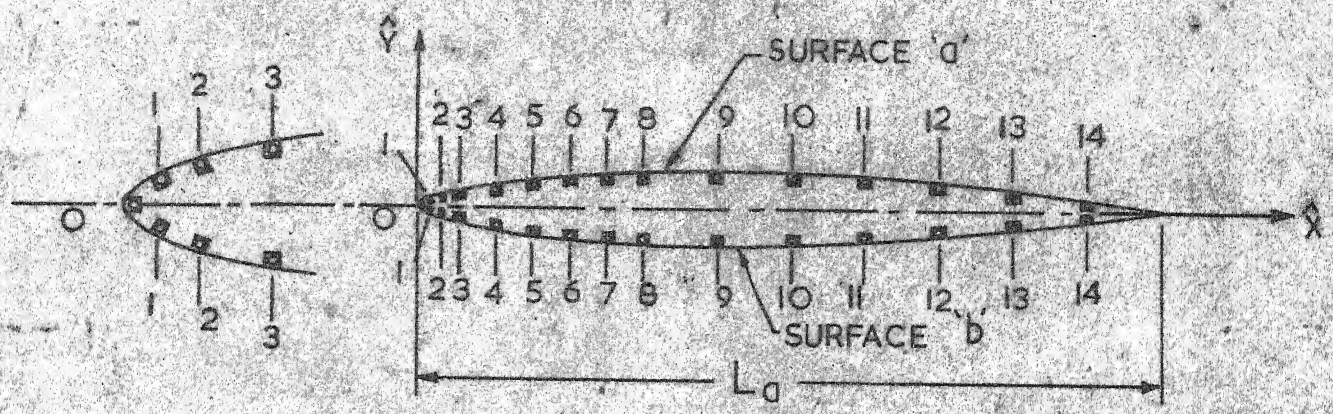

PROFILE NACA 66010, L_a = 406.4 mm

PRESSURE TAP NO.	SURFACE 'a'		SURFACE 'b'	
	$\hat{X}/L_a$ %	$\hat{Y}/L_a$ %	$\hat{X}/L_a$ %	$\hat{Y}/L_a$ %
0	0	0	-	-
1	1.3	0.755	1.3	0.755
2	2.5	1.516	2.5	1.516
3	5.0	2.087	5.0	2.087
4	7.5	2.536	7.5	2.536
5	10.0	2.917	10.0	2.917
6	15.0	3.530	15.0	3.530
7	20.0	4.001	20.0	4.001
8	25.0	4.363	25.0	4.363
9	30.0	4.636	30.0	4.636
10	40.0	4.953	40.0	4.953
11	50.0	4.971	50.0	4.971
12	59.0	4.665	59.0	4.665
13	70.0	3.787	70.0	3.787
14	80.0	2.494	80.0	2.494
15	90.0	1.054	90.0	1.054
-	100.0	0.0	100.0	0.0
	LEADING EDGE RADIUS 0.662 % L_a			

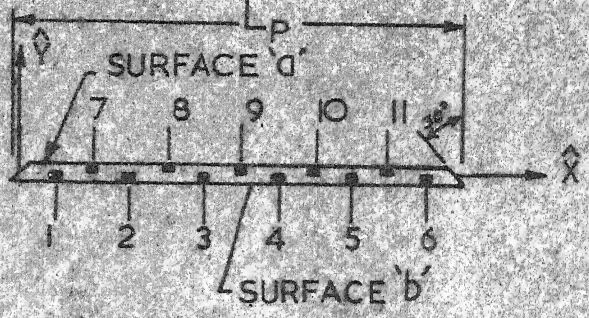

FLAT PLATE L_P = 153.4 MM. t = 6.35 MM.

PRESSURE TAP NO.	CO-ORDINATES X/L_P	REMARKS
1	0.084	SURFACE 'b'
2	0.250	
3	0.417	
4	0.584	
5	0.750	
6	0.916	
7	0.167	SURFACE 'a'
8	0.334	
9	0.50	
10	0.666	
11	0.833	

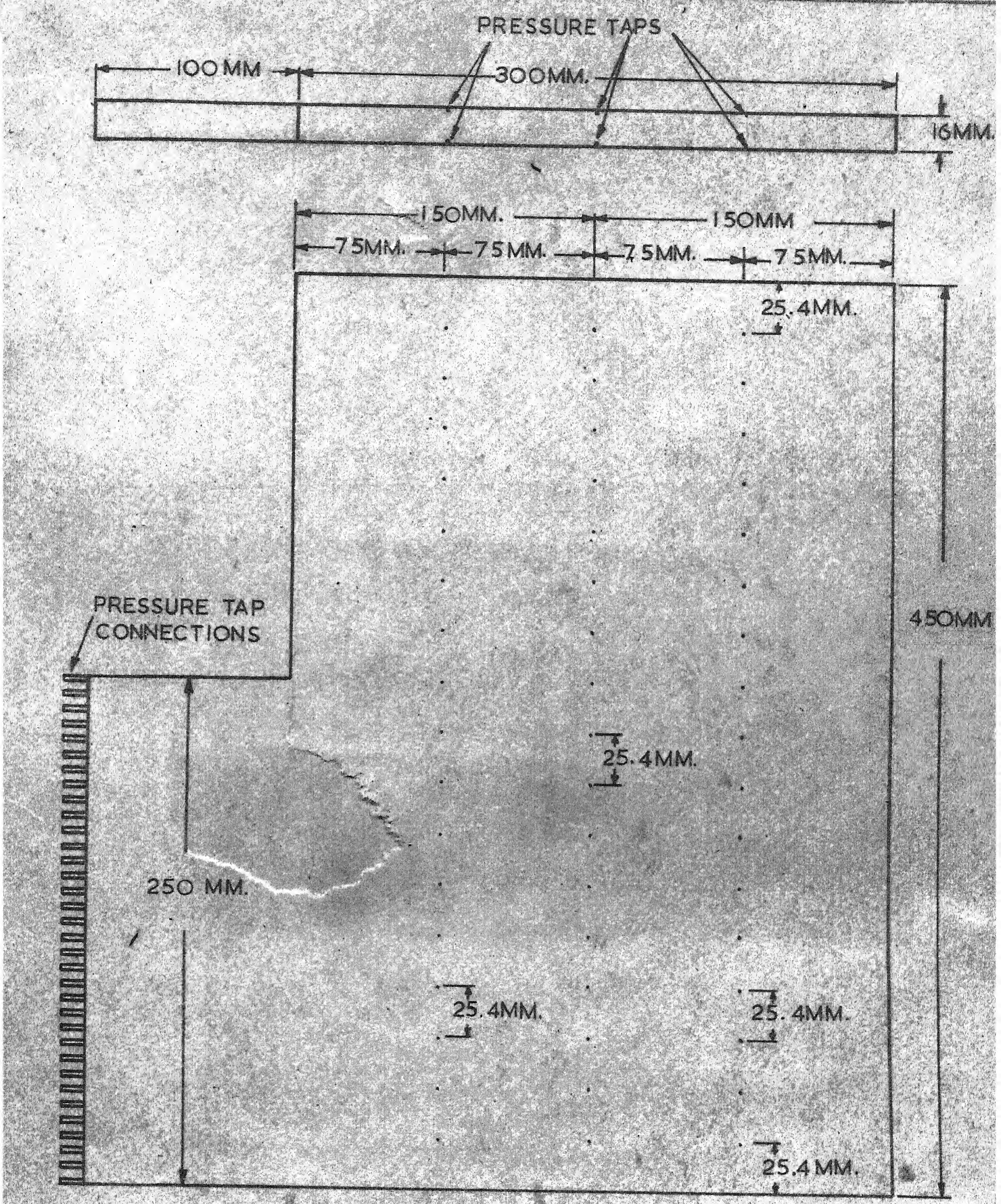
PRESSURE TAPS
100 MM
300MM.
16MM.
150MM.
150MM
75MM.
75MM.
75MM.
75MM.
25.4MM.
450MM
PRESSURE TAP CONNECTIONS
25.4MM.
250 MM.
25.4MM.
25.4MM.
25.4 MM.

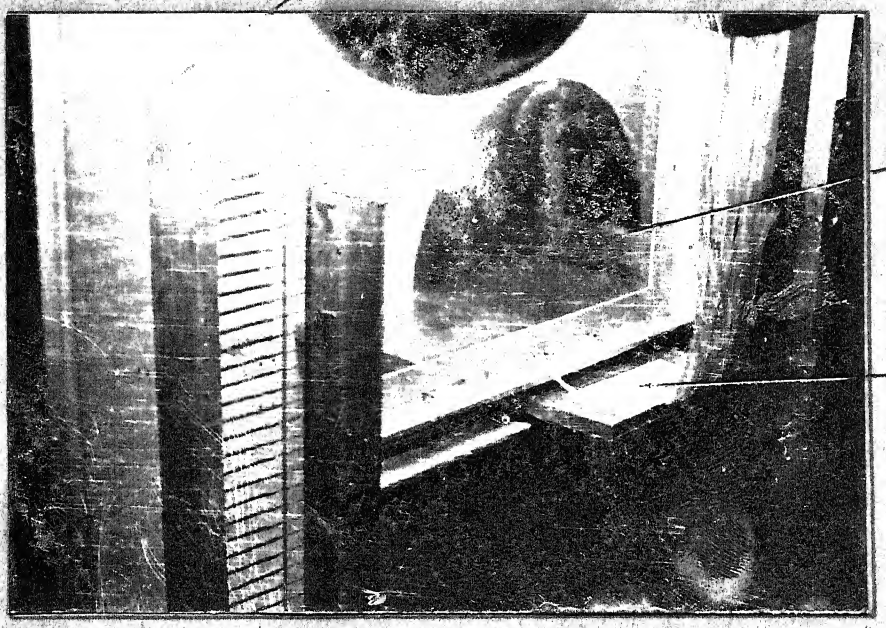

FLAT PLATE WITH SPLITTER PLATE

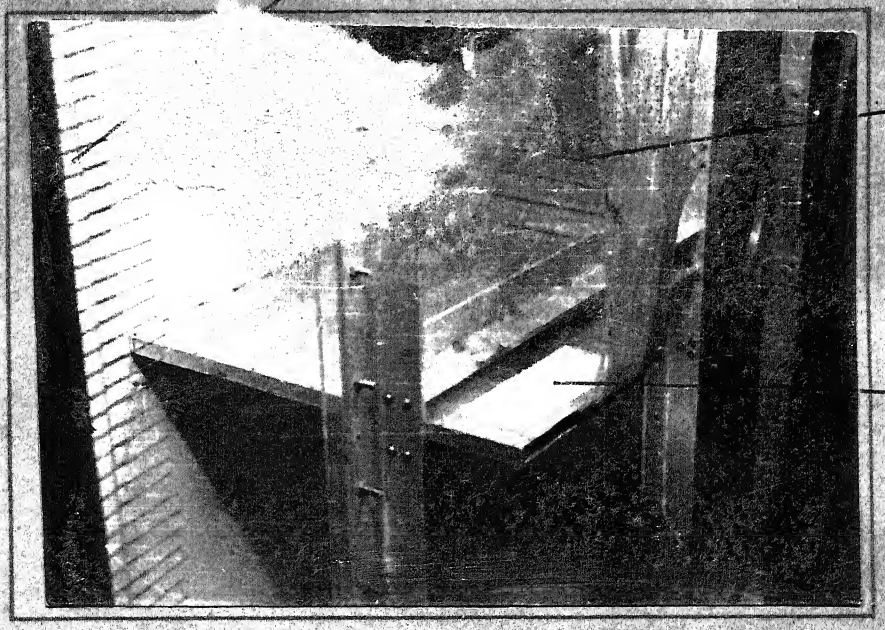

AIRFOIL WITH SPLITTER PLATE

WAKE SURVEY RAKE

FIG·7

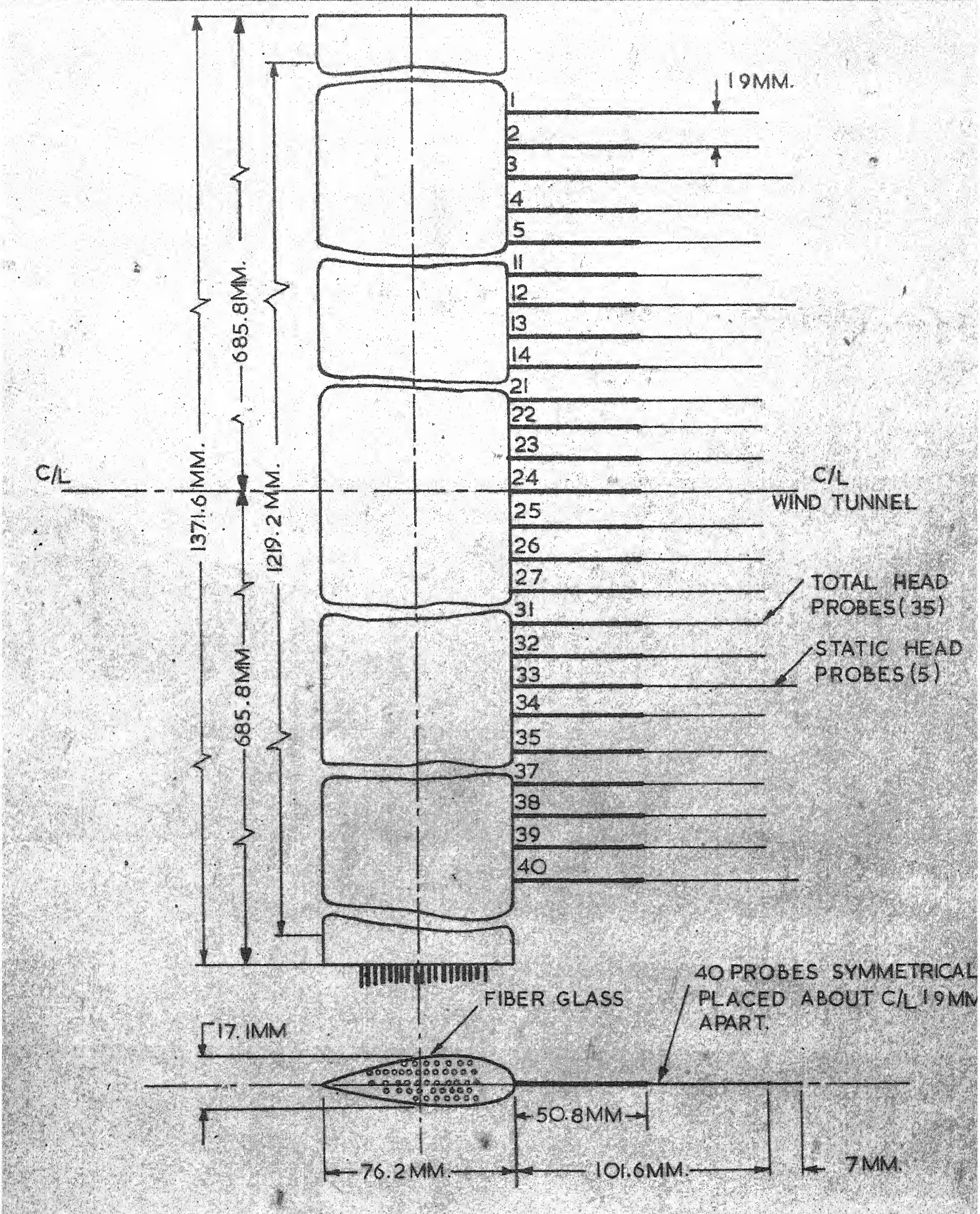

DRAWN: ISG PKM	DATE:	SQN. LDR. I.S. GUPTA	REPORT NO:

PRESSURE DISTRIBUTION ON NACA 66010 (TWO DIMENSIONALITY CHECK)

$\alpha = 20^\circ$

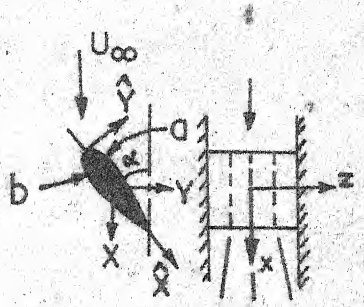

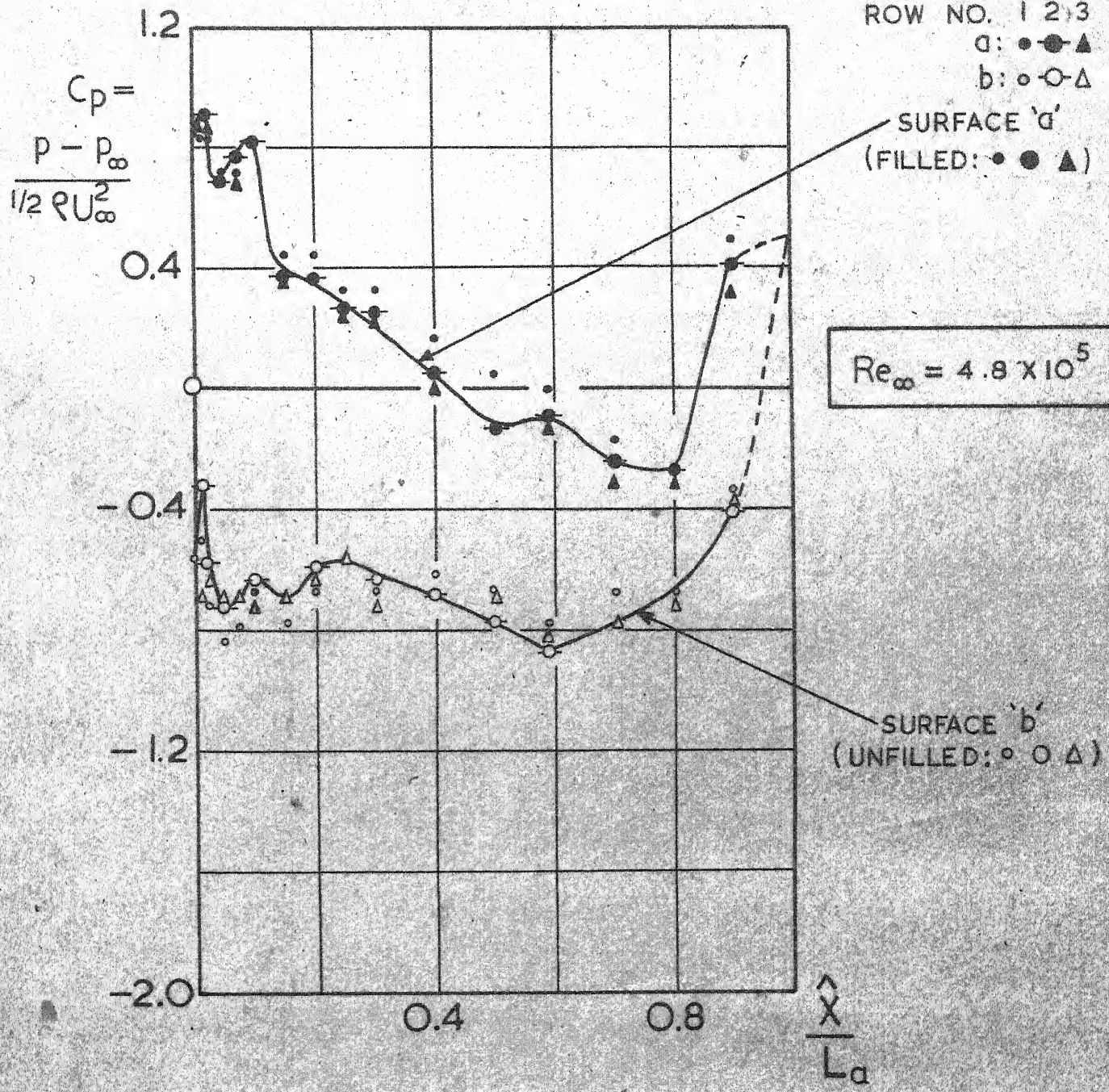

$Re_\infty = 4.8 \times 10^5$

DRAWN: I.S.G P.K.M	DATE:	SQN. LDR. I.S. GUPTA	REPORT NO:

PRESSURE DISTRIBUTION ON NACA 66010 (TWO DIMENSIONALITY CHECK)

FIG.9

$\alpha = 45^\circ$

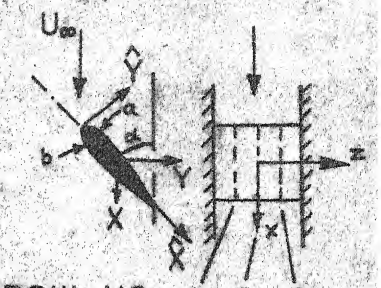

$C_p = \dfrac{p - p_\infty}{1/2\, \rho\, U_\infty^2}$

SURFACE 'a'
(FILLED: ● ⬣ ▲)

$Re_\infty = 9.0 \times 10^6$

SURFACE 'b'
(UNFILLED: ○ ⬦ △)

1.2
0.4
-0.4
-1.2
-2.0
0.4
0.8
$\frac{X}{L_a}$

DRAWN: I.S.GUPTA P.K.M.	DATE:	SQN LDR. I.S. GUPTA	REPORT NO:

PRESSURE DISTRIBUTION ON FLAT PLATE (TWO DIMENSIONALITY CHECK)

FIG·10

$\alpha = 90°$

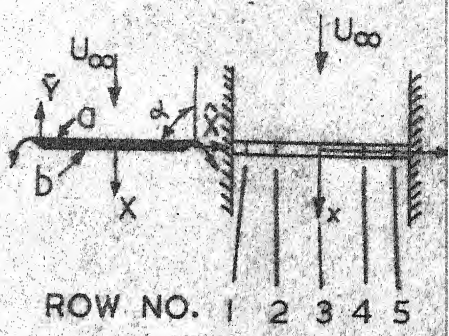

a : ● ■ ▲ ⧗ ⬣

b : ○ □ △ ⧗ ⬡

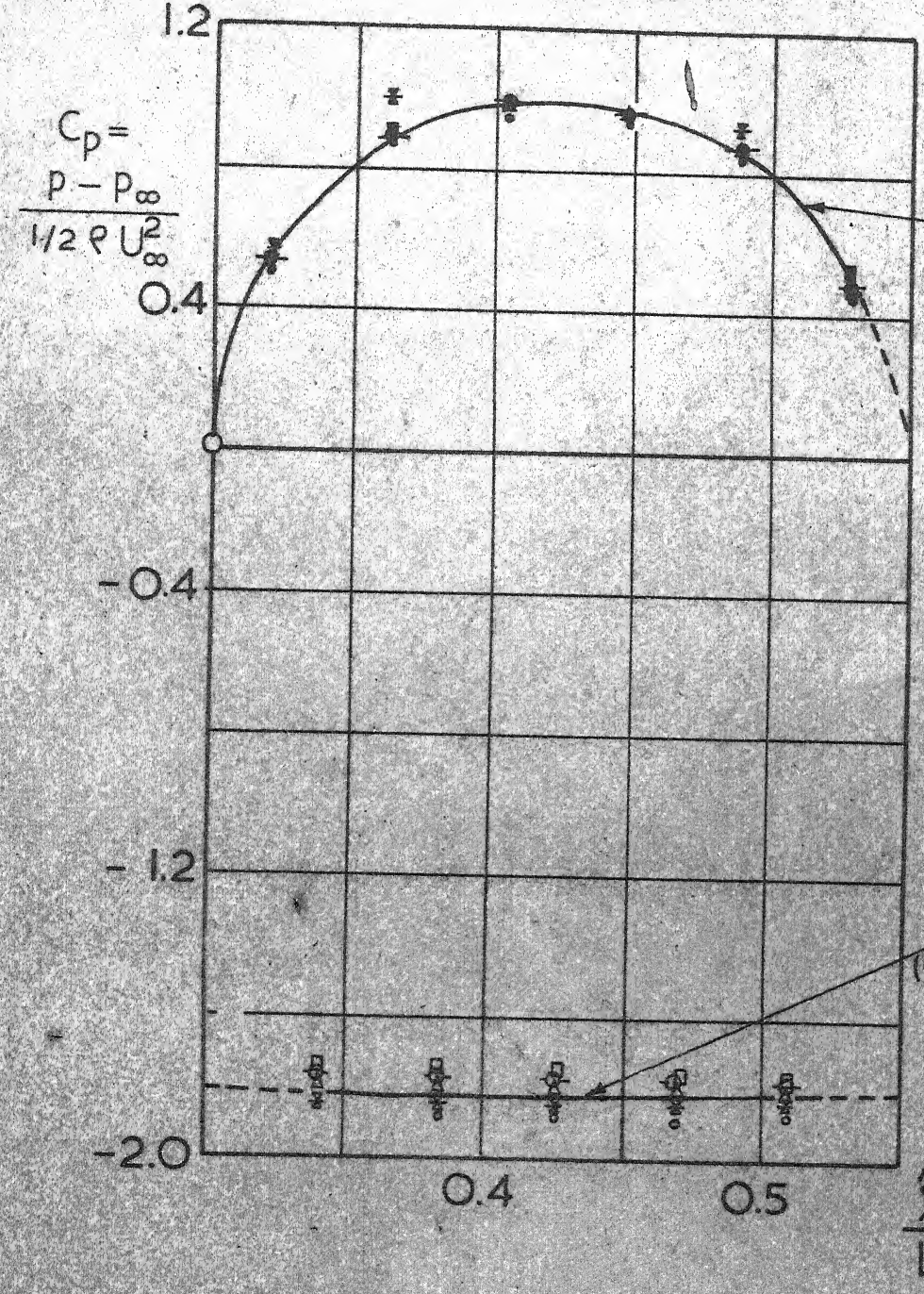

SURFACE 'a'
(FILLED: ● ■ ▲ ⧗ ⬣)

$Re_\infty = 4.8 \times 10^5$

SURFACE 'b'
(UNFILLED: ○ □ △ ⧗ ⬡)

DRAWN: ISG PKM	DATE:	SQN. LDR. I.S. GUPTA	REPORT NO:

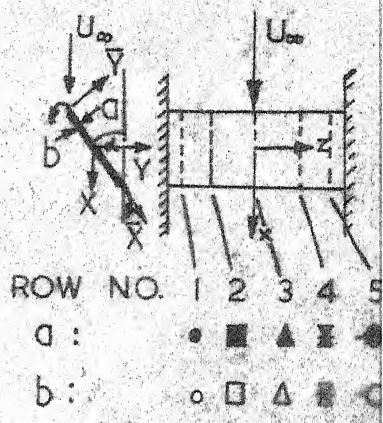

$\alpha = 45^\circ$

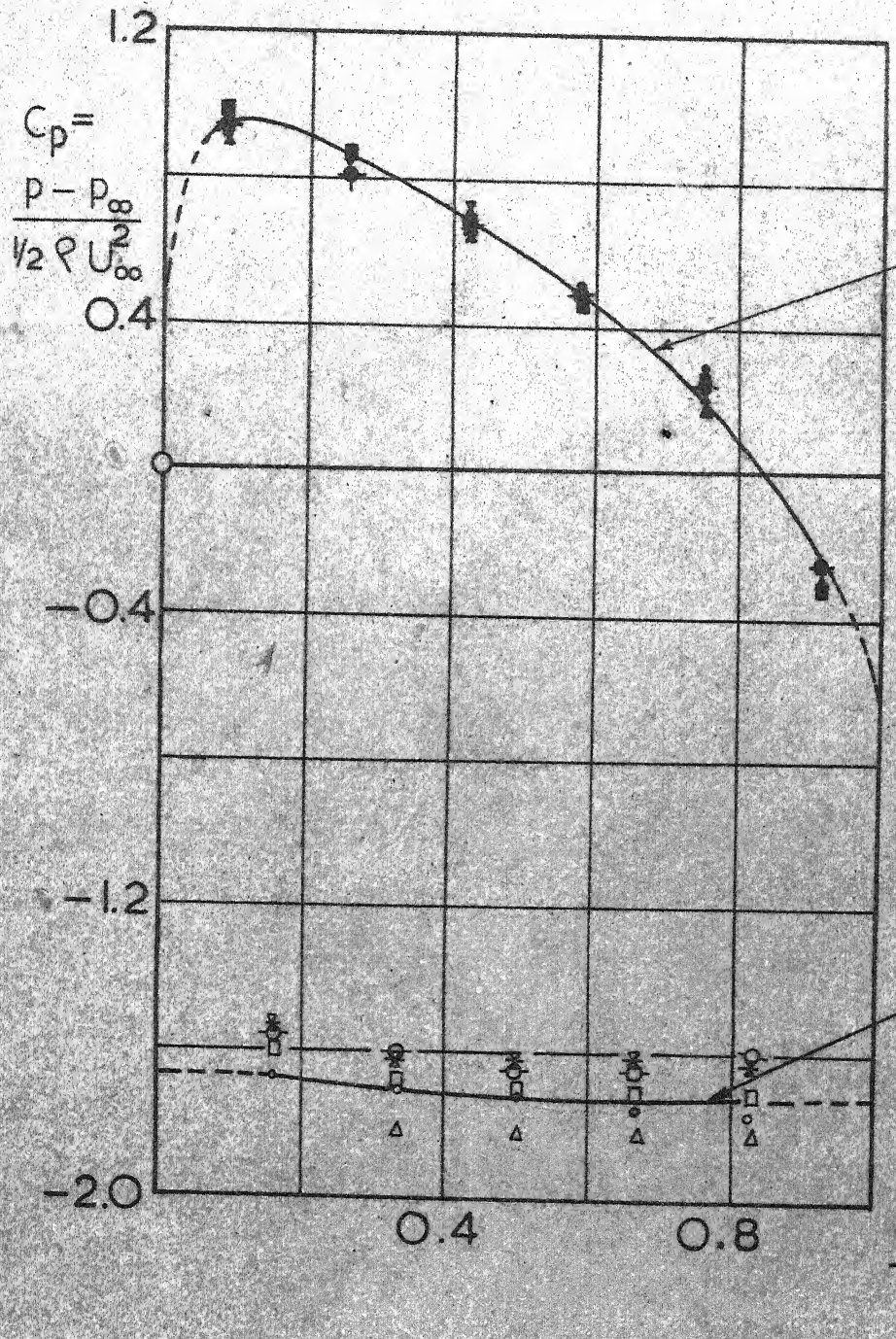

SURFACE 'a'
(FILLED: ● ■ ▲ ✱ ●)

$Re_\infty = 2.76 \times 10^5$

SURFACE 'b'
(UNFILLED: ○ □ △ ✱ ○)

LIFT CHARACTERISTICS NACA 66010 C_L Vs α

FIG·12

$Re_\infty = 9.2 \times 10^5$

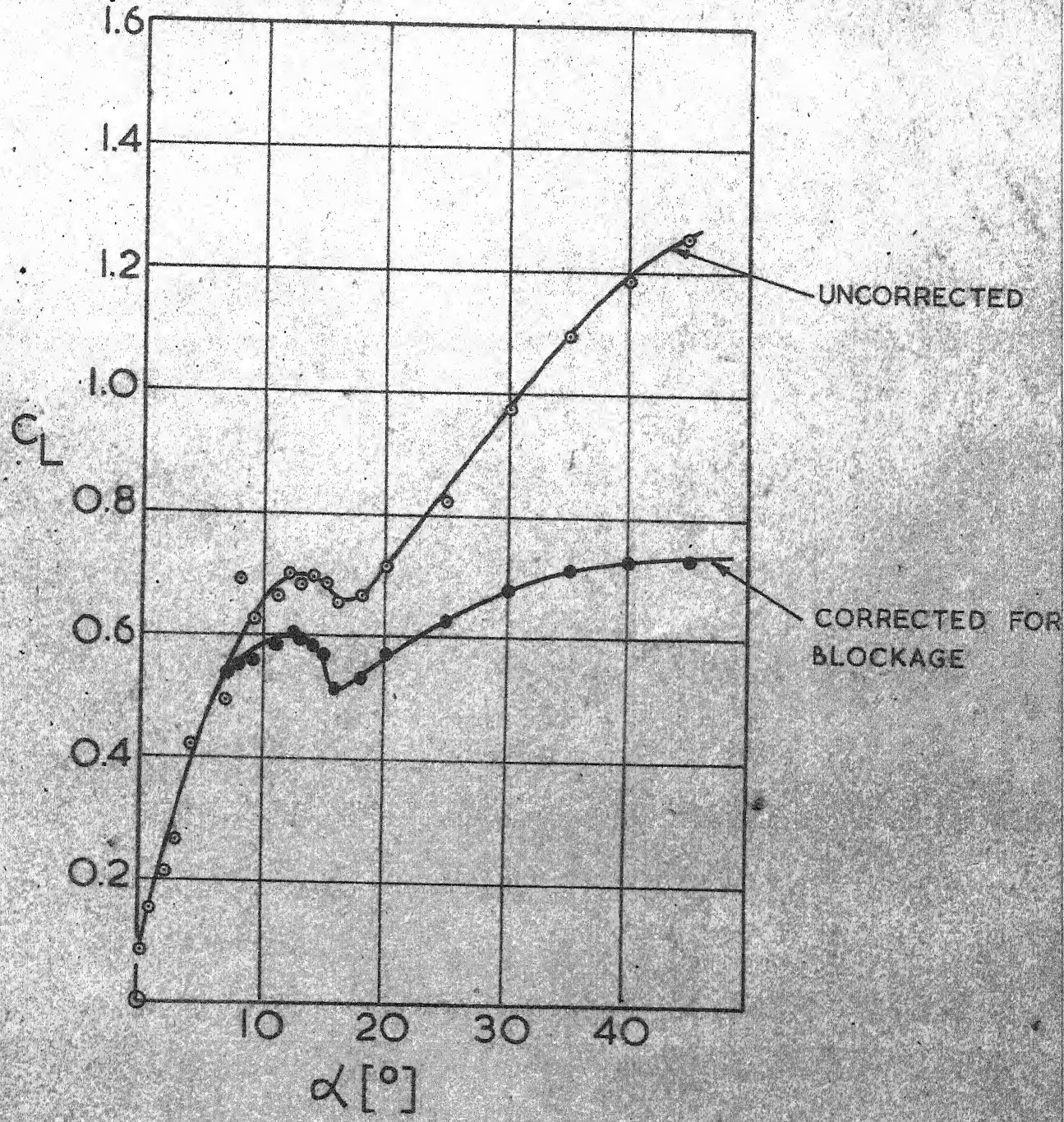

DRAWN: I.S.G P.K.M	DATE:	SQN LDR. I.S. GUPTA	REPORT NO:

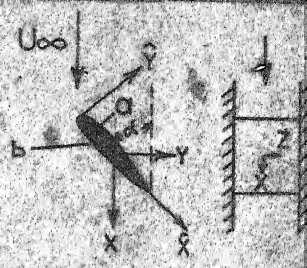
U∞
Y
a
b
Y
Z
X
X

$\alpha = 45°$

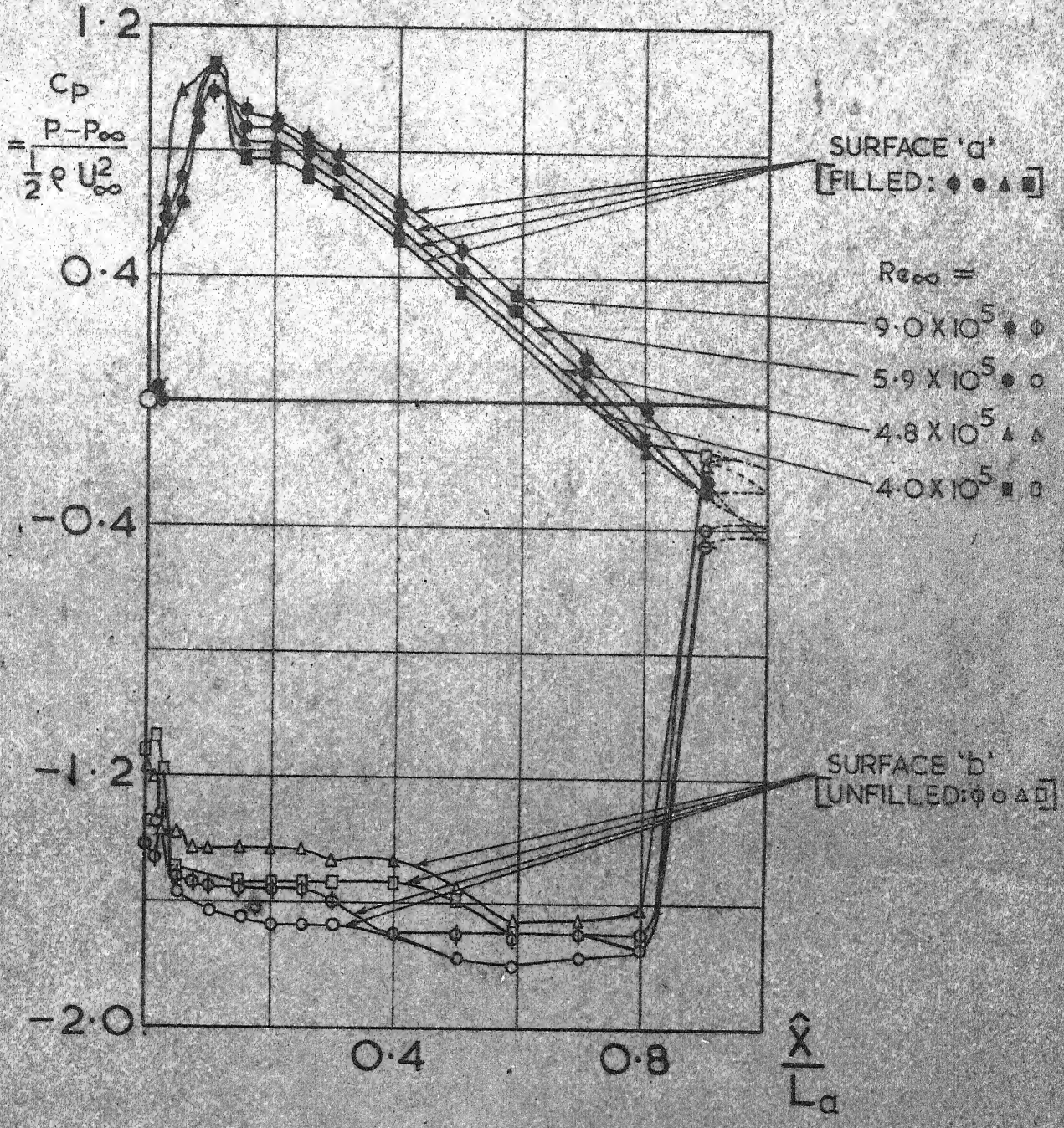
1·2
0·4
-0·4
-1·2
-2·0
0·4
0·8
$C_P = \frac{P-P_\infty}{\frac{1}{2}\rho U_\infty^2}$
$\frac{\hat{X}}{L_a}$
SURFACE 'a'
[FILLED: ◆ ● ▲ ■]
Re_∞ =
9.0×10^5 ◆ ◇
5.9×10^5 ● ○
4.8×10^5 ▲ △
4.0×10^5 ■ □
SURFACE 'b'
[UNFILLED: ◇ ○ △ □]

PRESSURE DISTRIBUTION ON NACA 66010

FIG·14

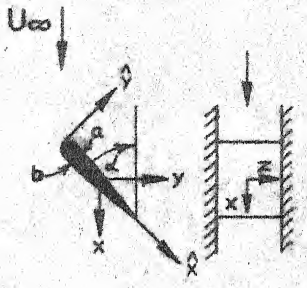

$\alpha = 4^0$

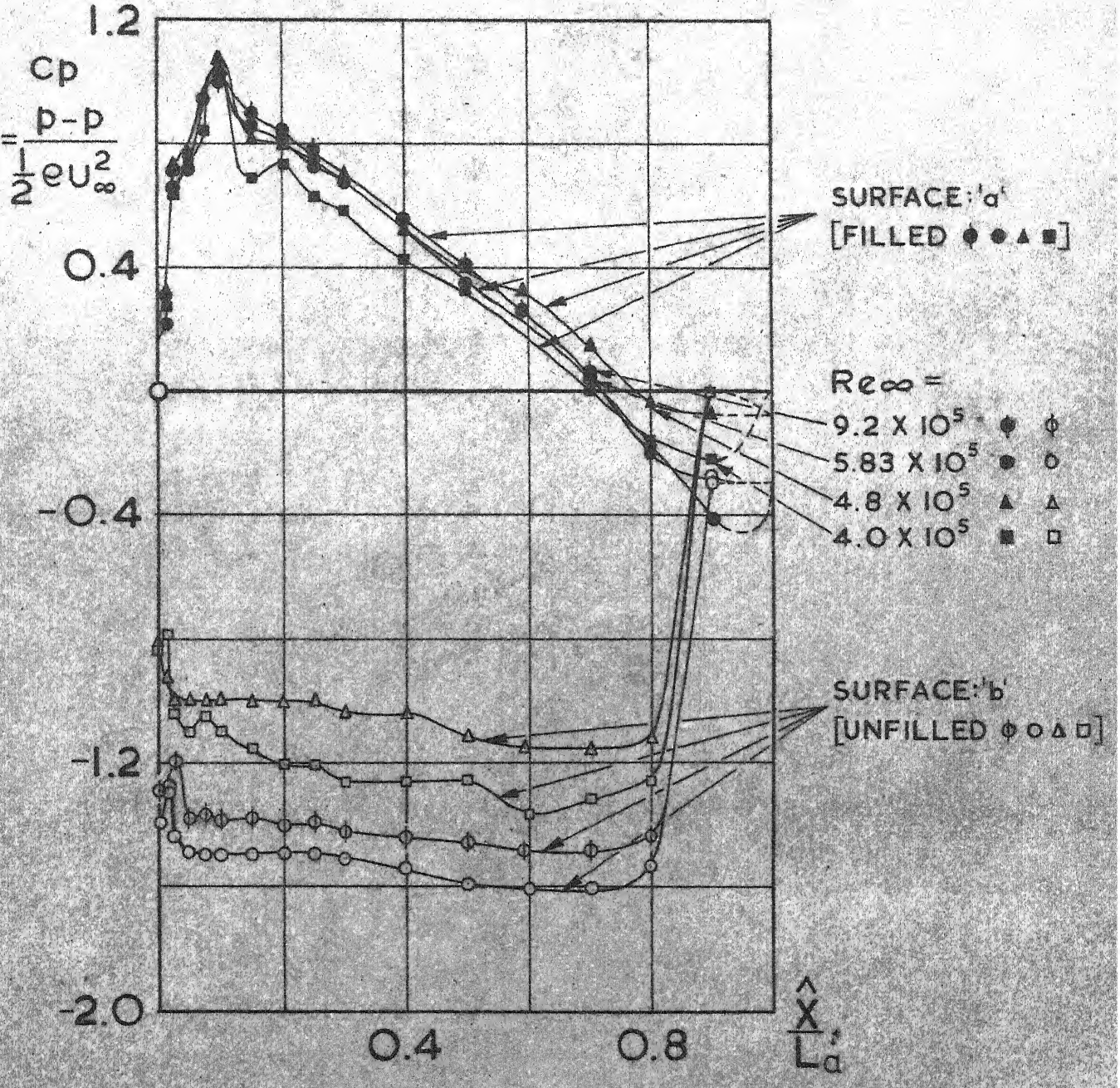

DRAWN I.S.G.	DATE:	SQN. LDR. I.S. GUPTA	REPORT NO:

DEPT. OF AERO ENGG	PRESSURE DISTRIBUTION ON NACA 66010	PAGE NO: 40
		FIG.15

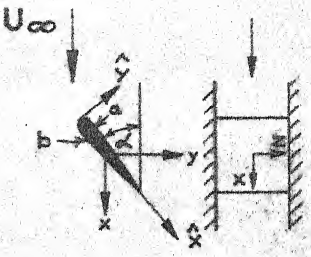

$\alpha = 35^\circ$

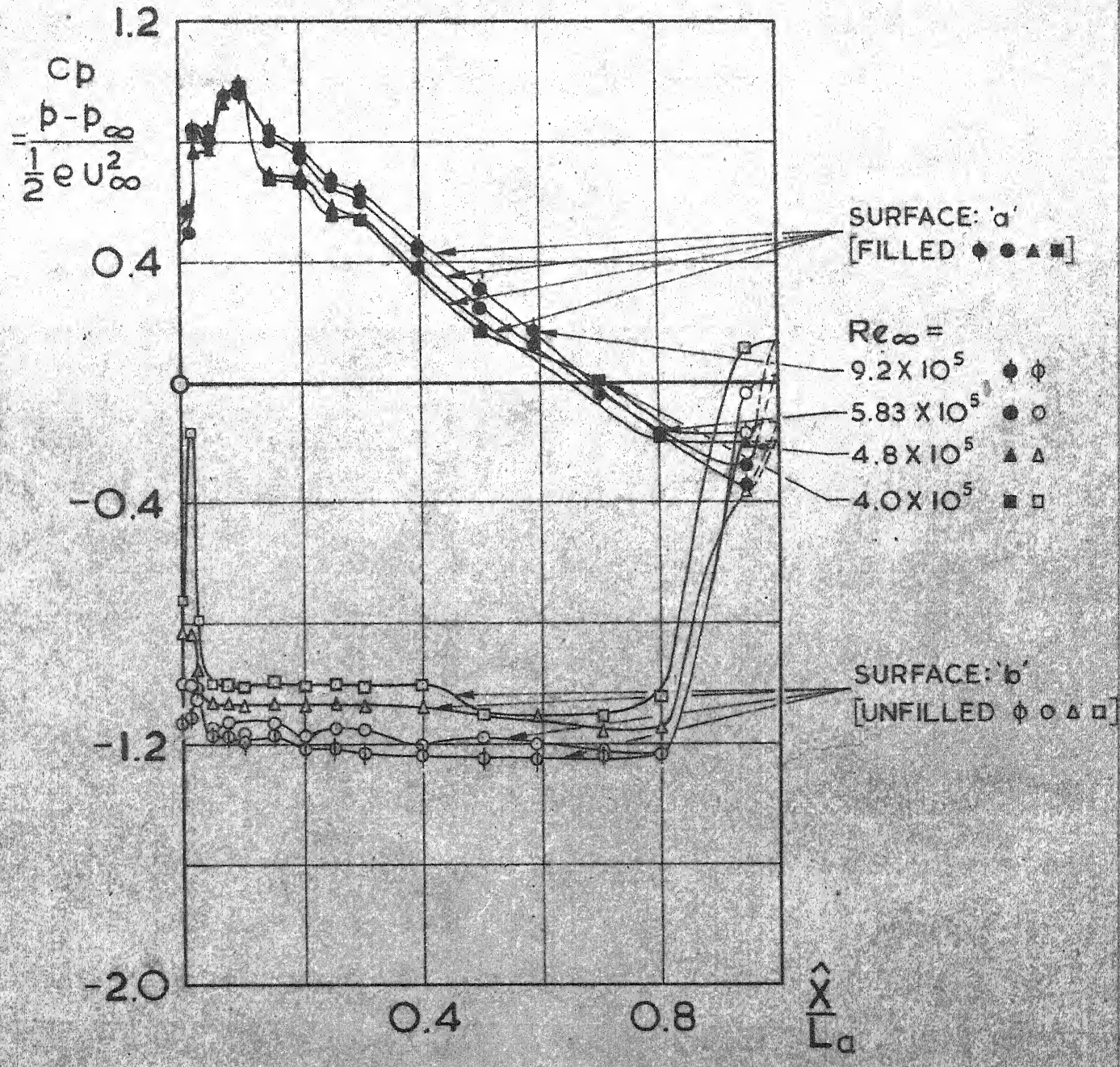

DRAWN: I.S.G.	DATE:	SQN. LDR. I.S.GUPTA	REPORT NO:

PRESSURE DISTRIBUTION ON NACA 66010

$\alpha = 30°$

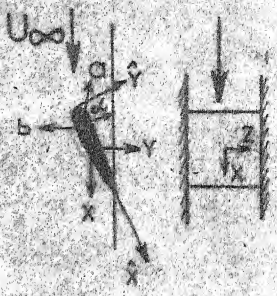

$$C_p = \frac{p - p_\infty}{\frac{1}{2}\rho U_\infty^2}$$

SURFACE 'a' [FILLED: ♦ ● ▲ ■]

$Re_\infty =$

9.2×10^5 ♦ ◊

5.83×10^5 ● ○

4.8×10^5 ▲ △

4.0×10^5 ■ □

SURFACE 'b' [UNFILLED: ◊ ○ △ □]

1.2, 0.4, -0.4, -1.2, -2.0

0.4, 0.8

$\frac{\hat{x}}{L_a}$

PRESSURE DISTRIBUTION ON NACA 66010

FIG.17

$\alpha = 25^\circ$

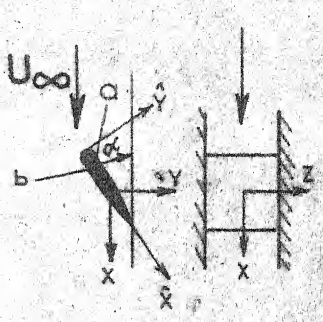

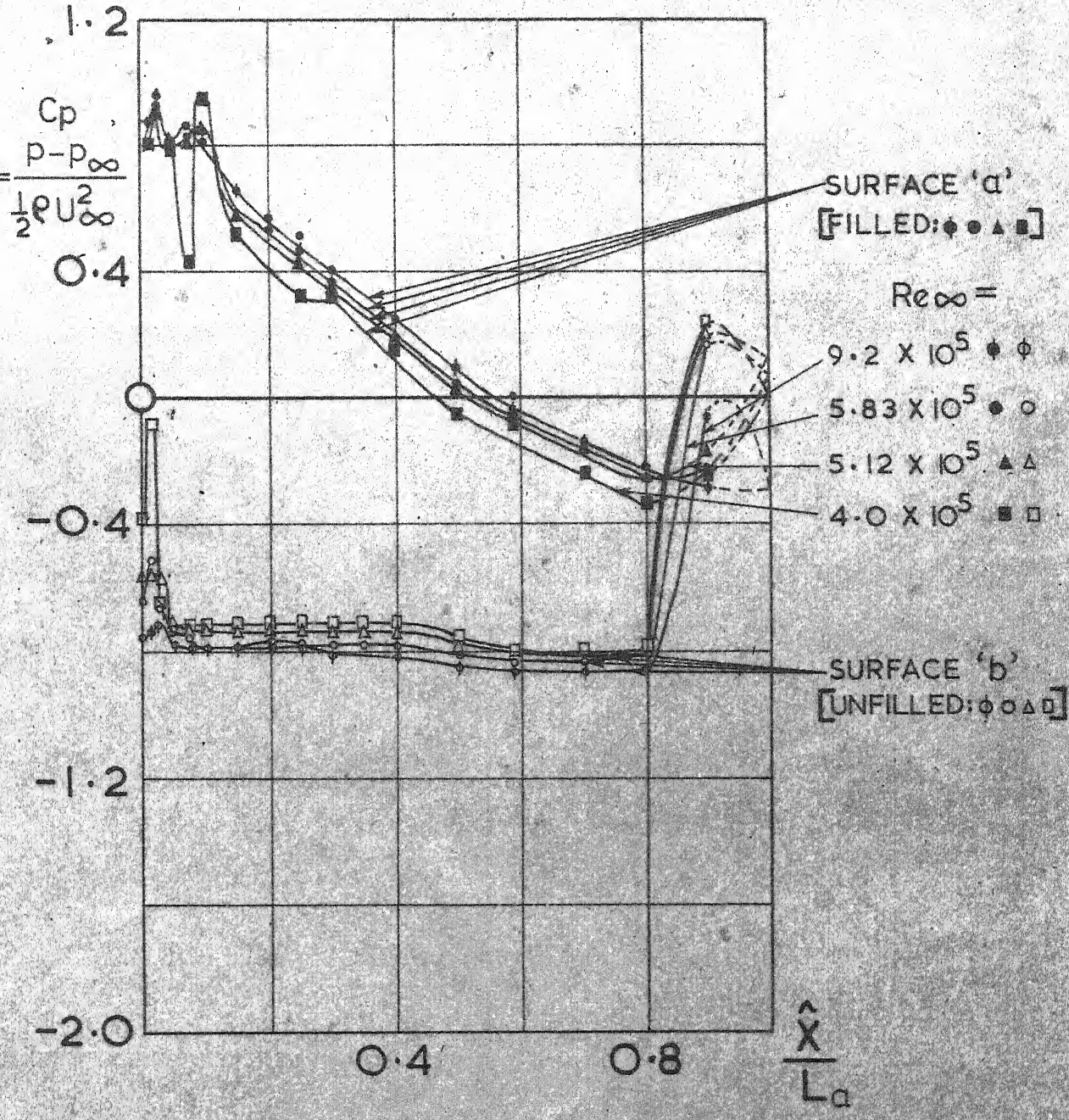

DRAWN: I.S.G.	DATE:	SQN. LDR. I. S. GUPTA	REPORT NO:

PRESSURE DISTRIBUTION ON NACA 66010

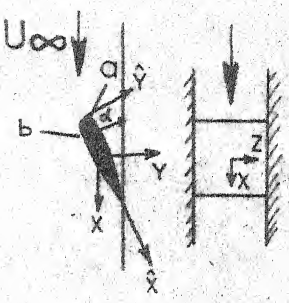

$\alpha = 20°$

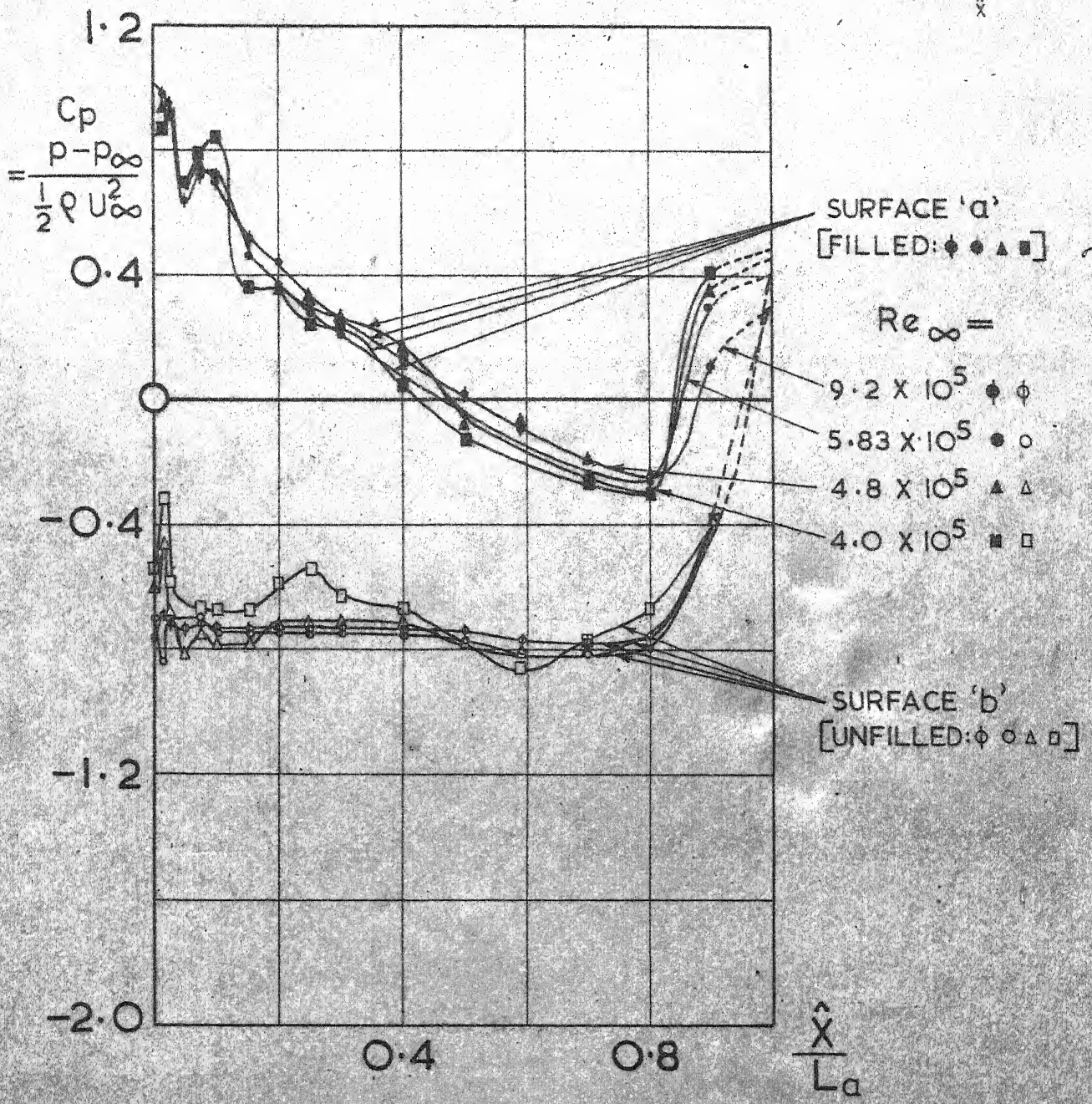

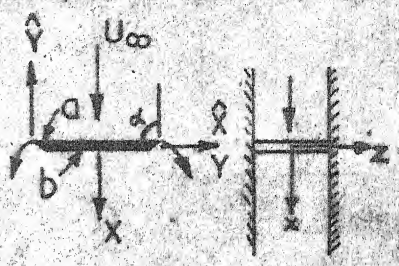

$\alpha = 90^\circ$

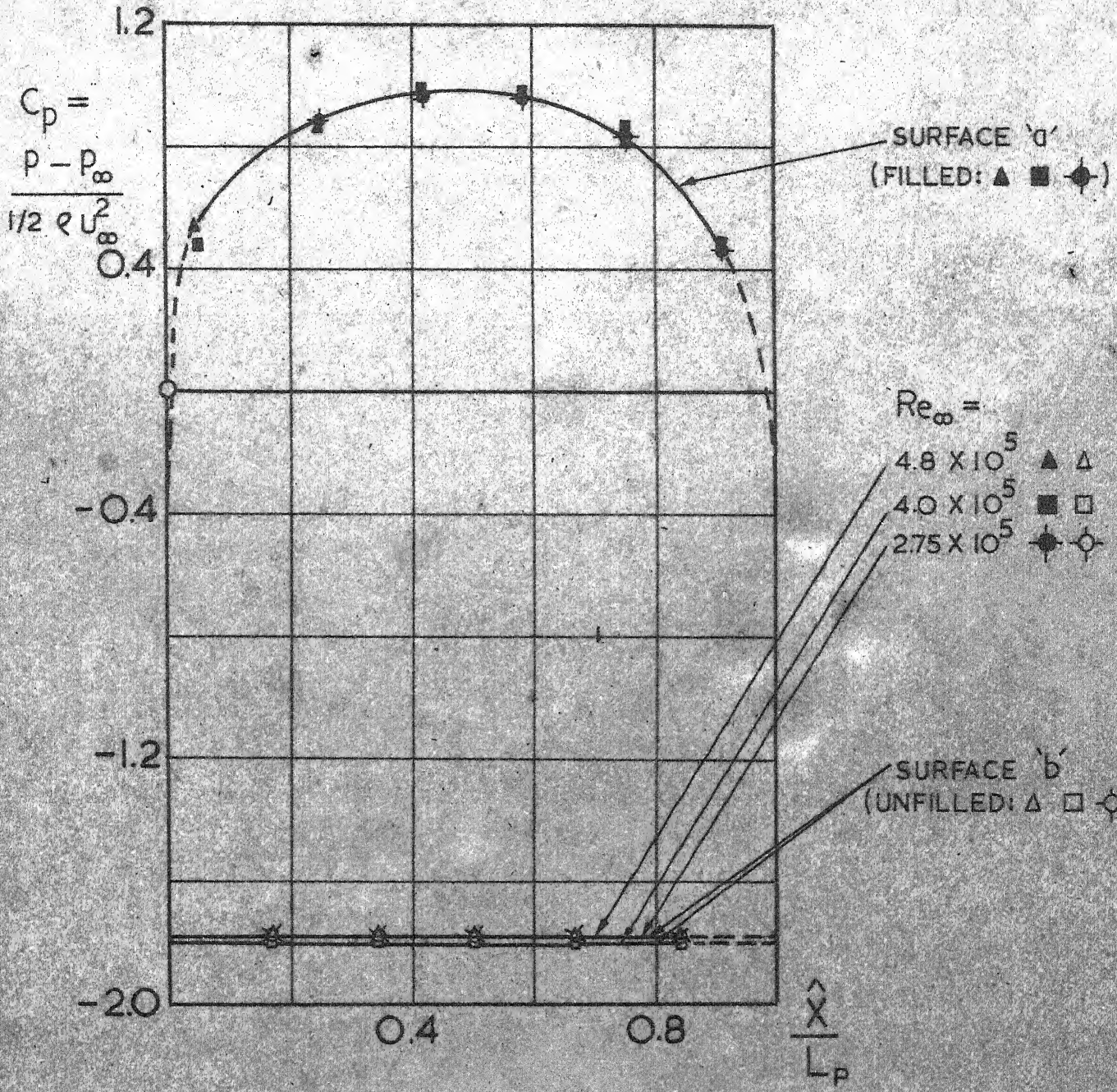

FIG. 20

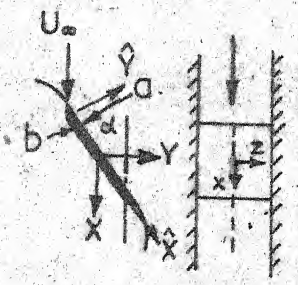

$\alpha = 60°$

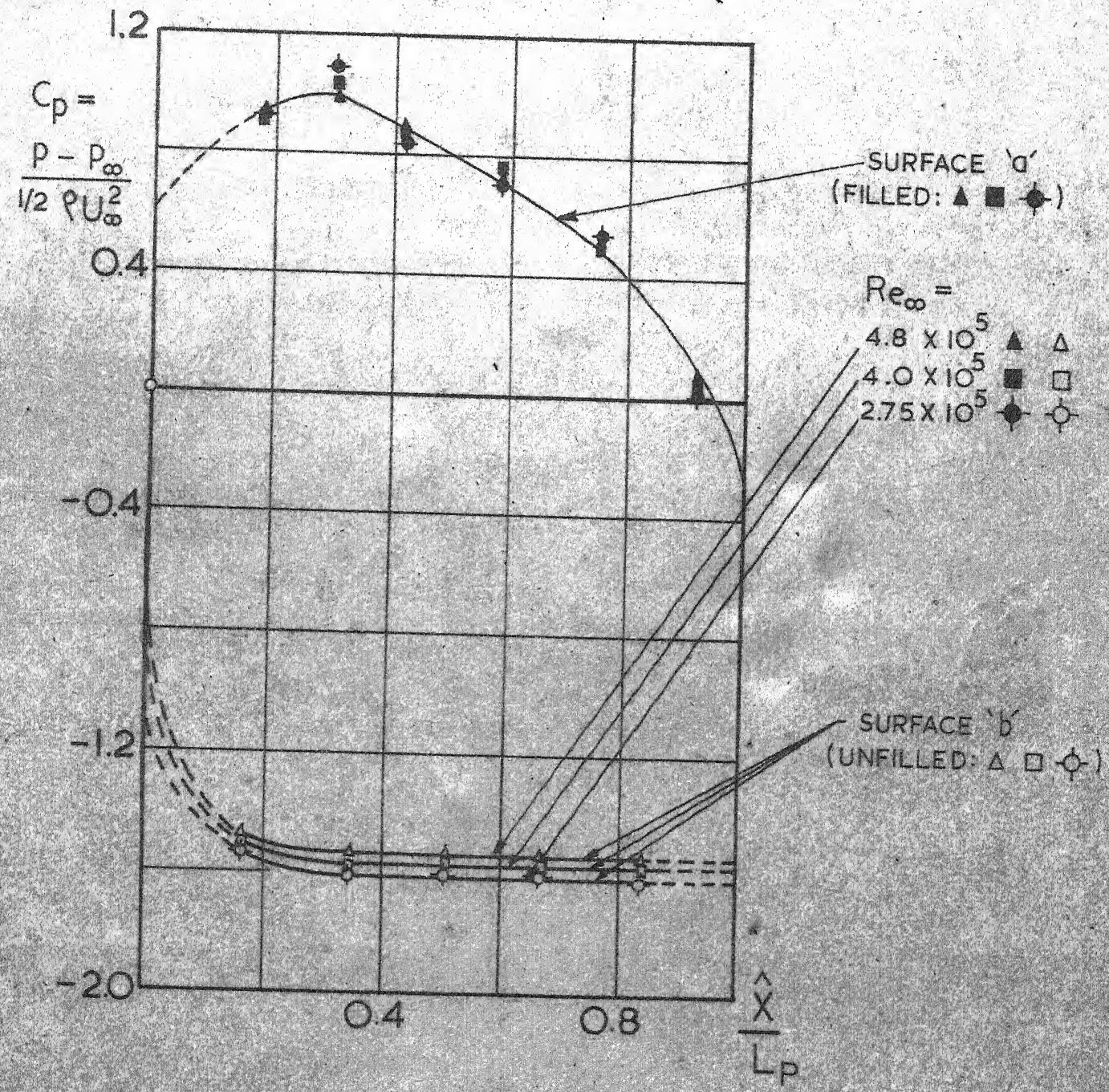

DRAWN: I S G P K M	DATE:	SQN. LDR. I. S. GUPTA	REPORT NO:

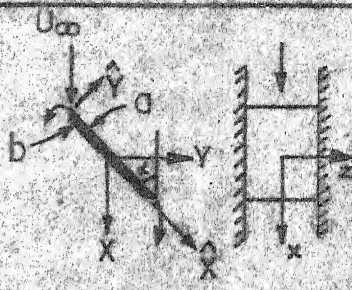

$\alpha = 45^\circ$

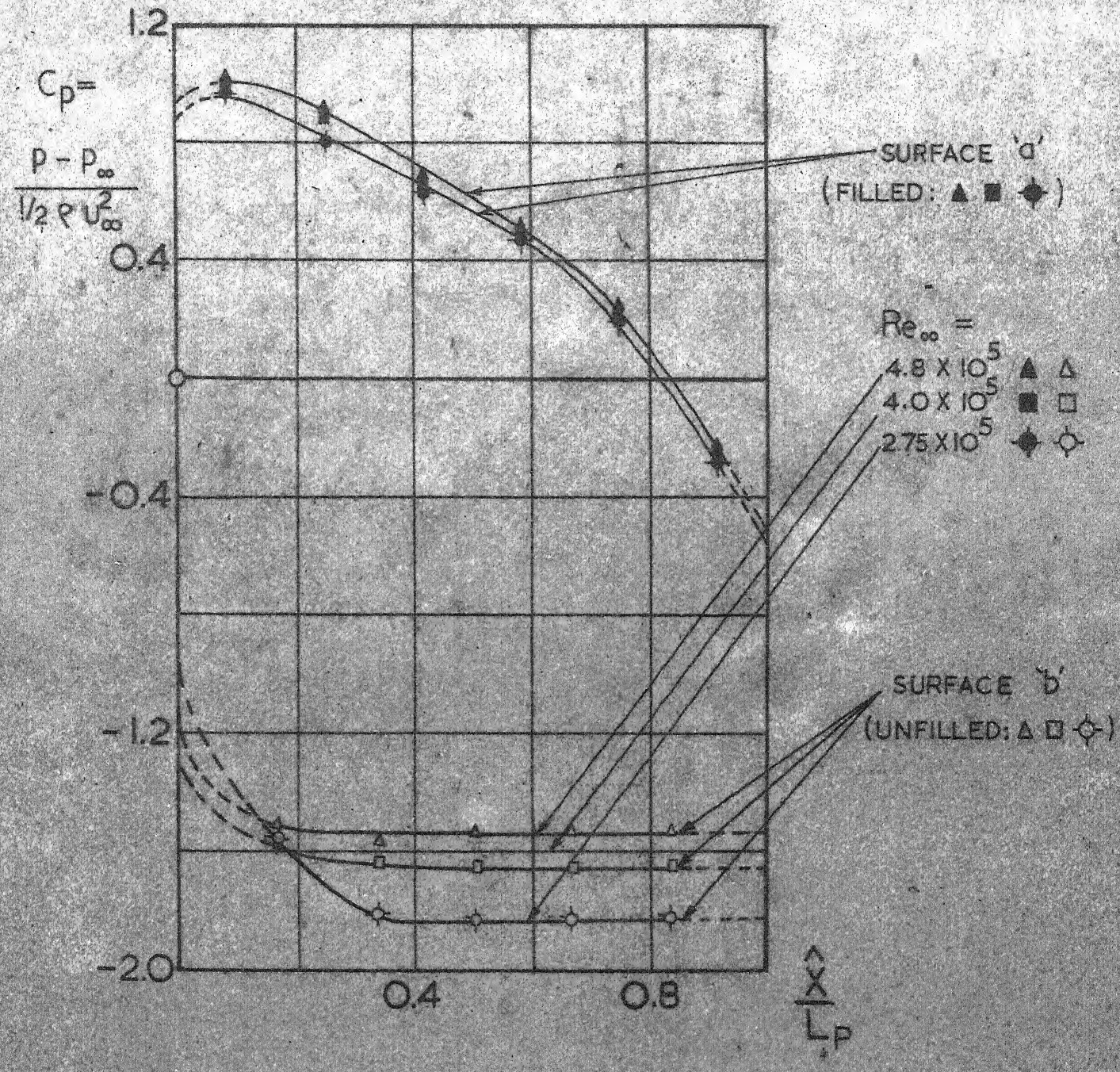

$\alpha = 30^\circ$

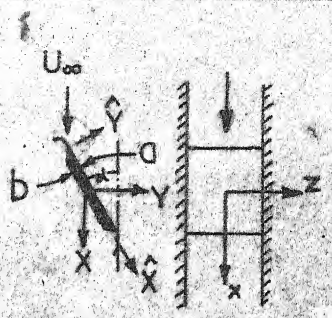

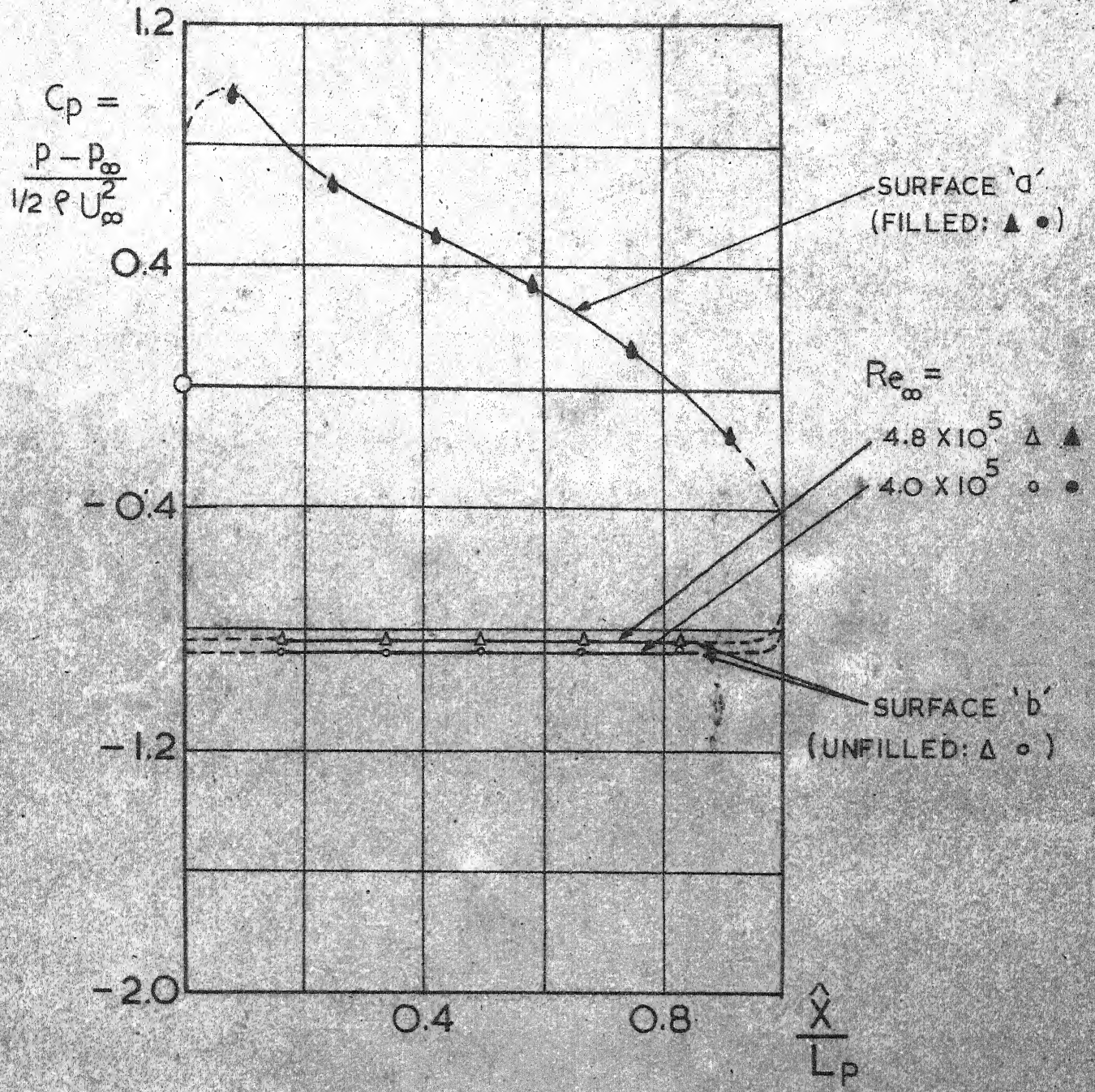

DRAWN: I.S.G R.K.M.	DATE	SQN LDR. I.S.GUPTA	REPORT NO

PRESSURE DISTRIBUTION ON NACA 66010 WITH SPLITTER PLATE FORE-MOST

FIG. 23

$\alpha = 45°$

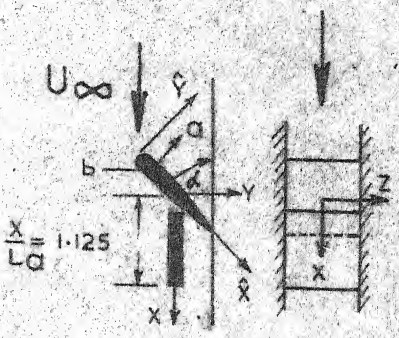

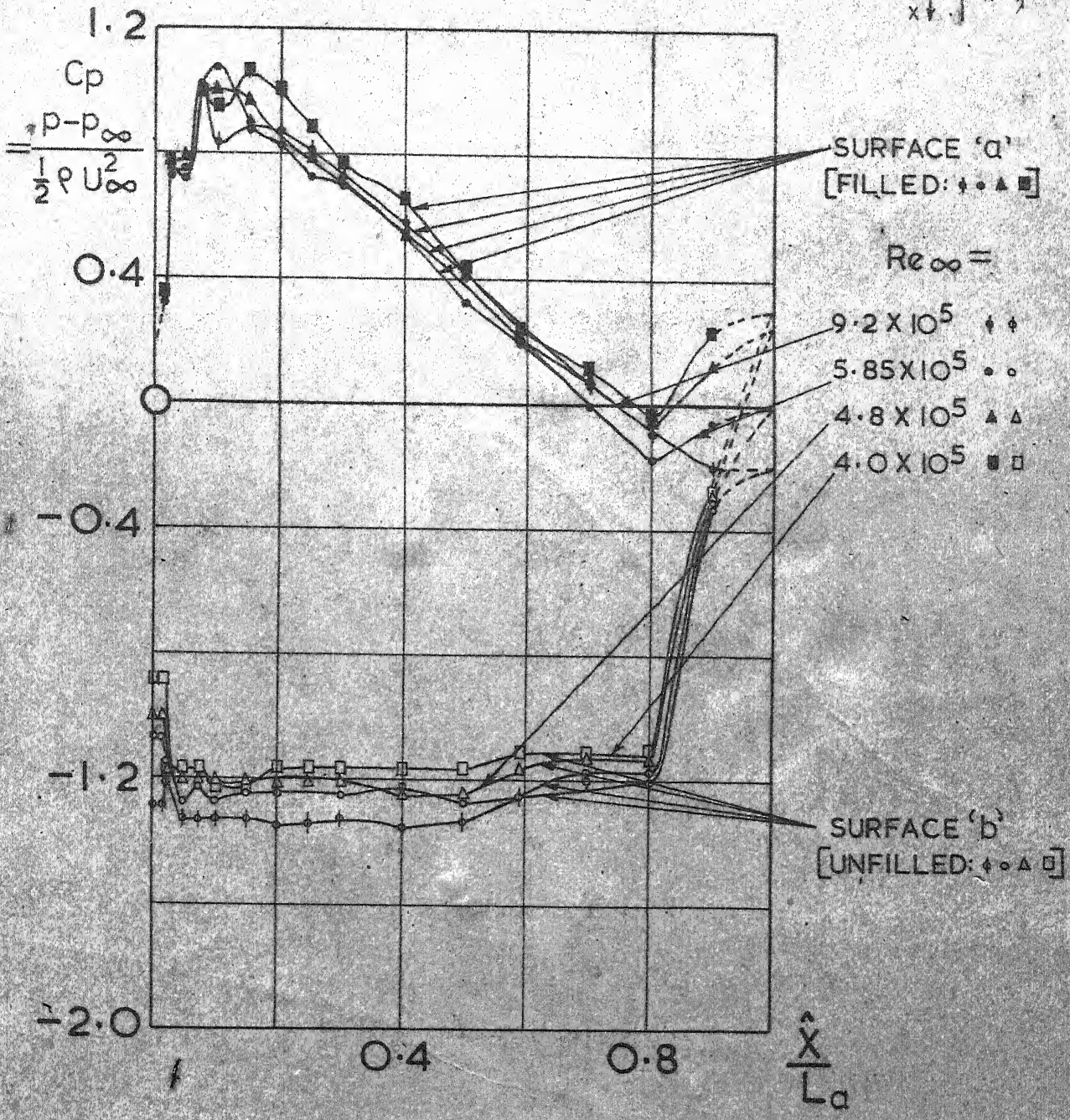

PRESSURE DISTRIBUTION ON NACA 6610 WITH SPLITTER PLATE FOREMOST

FIG·24

$\alpha = 40°$

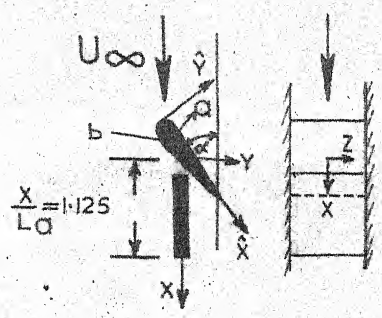

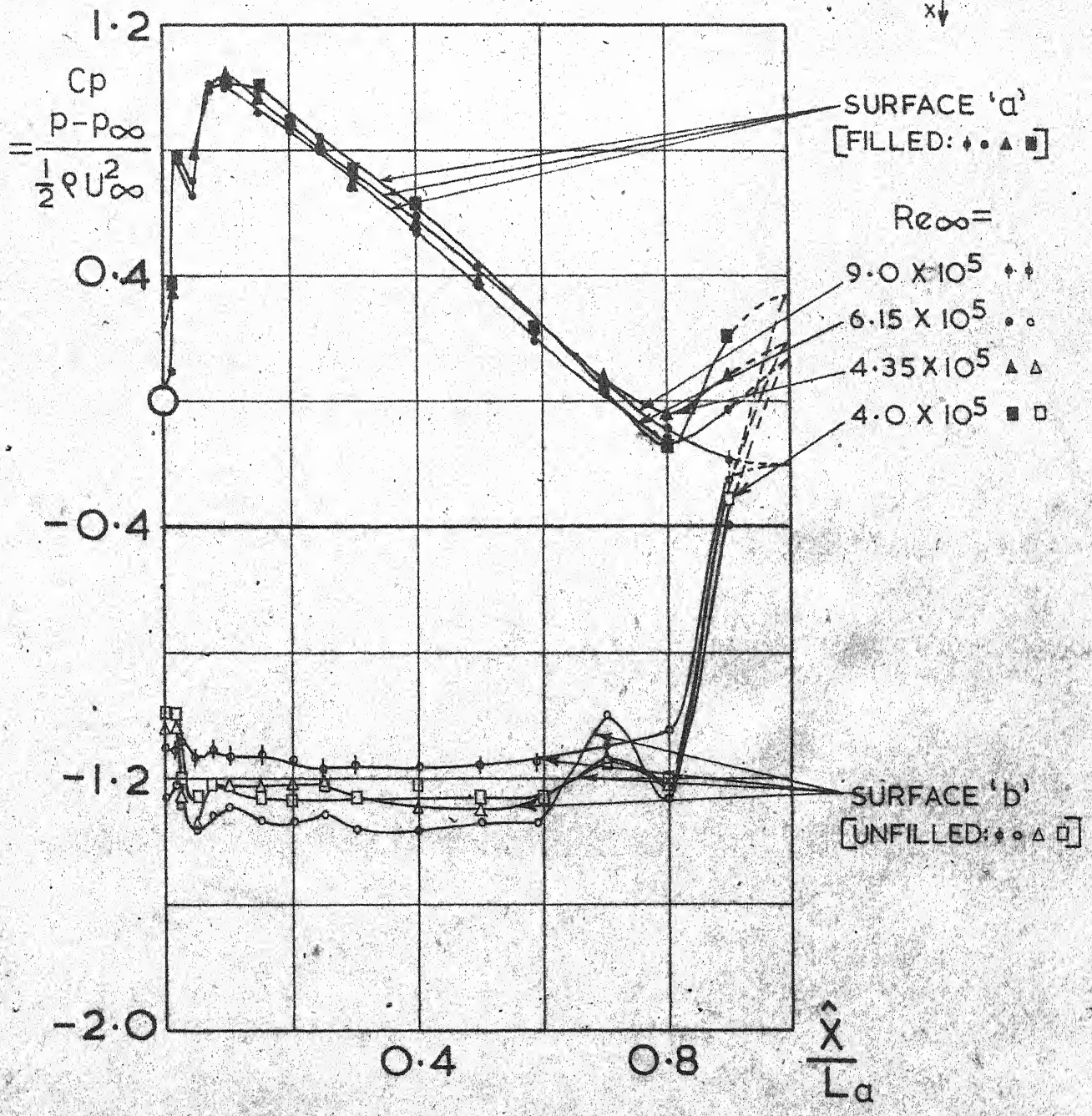

DRAWN: I.S.G.	DATE:	SQN·LDR. I.S. GUPTA	REPORT NO:

PRESSURE DISTRIBUTION ON NACA 66010 WITH SPLITTER PLATE FORE-MOST

FIG·25

$\alpha = 35^{\circ}$

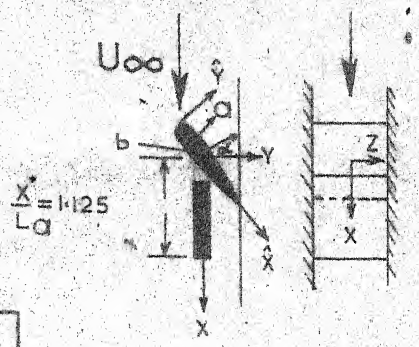

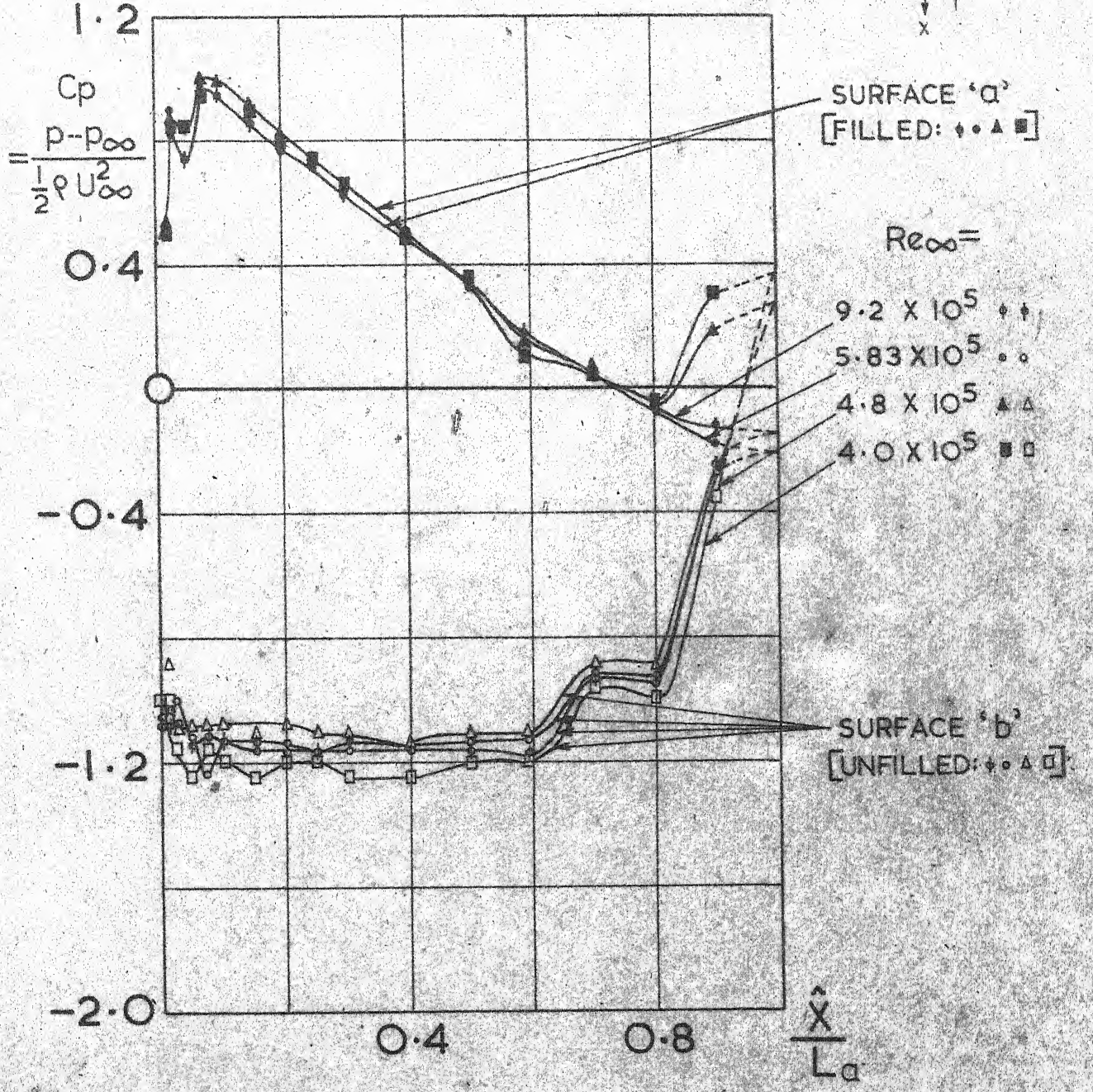

DRAWN: I.S.G.	DATE:	SQN. LDR. I.S. GUPTA	REPORT NO:

PRESSURE DISTRIBUTION ON NACA 66010 WITH SPLITTER PLATE FOREMOST

FIG·26

$\alpha = 30°$

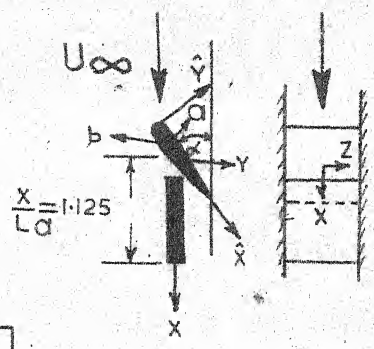

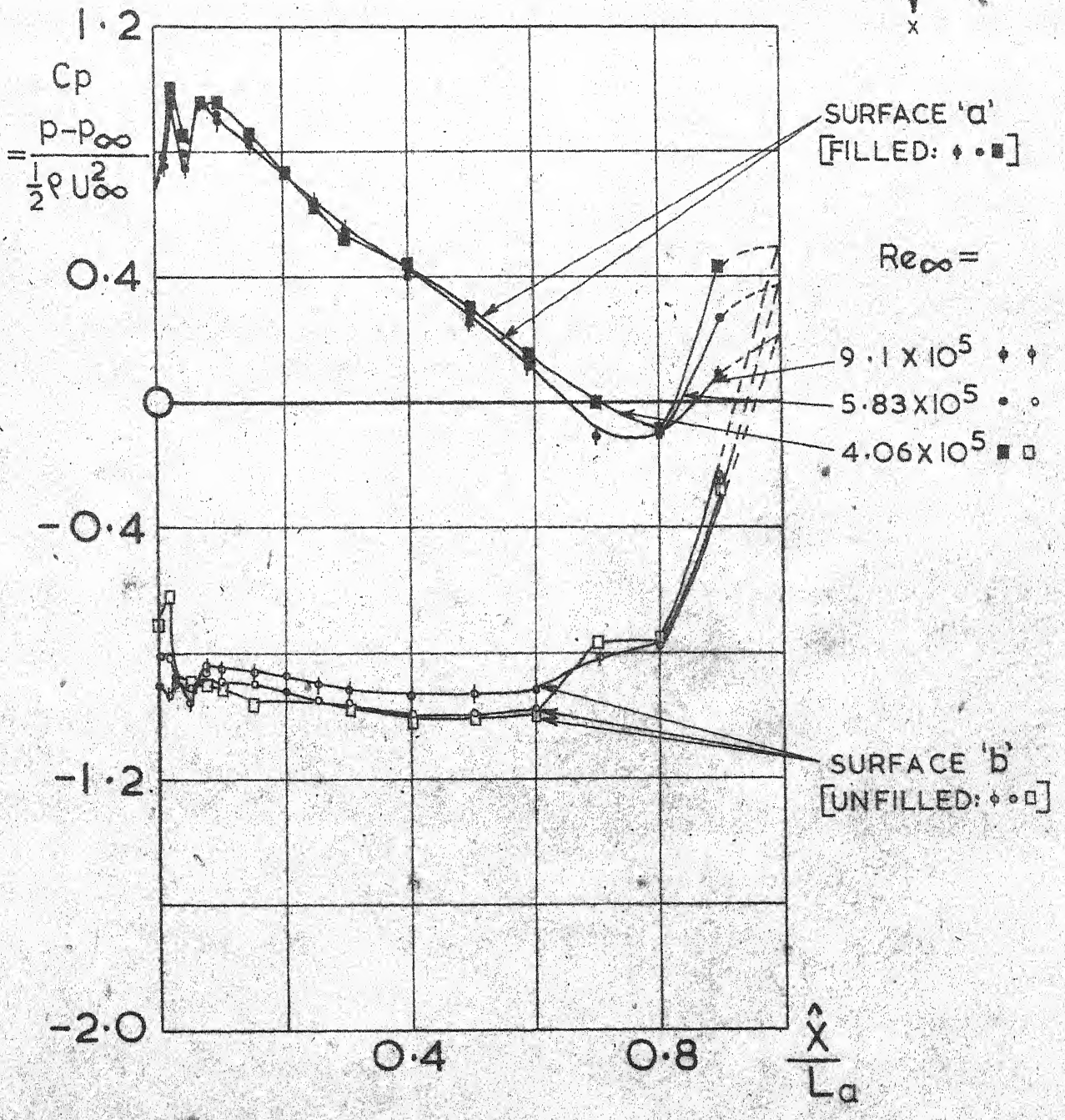

DRAWN: I.S.G.	DATE:	SQN. LDR. I.S. GUPTA	REPORT NO:

PRESSURE DISTRIBUTION ON NAÇA 66010 WITH SPLITTER PLATE FORE-MOST

FIG. 27

$\alpha = 25°$

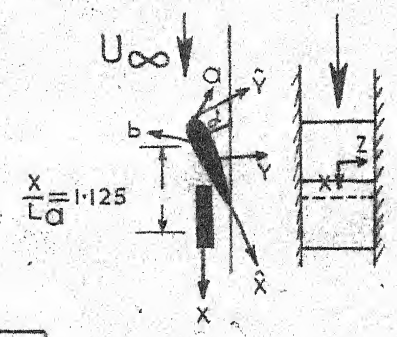

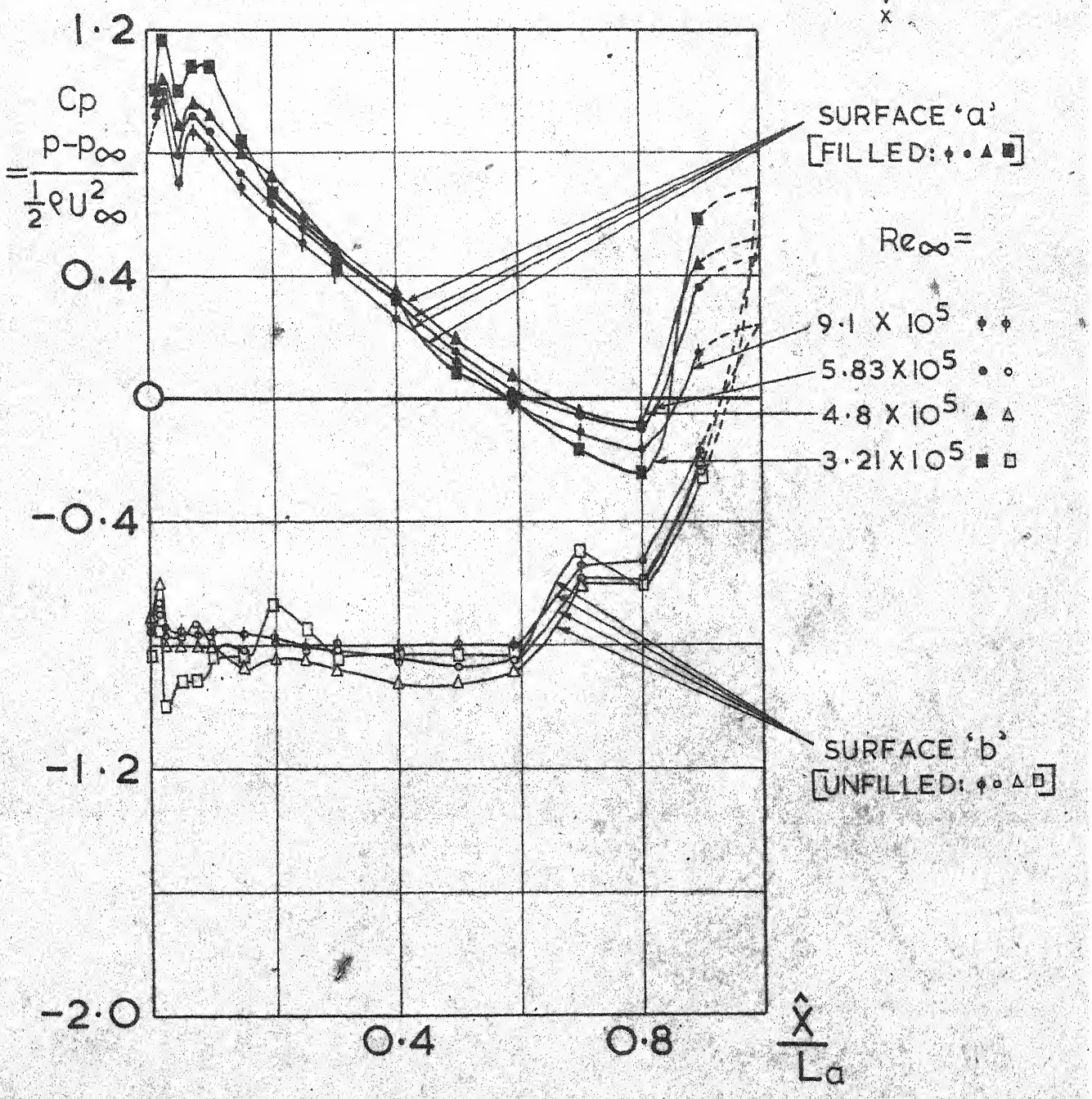

DRAWN: I.S.G.	DATE:	SQN. LDR. I. S. GUPTA	REPORT NO:

$\alpha = 20°$

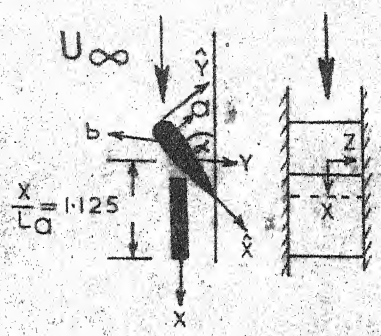
U∞
Ŷ
α
b
Y
Z
X/La = 1·125
X̂
X

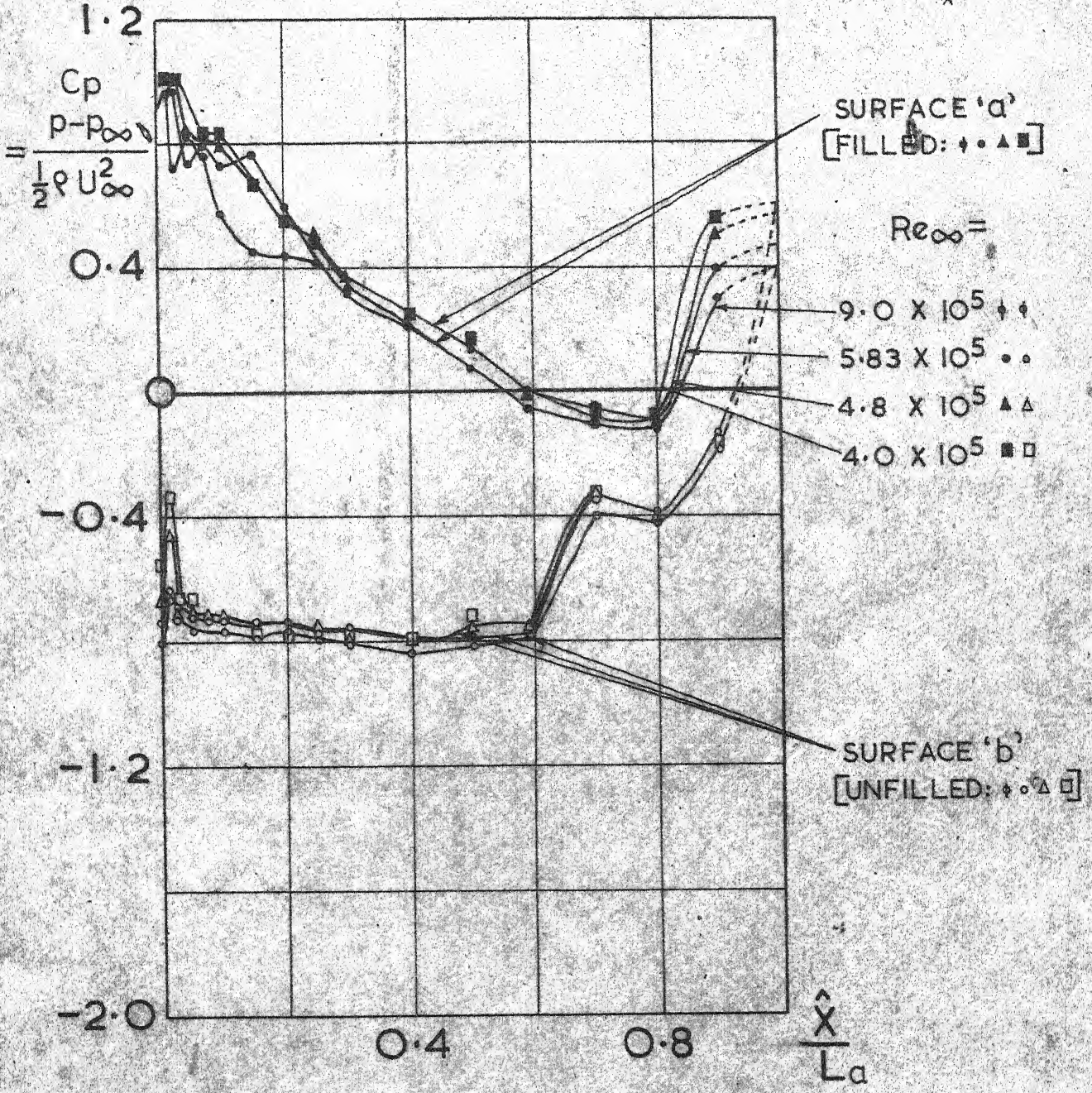
1·2
Cp = (p−p∞) / ½ρU∞²
0·4
−0·4
−1·2
−2·0
0·4
0·8
X̂/La
SURFACE 'a'
[FILLED: ♦ • ▲ ■]
Re∞ =
9·0 X 10⁵ ♦ ◊
5·83 X 10⁵ • ∘
4·8 X 10⁵ ▲ △
4·0 X 10⁵ ■ □
SURFACE 'b'
[UNFILLED: ◊ ∘ △ □]

PRESSURE DISTRIBUTION ON NACA 66010 WITH SPLITTER PLATE REARMOST

FIG.29

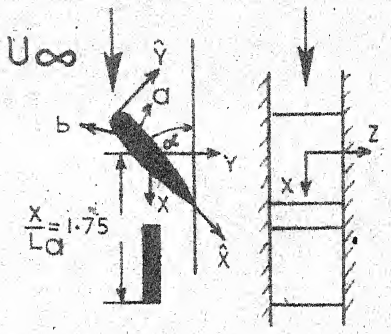

$\alpha = 45^\circ$

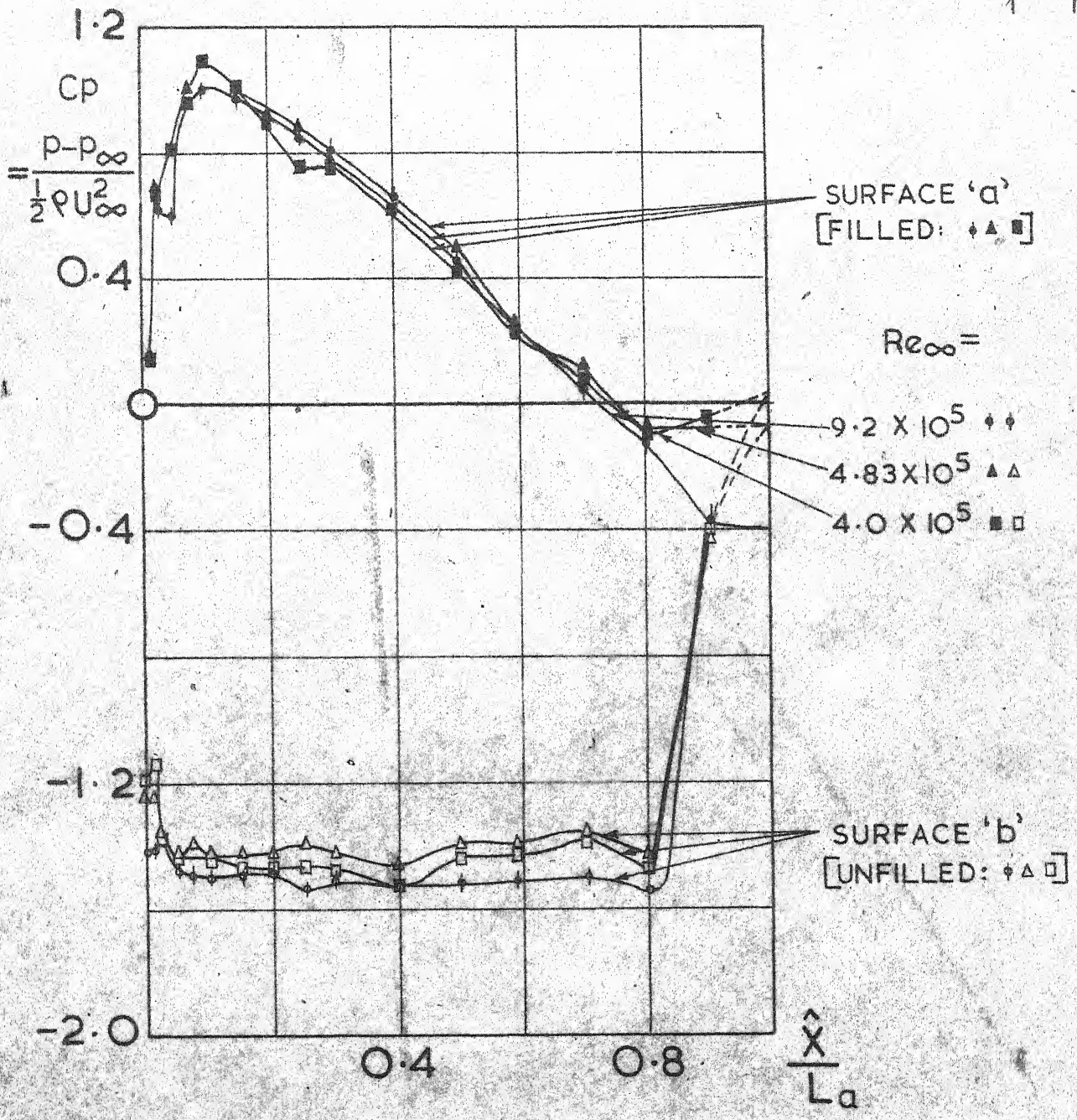

DRAWN: I.S.G.	DATE:	SQN. LDR. I.S.GUPTA	REPORT NO:

PRESSURE DISTRIBUTION ON NACA 6601O WITH SPLITTER PLATE REARMOST

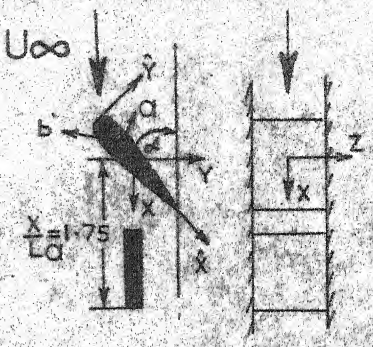

$\alpha = 40°$

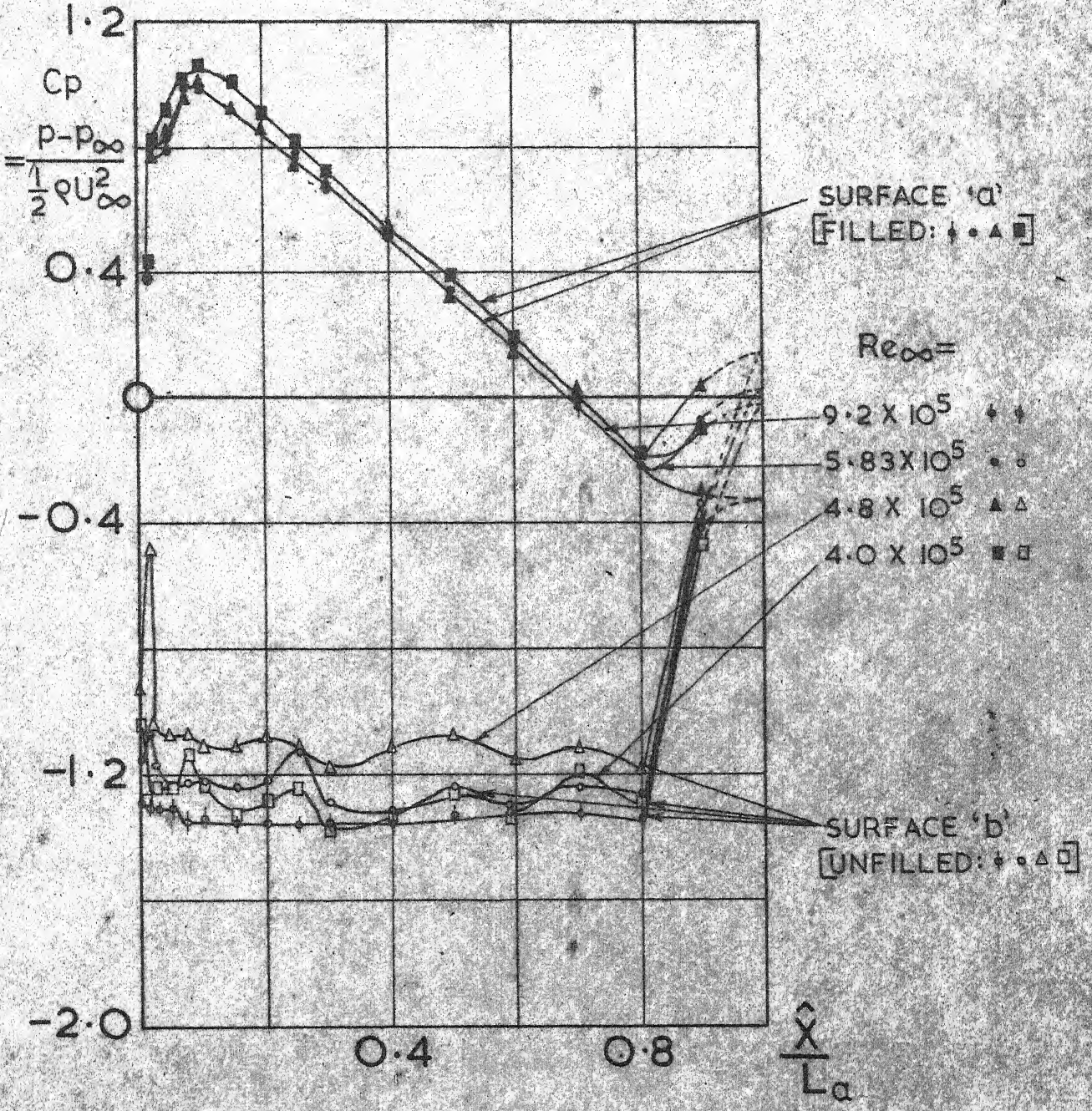

PRESSURE DISTRIBUTION ON NACA 66010 WITH SPLITTER PLATE REARMOST

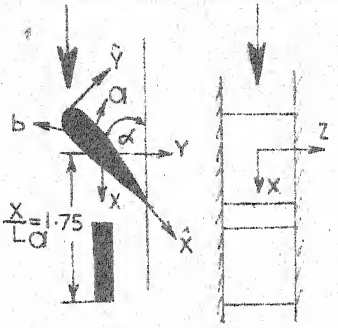

$\alpha = 35°$

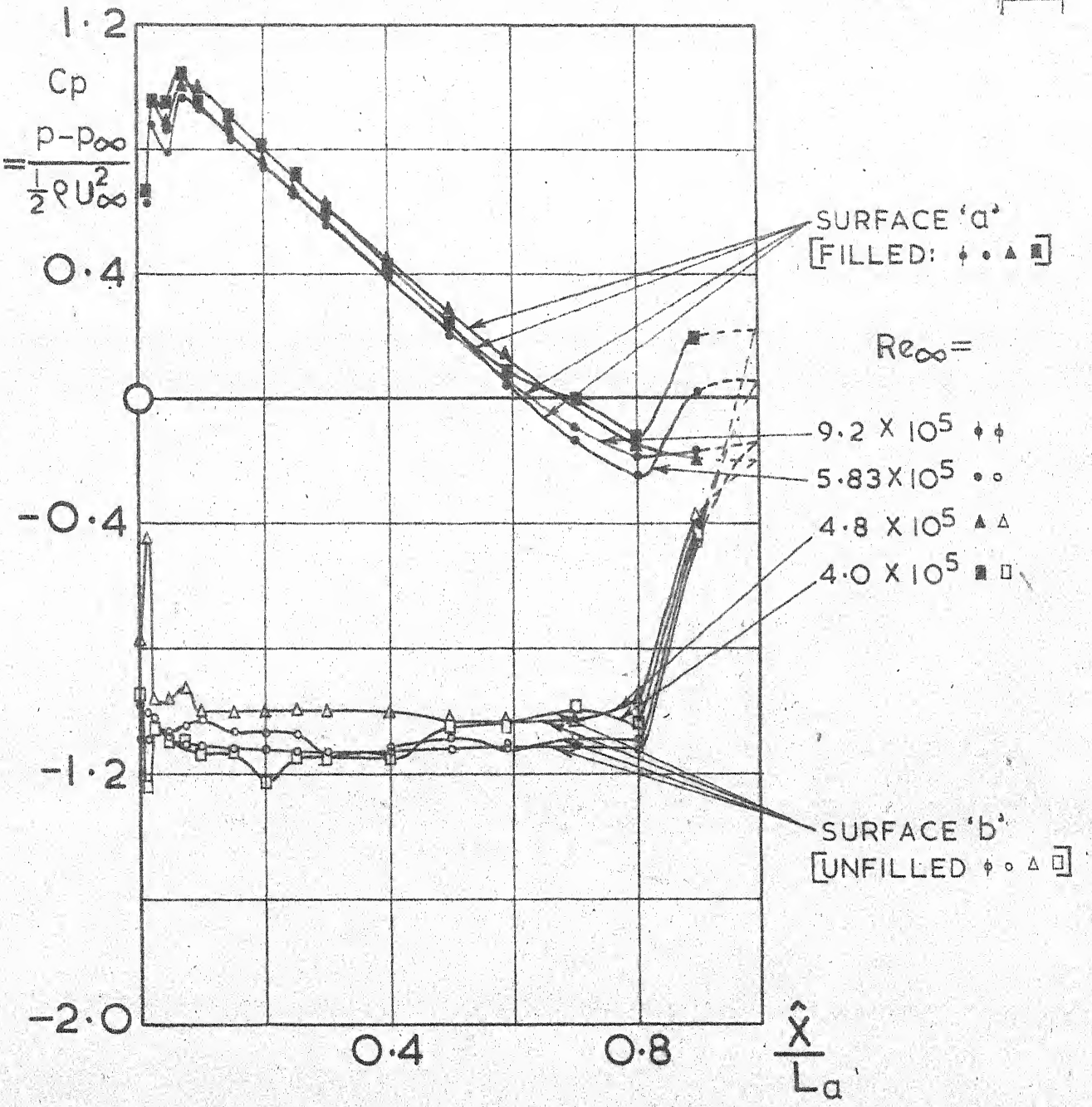

PRESSURE DISTRIBUTION ON NACA 66010 WITH SPLITTER PLATE REARMOST

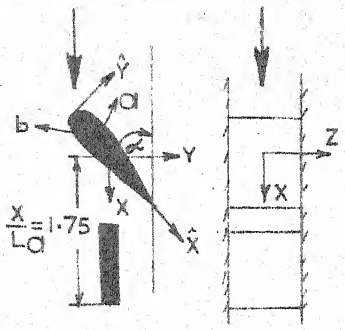

$\alpha = 30°$

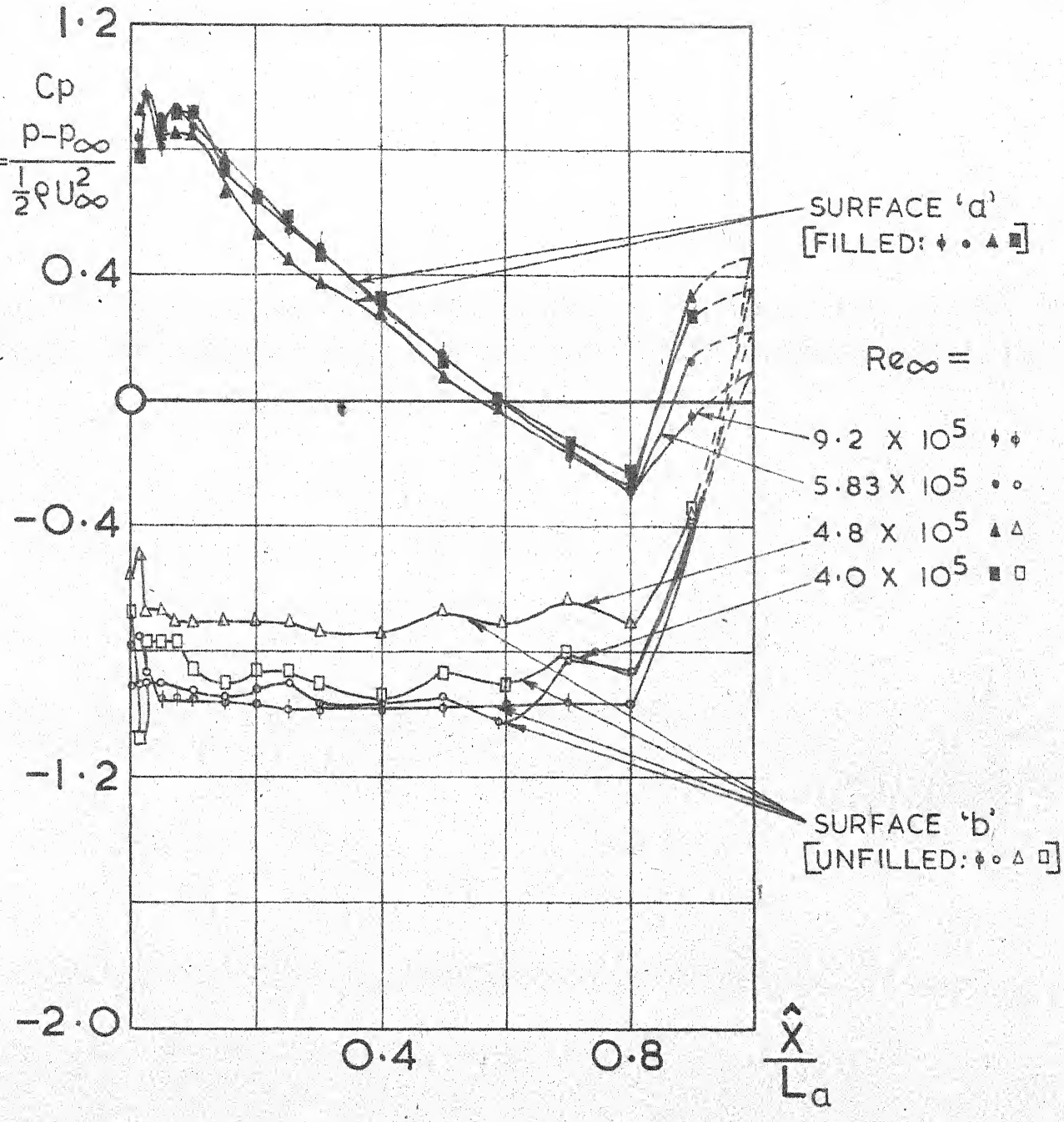

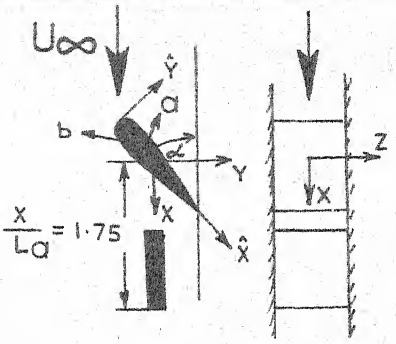

$\alpha = 25^\circ$

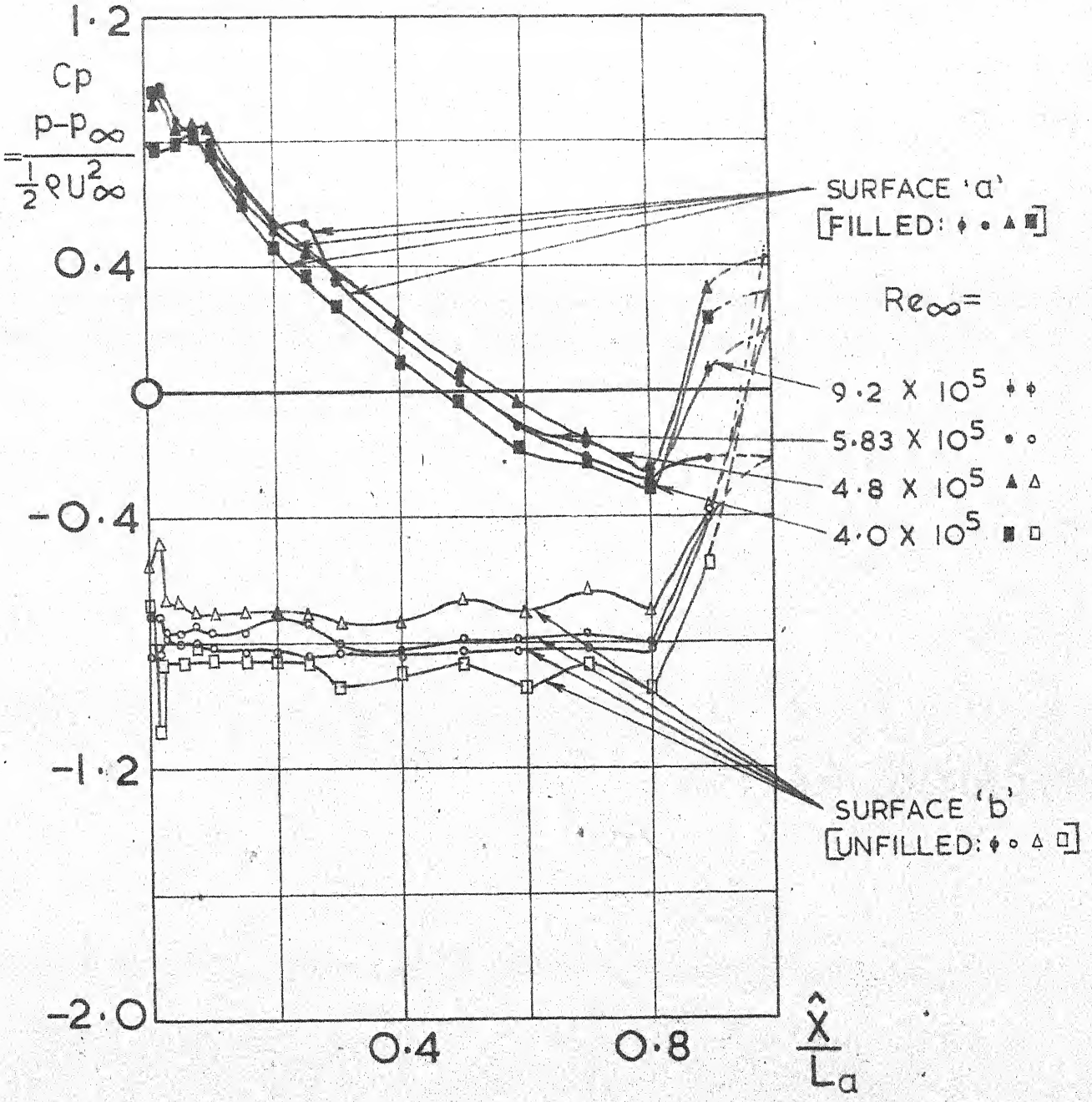

DRAWN: I. S. G.	DATE:	SQN. LDR. I. S. GUPTA	REPORT NO:

PRESSURE DISTRIBUTION ON NACA 66010 WITH SPLITTER PLATE REARMOST

FIG·34

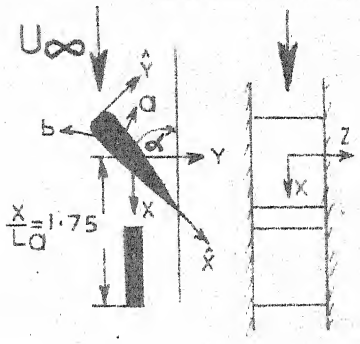

$\alpha = 20°$

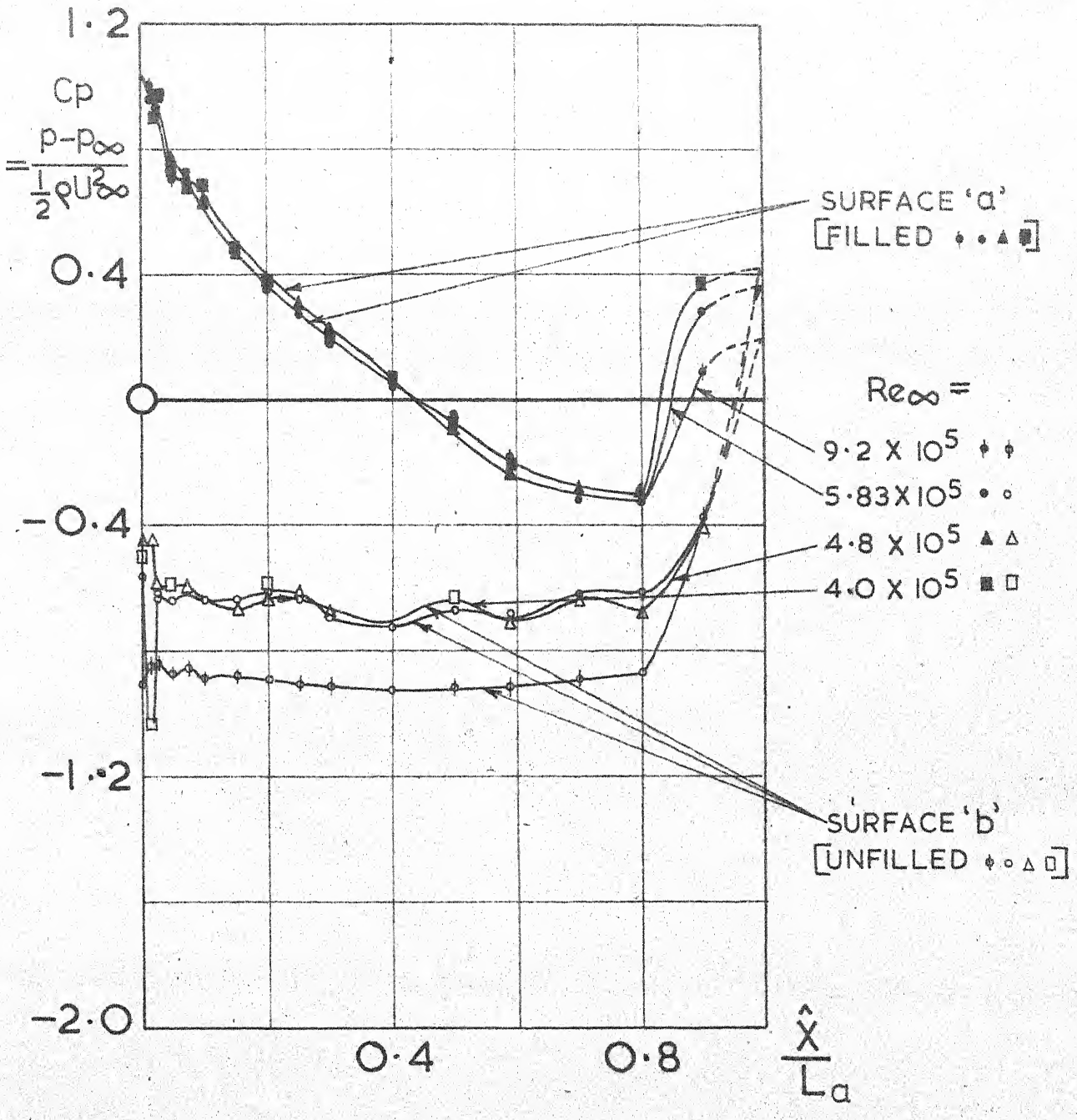

DRAWN: I.S.G. | DATE: | SQN. LDR. I.S. GUPTA | REPORT NO:

PRESSURE DISTRIBUTION ON FLAT PLATE WITH SPLITTER PLATE FOREMOST

FIG. 35

$\alpha = 90°$

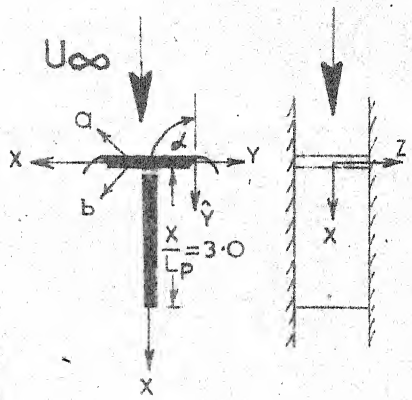

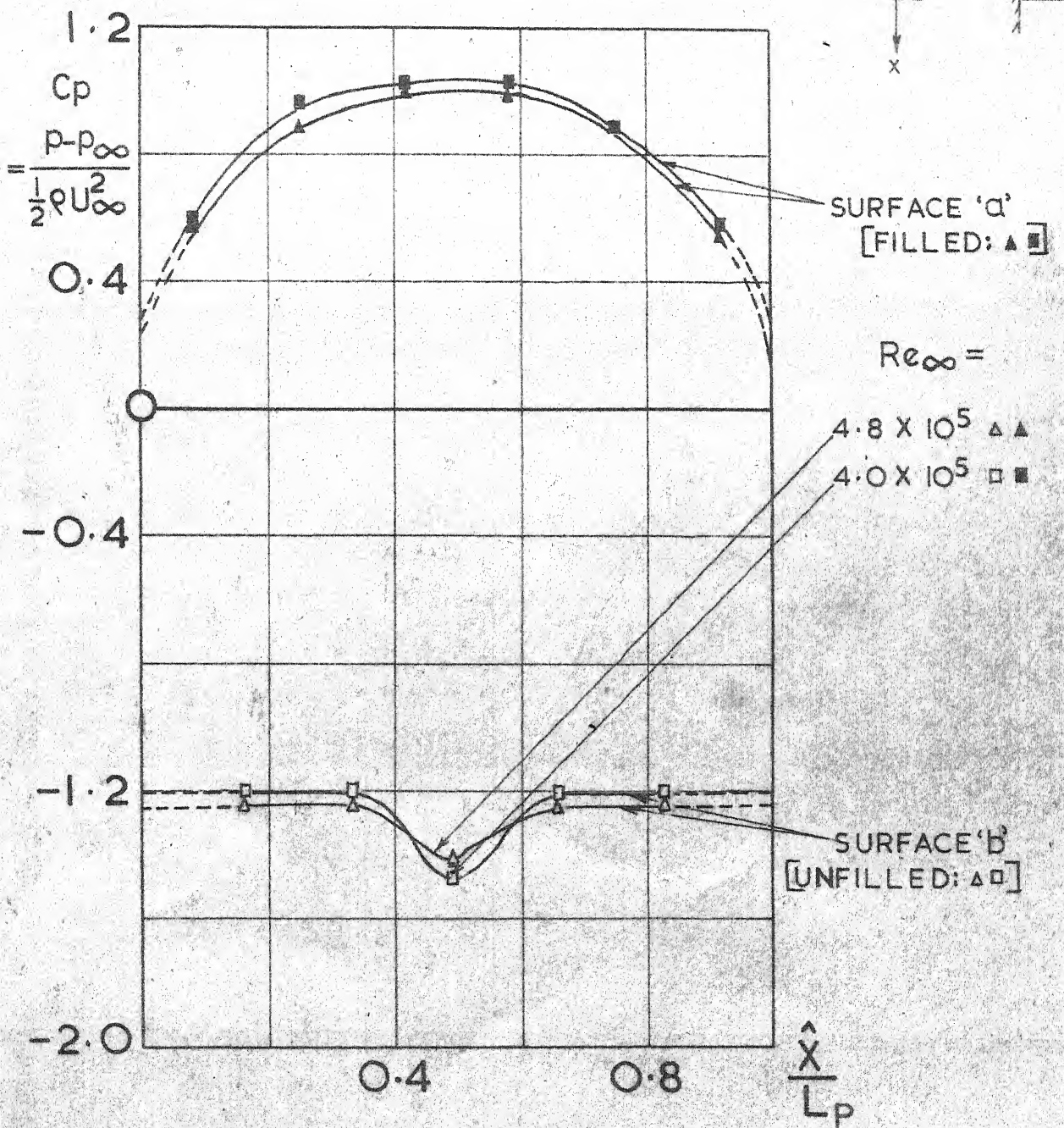

DRAWN: I.S.G.	DATE:	SQN. LDR. I.S. GUPTA	REPORT NO:

PRESSURE DISTRIBUTION ON FLAT PLATE WITH SPLITTER PLATE FOREMOST

FIG. 36

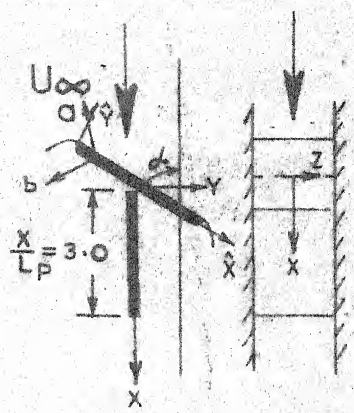

$\alpha = 60°$

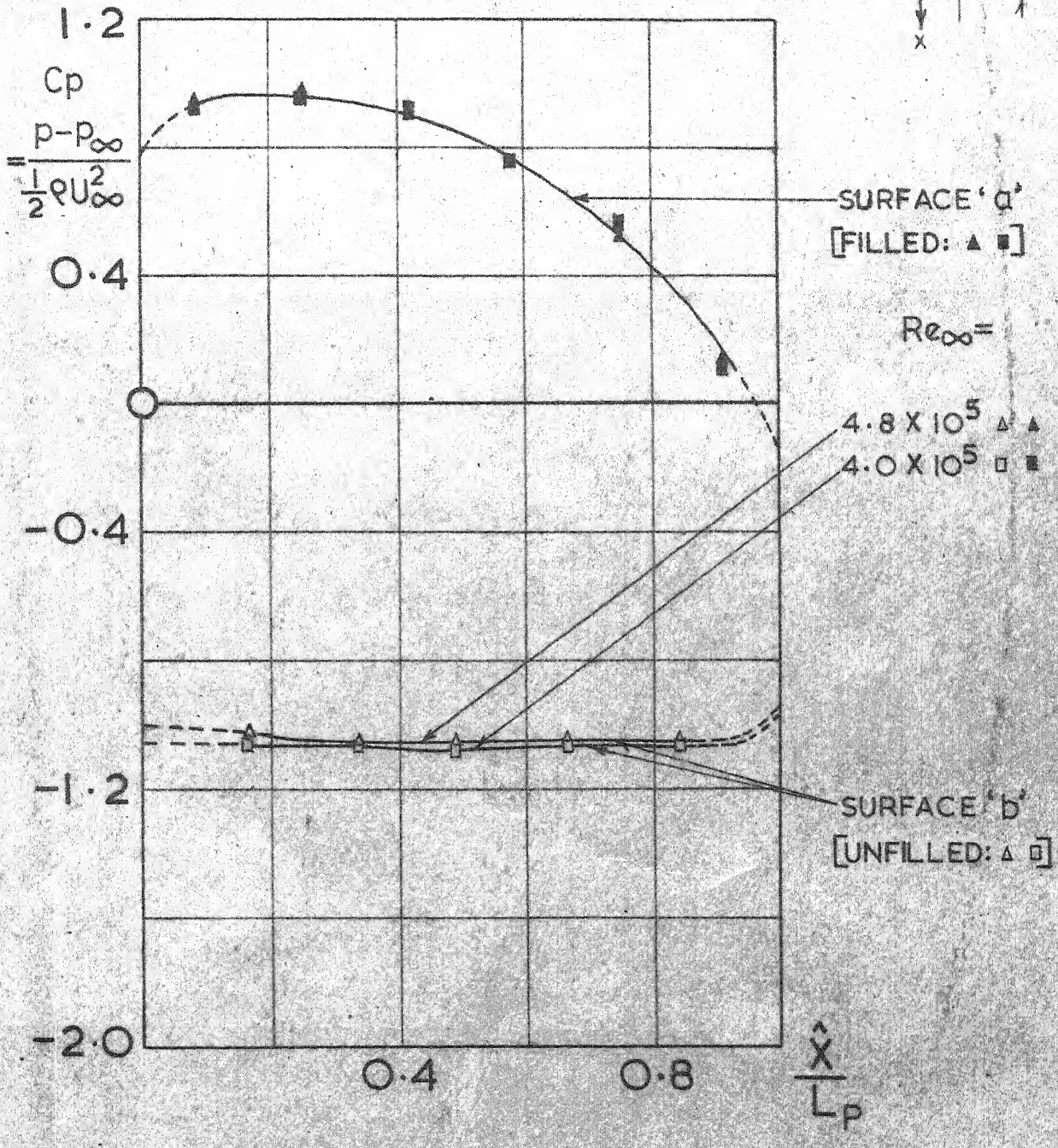

DRAWN: I.S.G.	DATE:	SQN. LDR. I.S.GUPTA	REPORT NO:

DEPT. OF AERO ENGG.

PRESSURE DISTRIBUTION ON FLAT PLATE WITH SPLITTER PLATE FOREMOST

FIG. 37

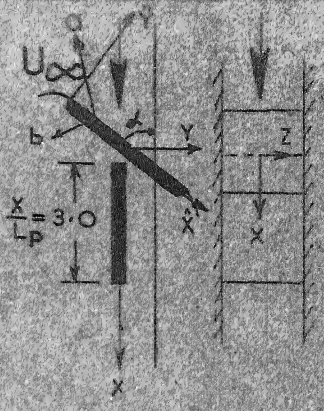

$\alpha = 45^\circ$

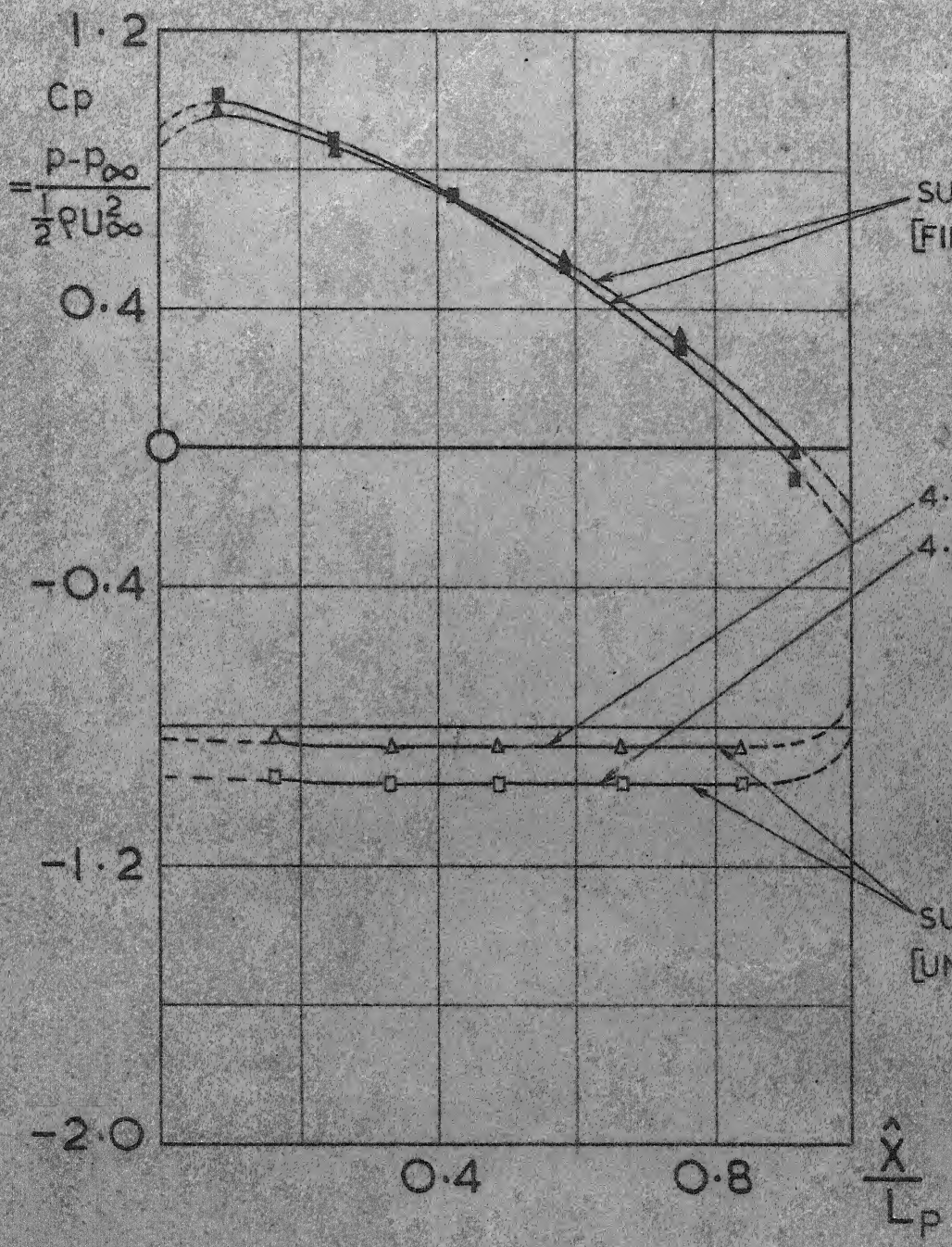

DRAWN: I.S.G.	DATE:	SQN. LDR. I.S. GUPTA	REPORT NO:

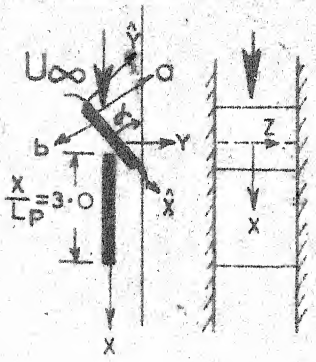
U_∞
a
b
Y
Z
X
$\frac{X}{L_P}=3.0$
$\hat{Y}$
$\hat{X}$
X

$\alpha = 30°$

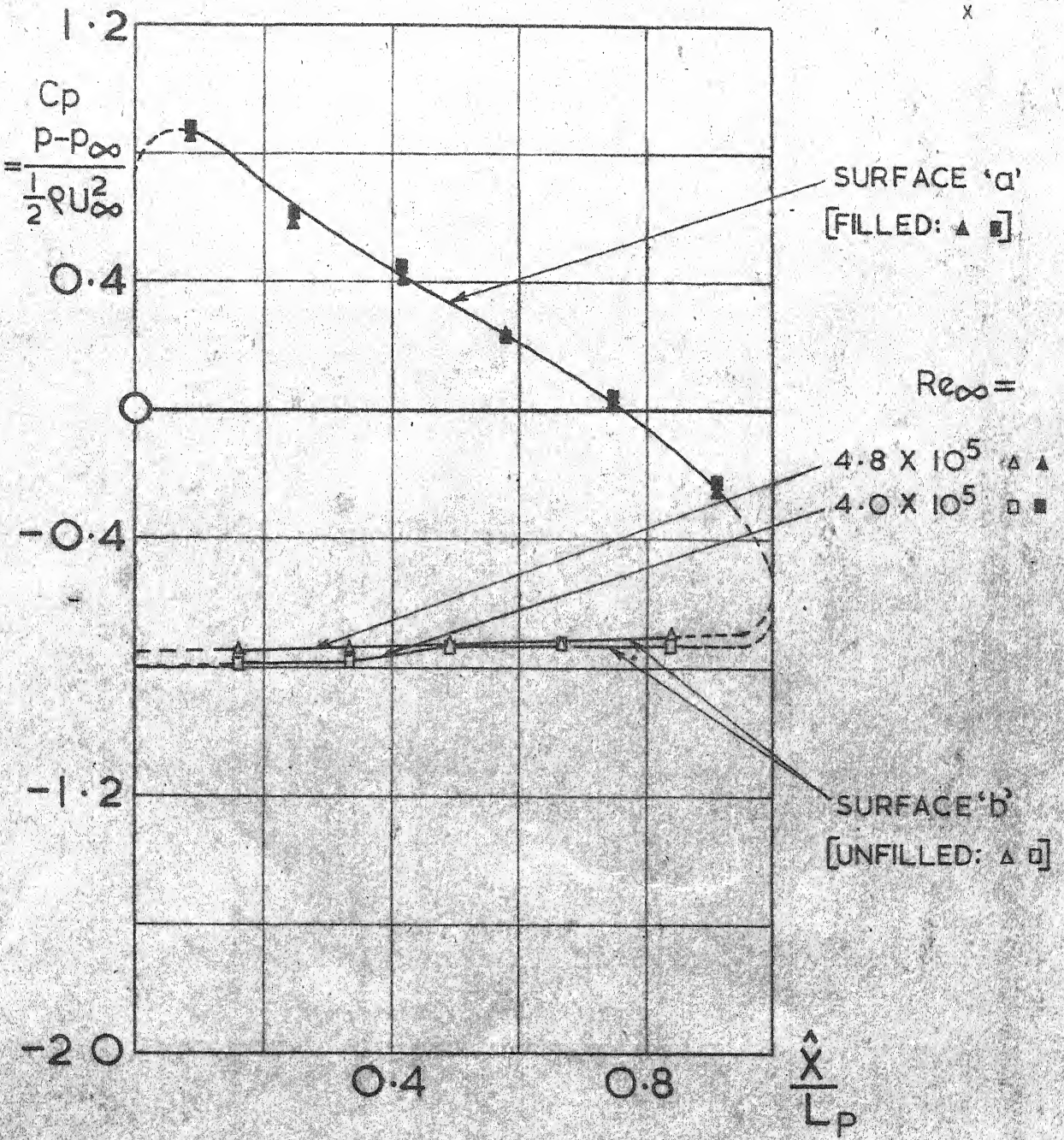
1·2
Cp
$=\frac{p-p_\infty}{\frac{1}{2}\rho U_\infty^2}$
0·4
-0·4
-1·2
-2 0
0·4
0·8
$\frac{\hat{X}}{L_P}$
SURFACE 'a'
[FILLED: ▲ ■]
$Re_\infty =$
4·8 X 10⁵ △ ▲
4·0 X 10⁵ □ ■
SURFACE 'b'
[UNFILLED: △ □]

$\alpha = 90°$

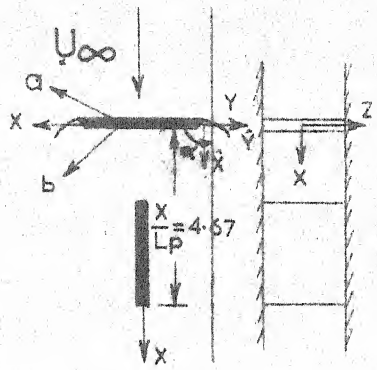
U∞
a
b
X
Y
Z
X
X/Lp = 4.67
X

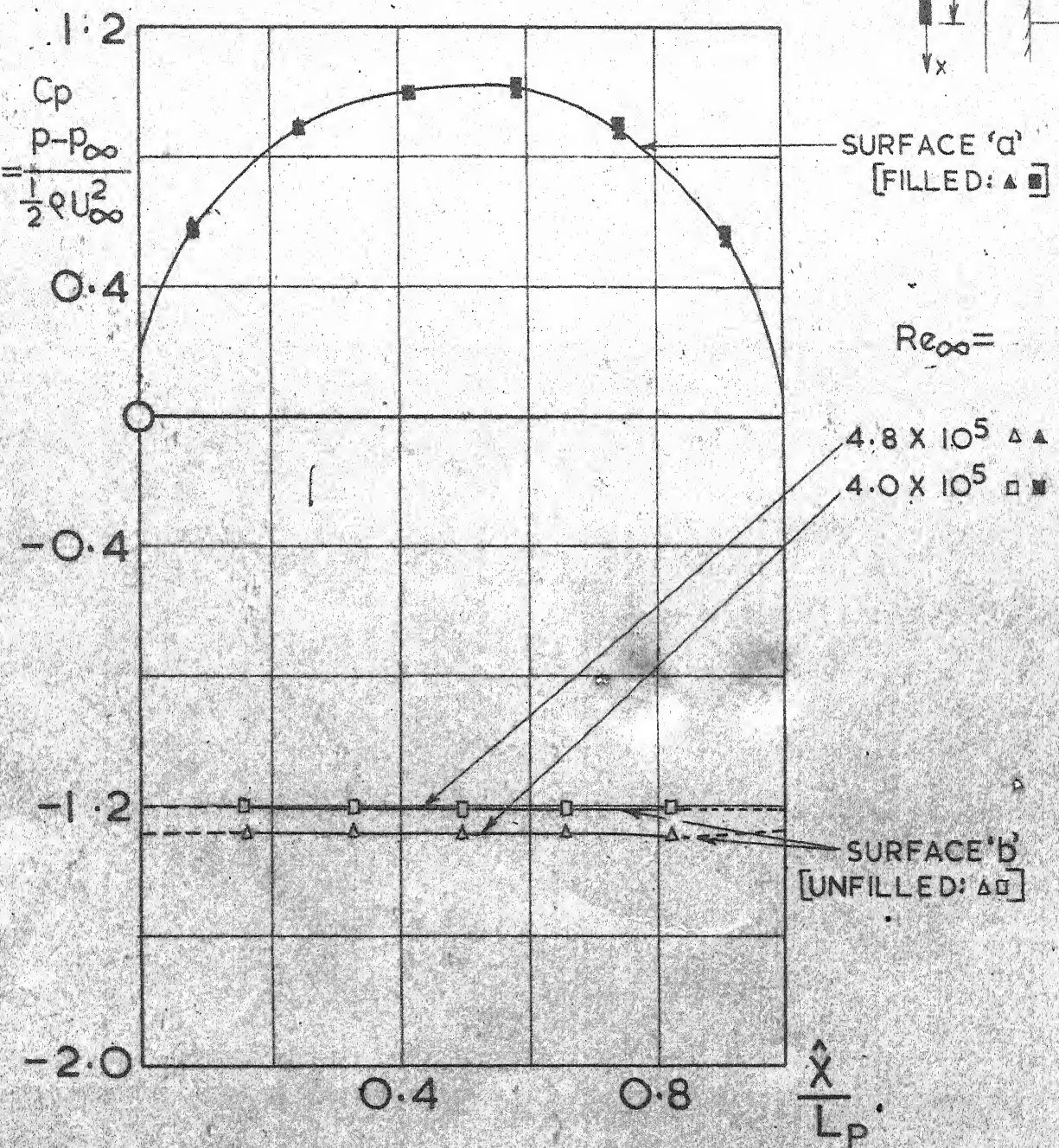
1·2
Cp
p-p∞
=
½ρU∞²
0·4
-0·4
-1·2
-2·0
0·4
0·8
X̂/Lp
SURFACE 'a'
[FILLED: ▲ ■]
Re∞=
4·8 X 10⁵ △ ▲
4·0 X 10⁵ □ ■
SURFACE 'b'
[UNFILLED: △ □]

DEPT. OF AERO ENGG	PRESSURE DISTRIBUTION ON FLAT PLATE WITH SPLITTER PLATE REARMOST.	PAGE NO: 65
		FIG·40

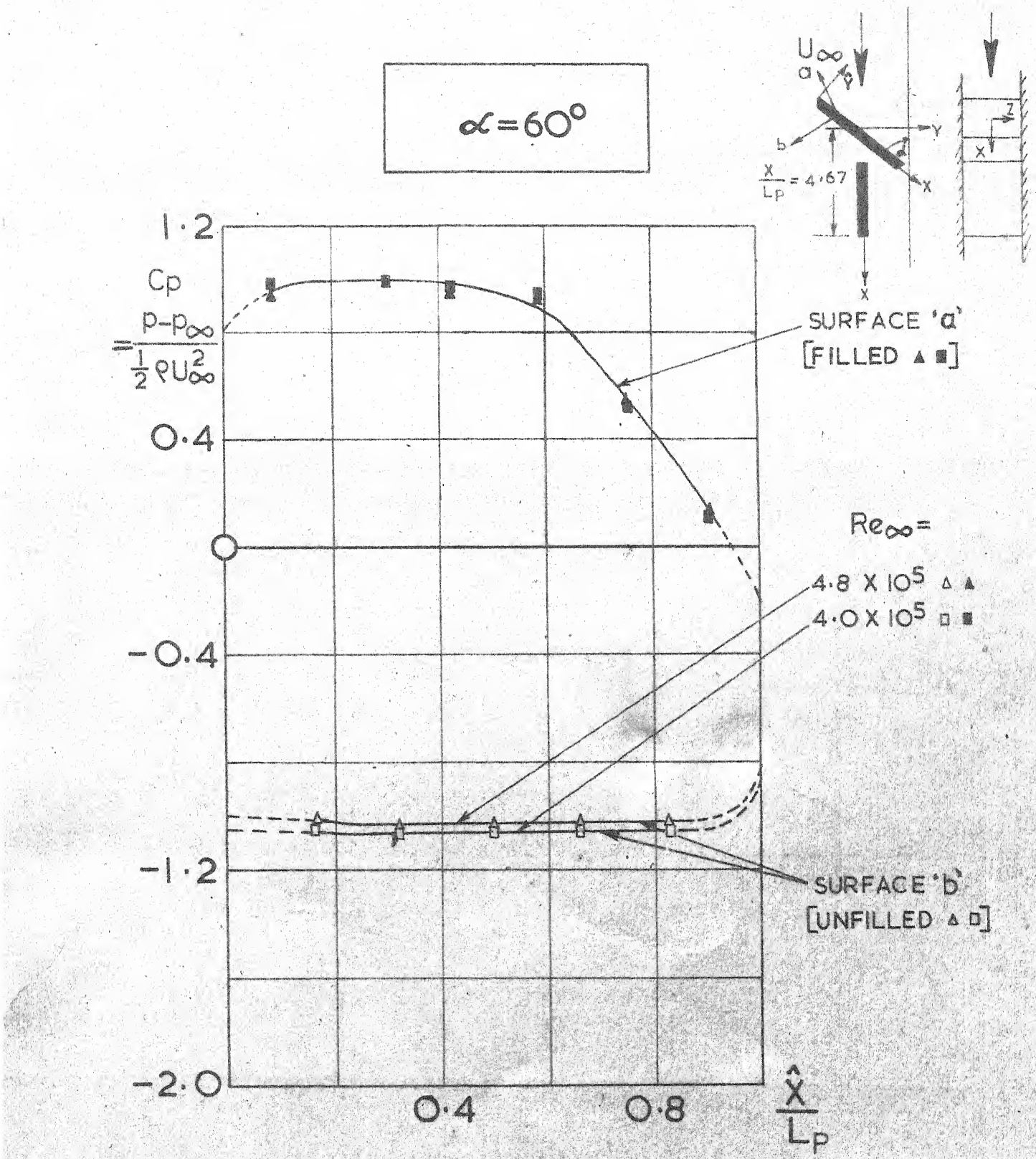

DRAWN: I.S.G.	DATE:	SQN. LDR. I.S. GUPTA	REPORT NO:

PRESSURE DISTRIBUTION ON FLAT PLATE WITH SPLITTER PLATE REARMOST

FIG·41

$\alpha = 45°$

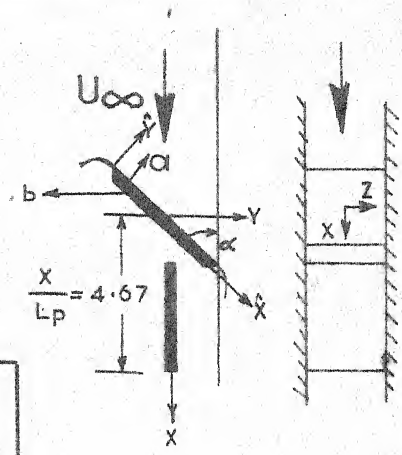

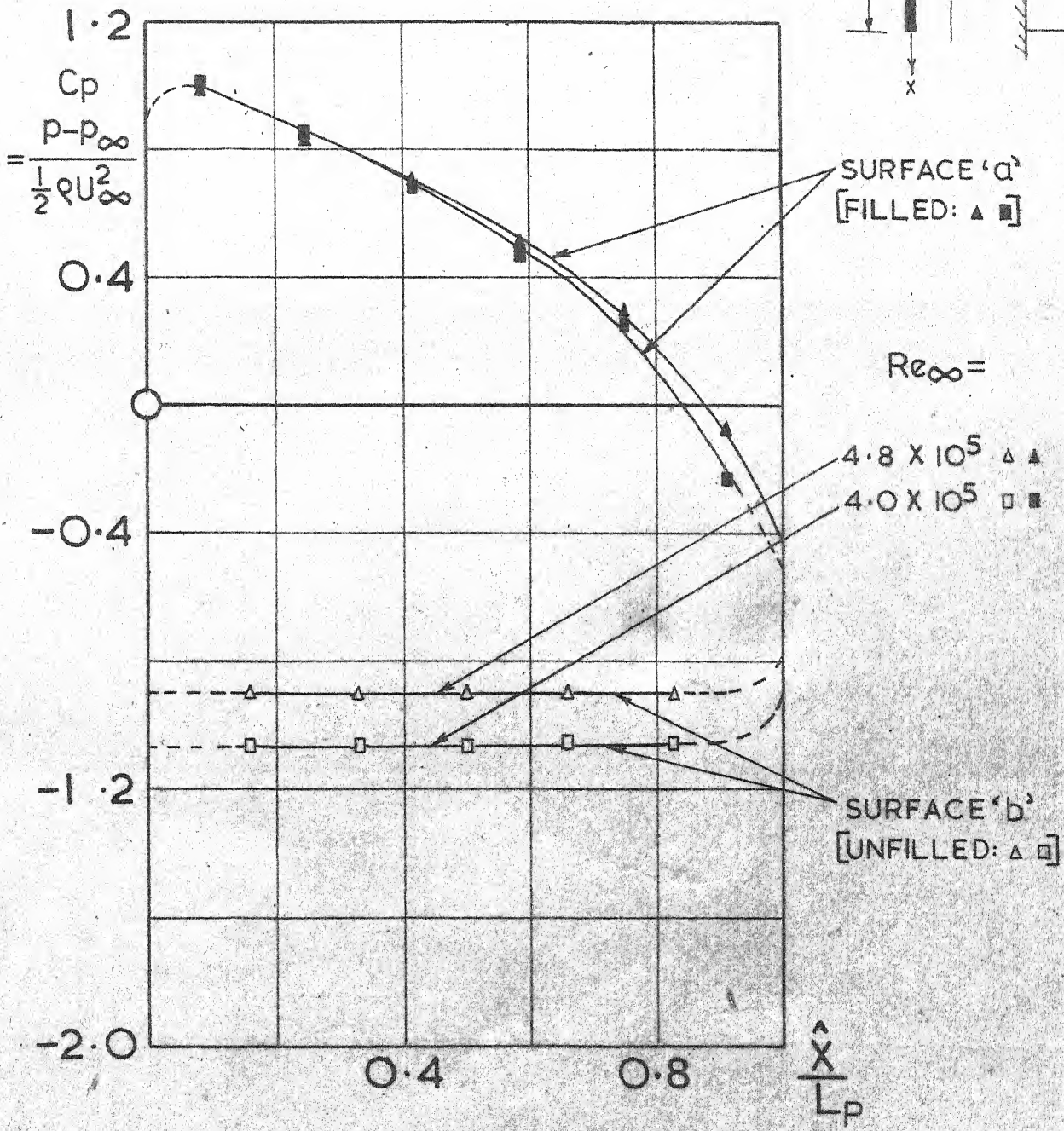

DRAWN: I.S.G.	DATE:	SQN.LDR.I.S.GUPTA	REPORT NO:

DEPT. OF AERO ENGG	PRESSURE DISTRIBUTION ON FLAT PLATE WITH SPLITTER PLATE REARMOST	PAGE NO: 67
		FIG. 42

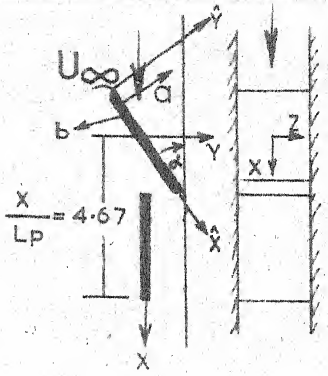

$\alpha = 30°$

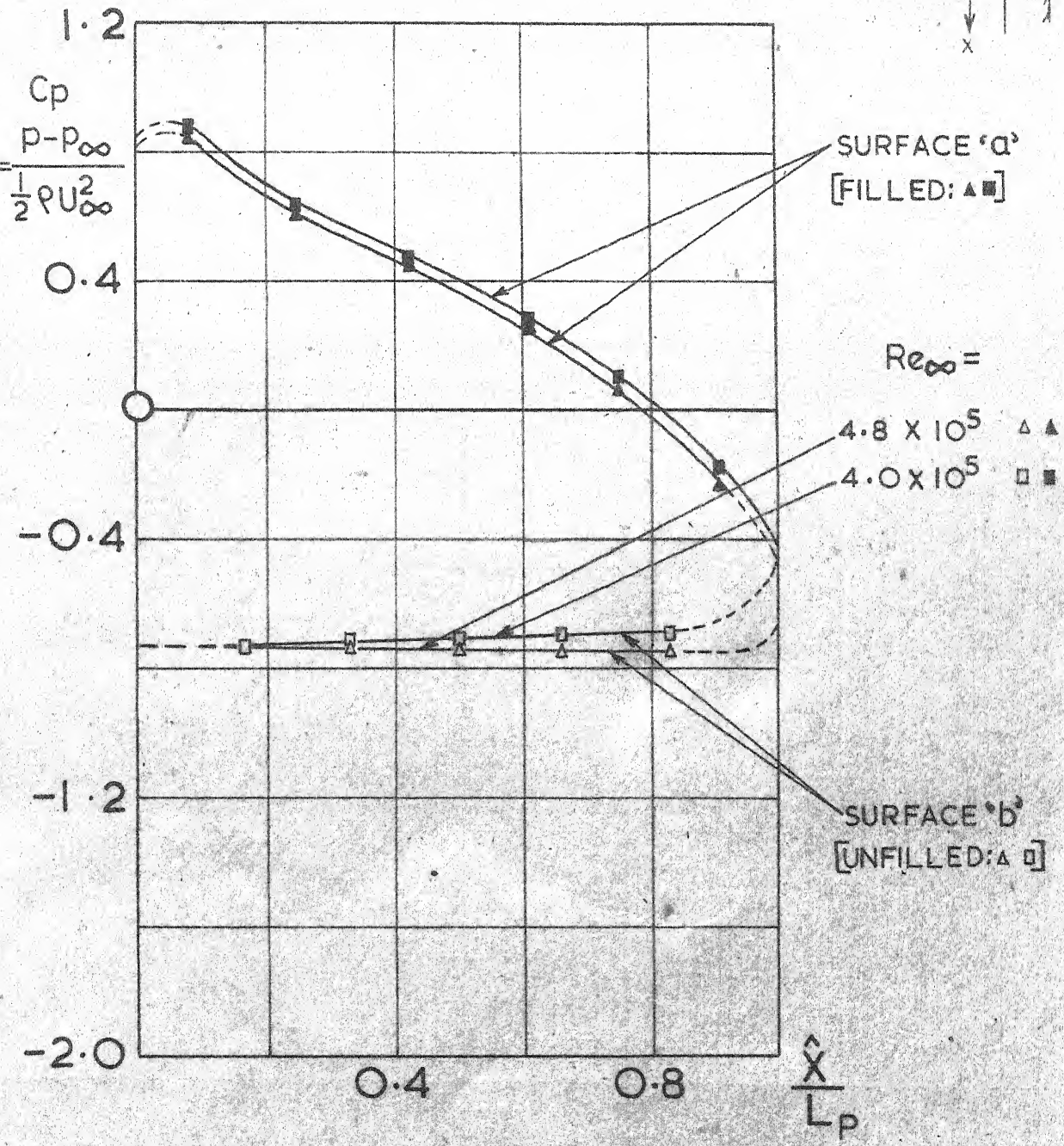

DRAWN: I.S.G.	DATE:	SQN. LDR. I.S. GUPTA	REPORT NO:

$\alpha = 45°$

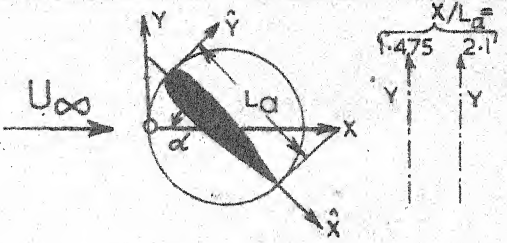

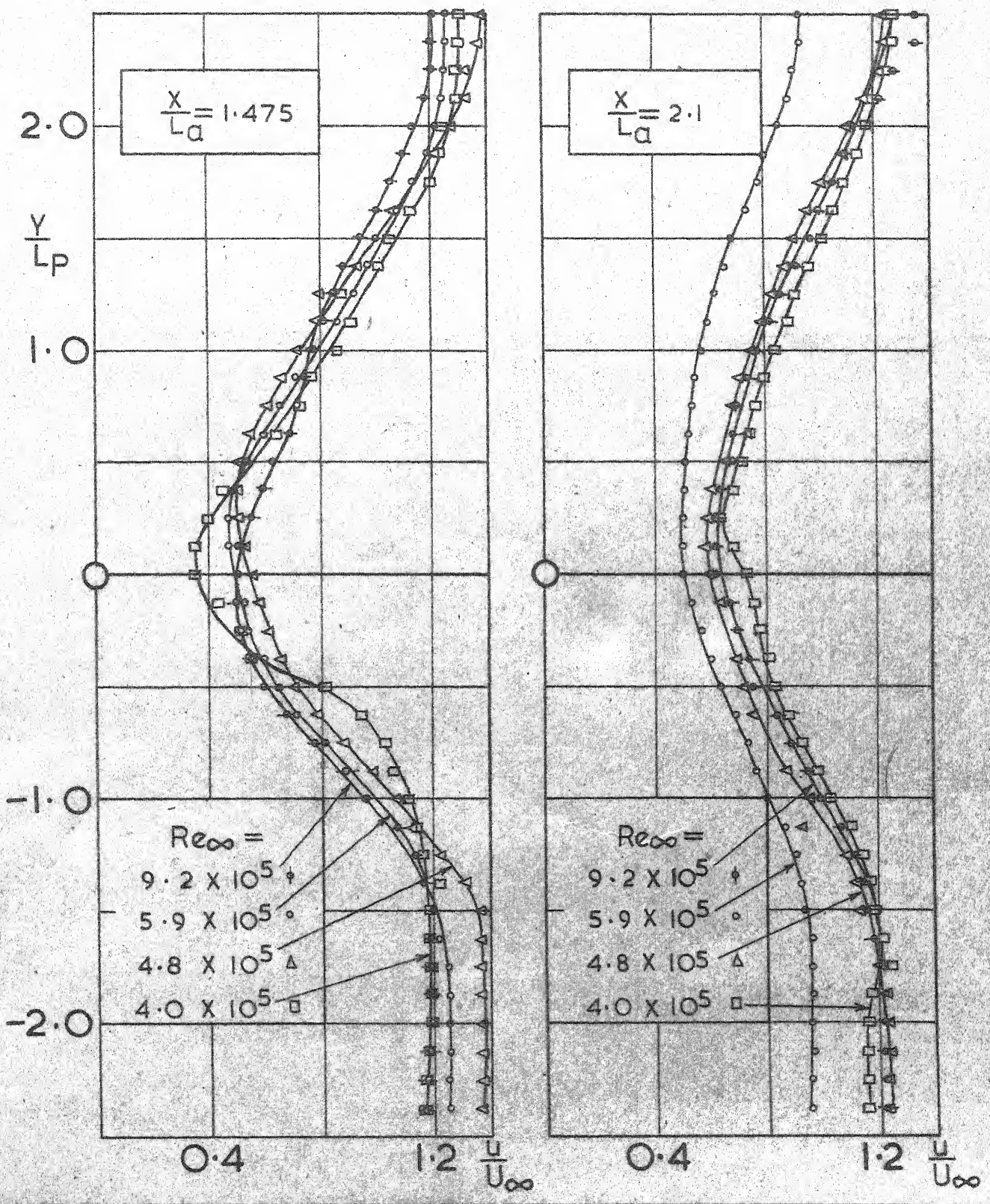

DRAWN: I.S.G.	DATE:	SQN. LDR. I.S. GUPTA	REPORT NO:

$\alpha = 40°$

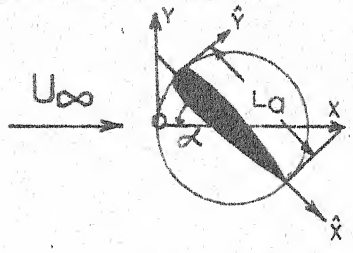

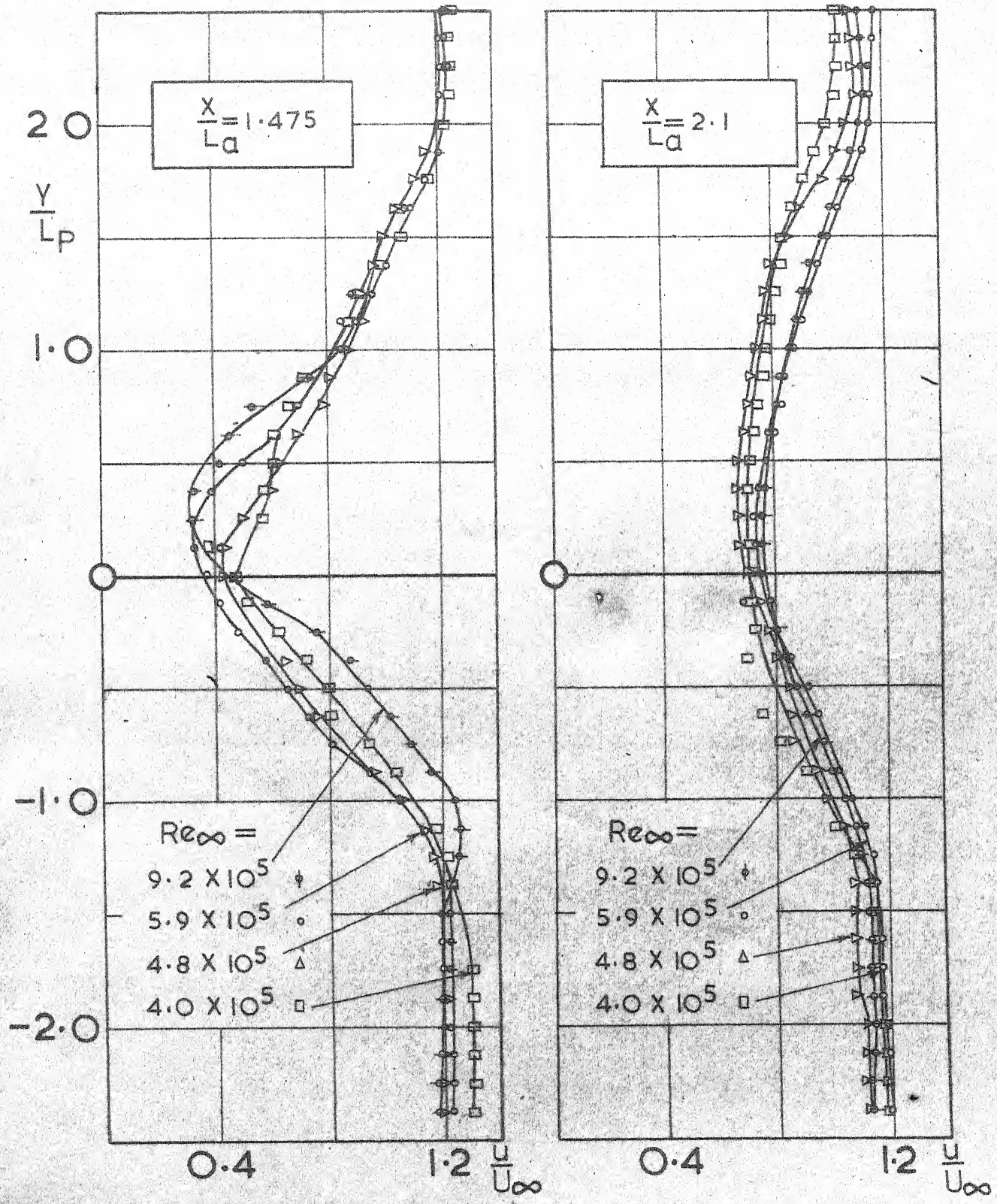

DRAWN: I. S. G.	DATE:	SQN. LDR. I. S. GUPTA	REPORT NO:

$\alpha = 35^\circ$

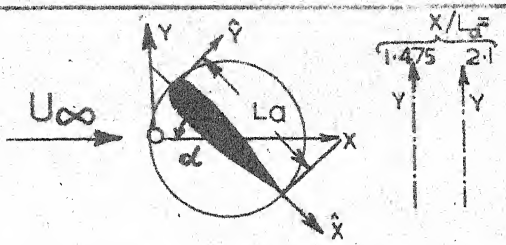

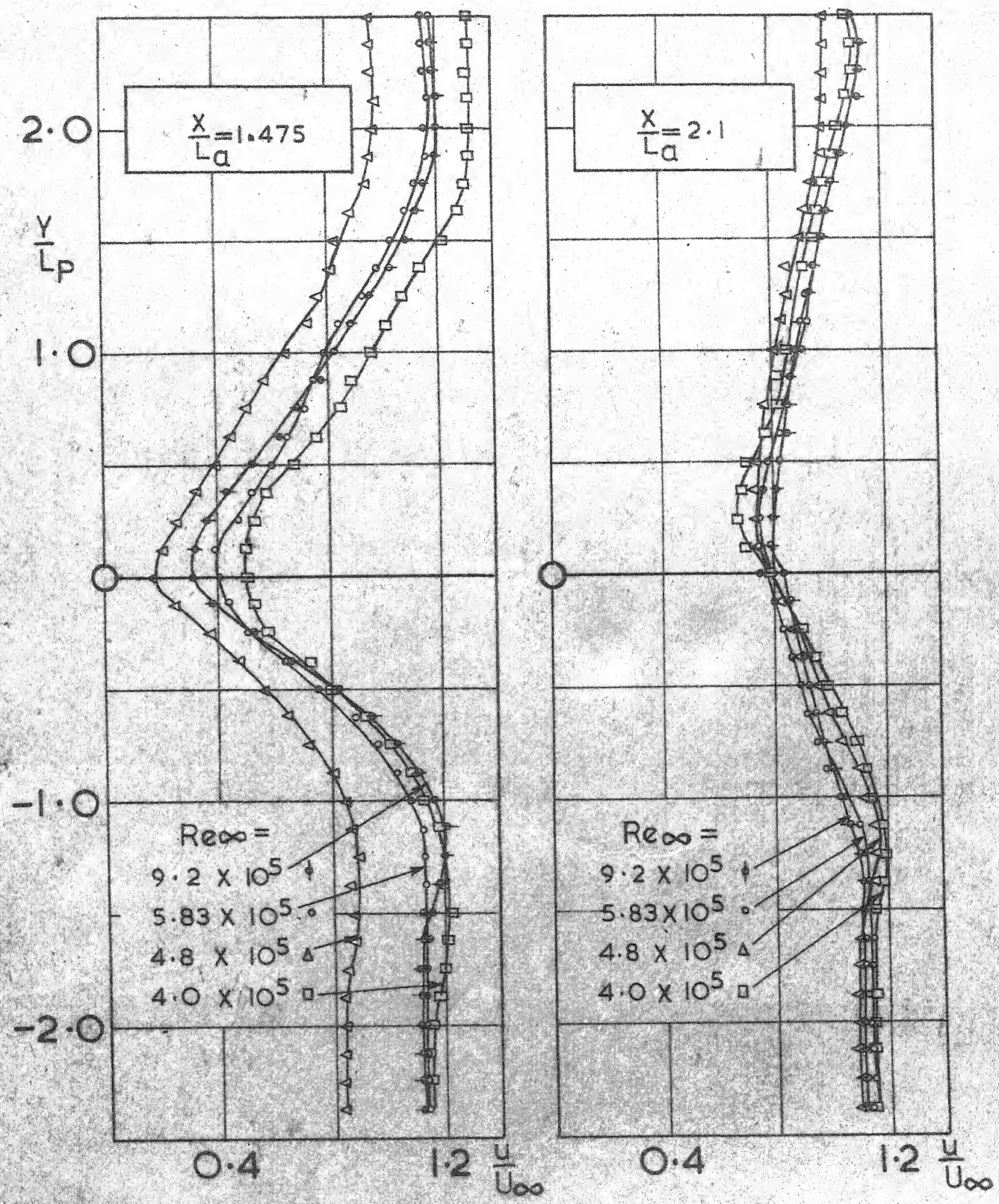

$\alpha = 30°$

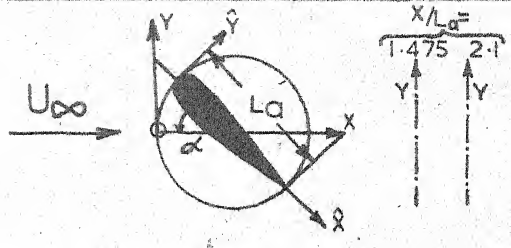
U_∞
Y
Y
La
X
X
α
X/La=
1·475
2·1
Y
Y

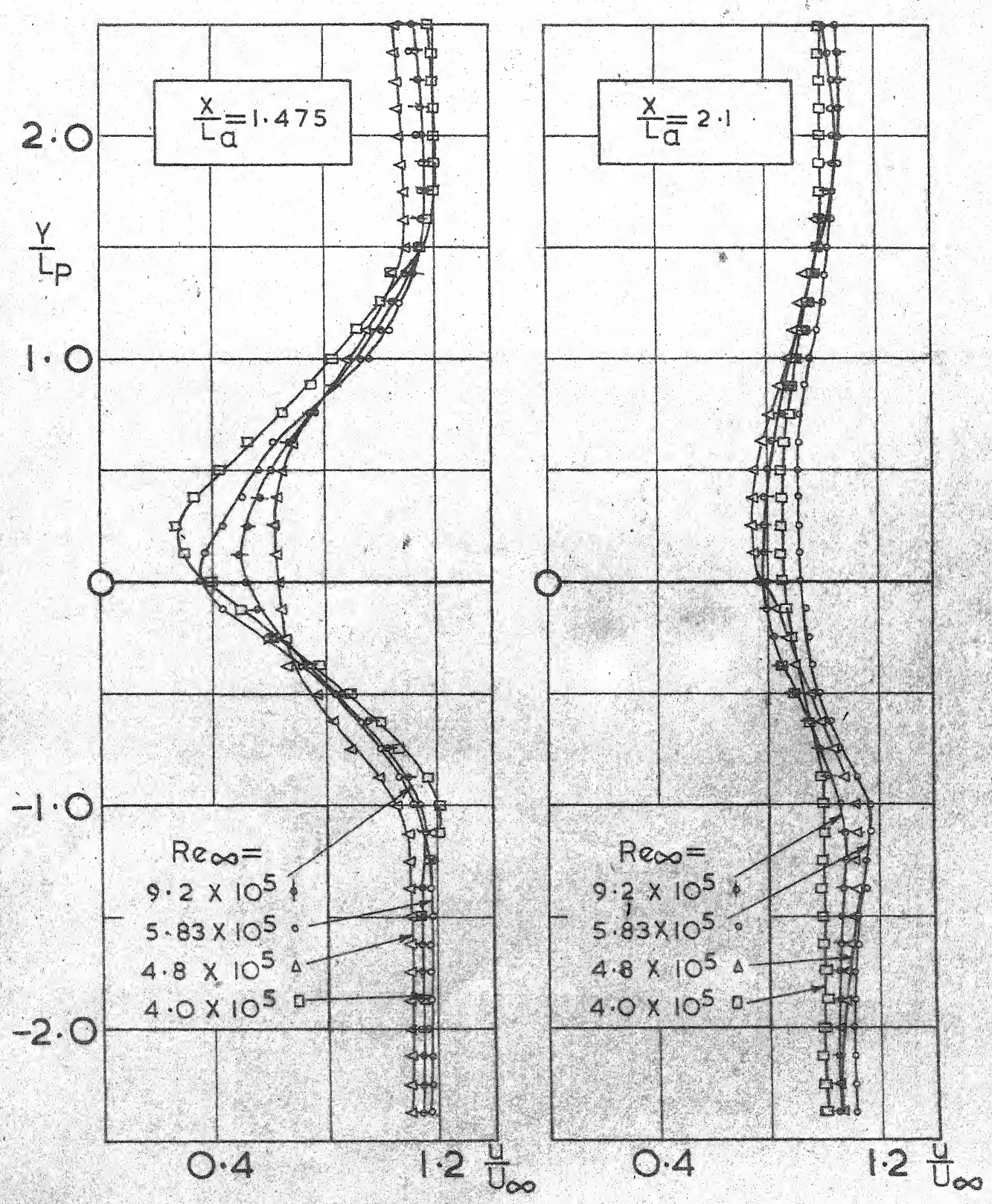
X/La = 1·475
X/La = 2·1
2·0
1·0
-1·0
-2·0
Y/Lp
Re∞=
9·2 X 10^5
5·83 X 10^5
4·8 X 10^5
4·0 X 10^5
0·4
1·2
U/U∞

$\alpha = 25^\circ$

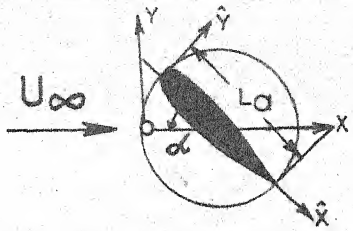

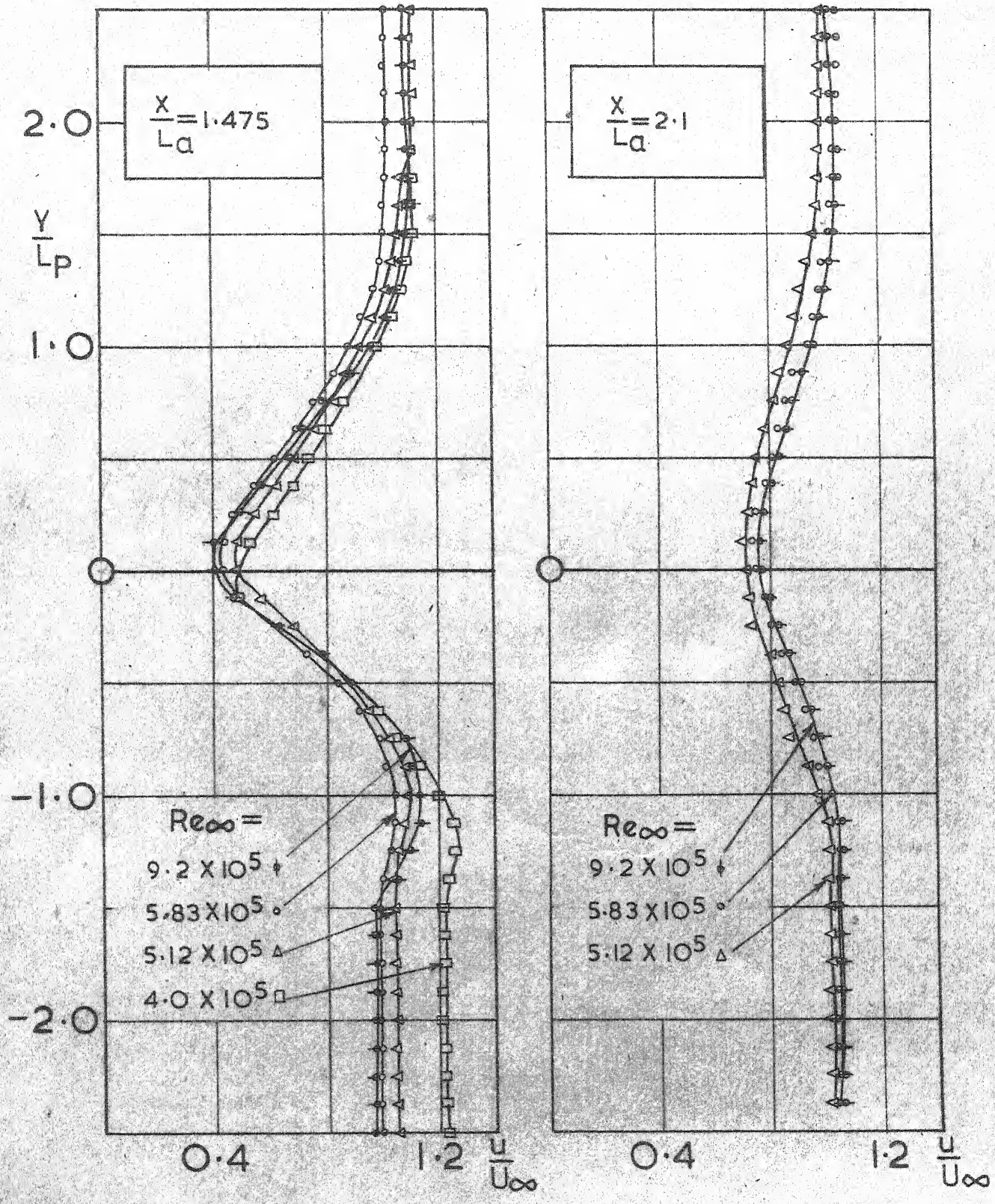

DRAWN: I. S. G.	DATE:	SQN. LDR. I. S. GUPTA	REPORT NO:

$\alpha = 20°$

U_∞

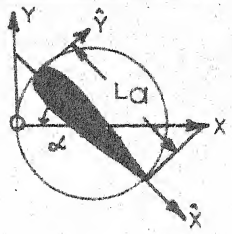

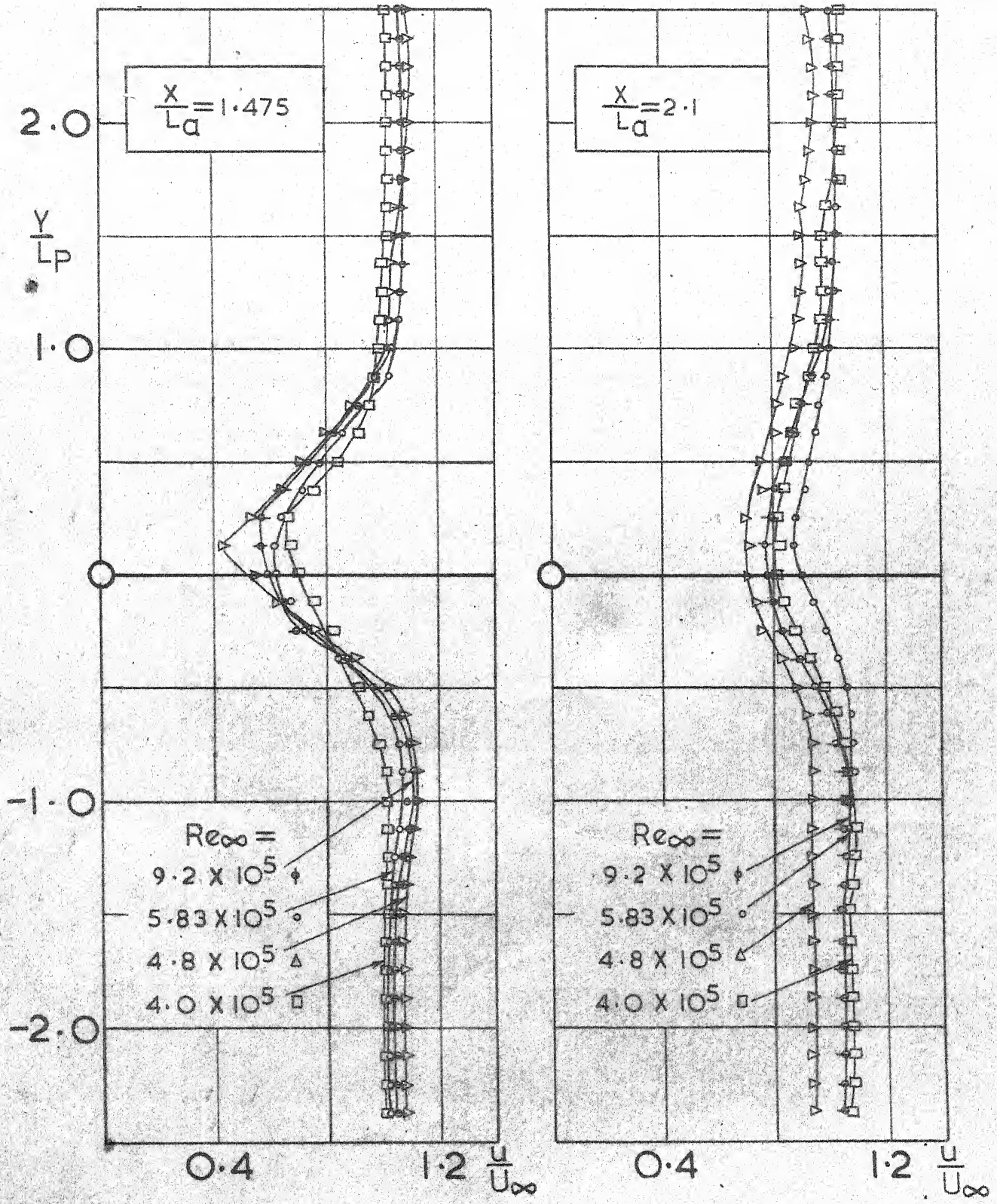

DRAWN: I. S. G.	DATE:	SQN. LDR. I. S. GUPTA	REPORT NO:

WAKE VELOCITY PROFILES FLAT PLATE

$\alpha = 90°$

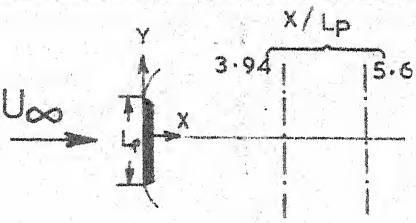

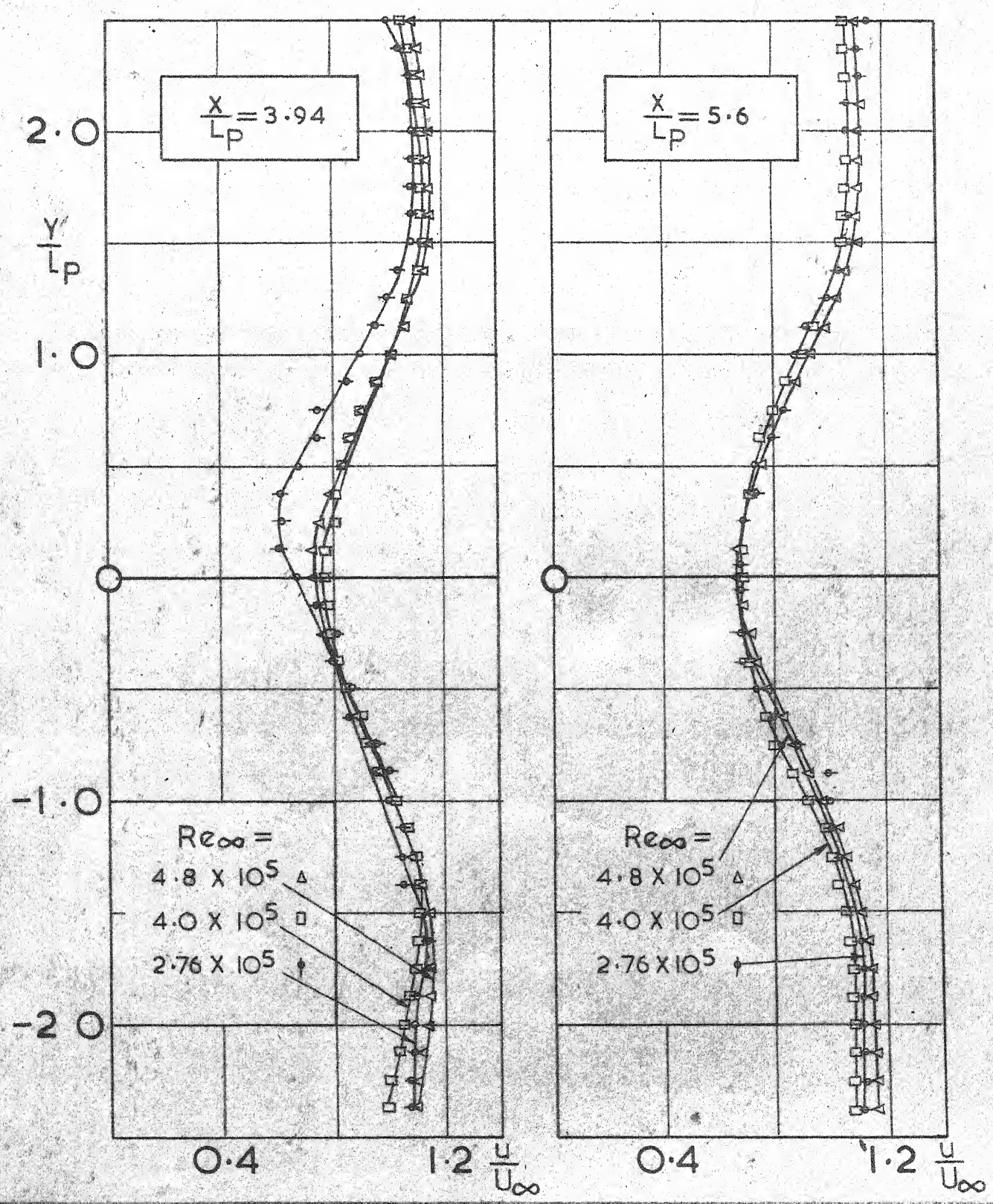

WAKE VELOCITY PROFILES FLAT PLATE

FIG·50

$\alpha = 45°$

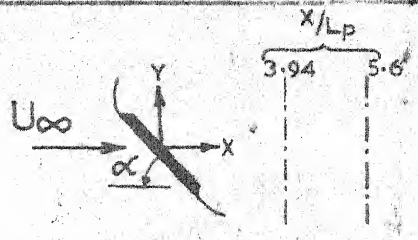

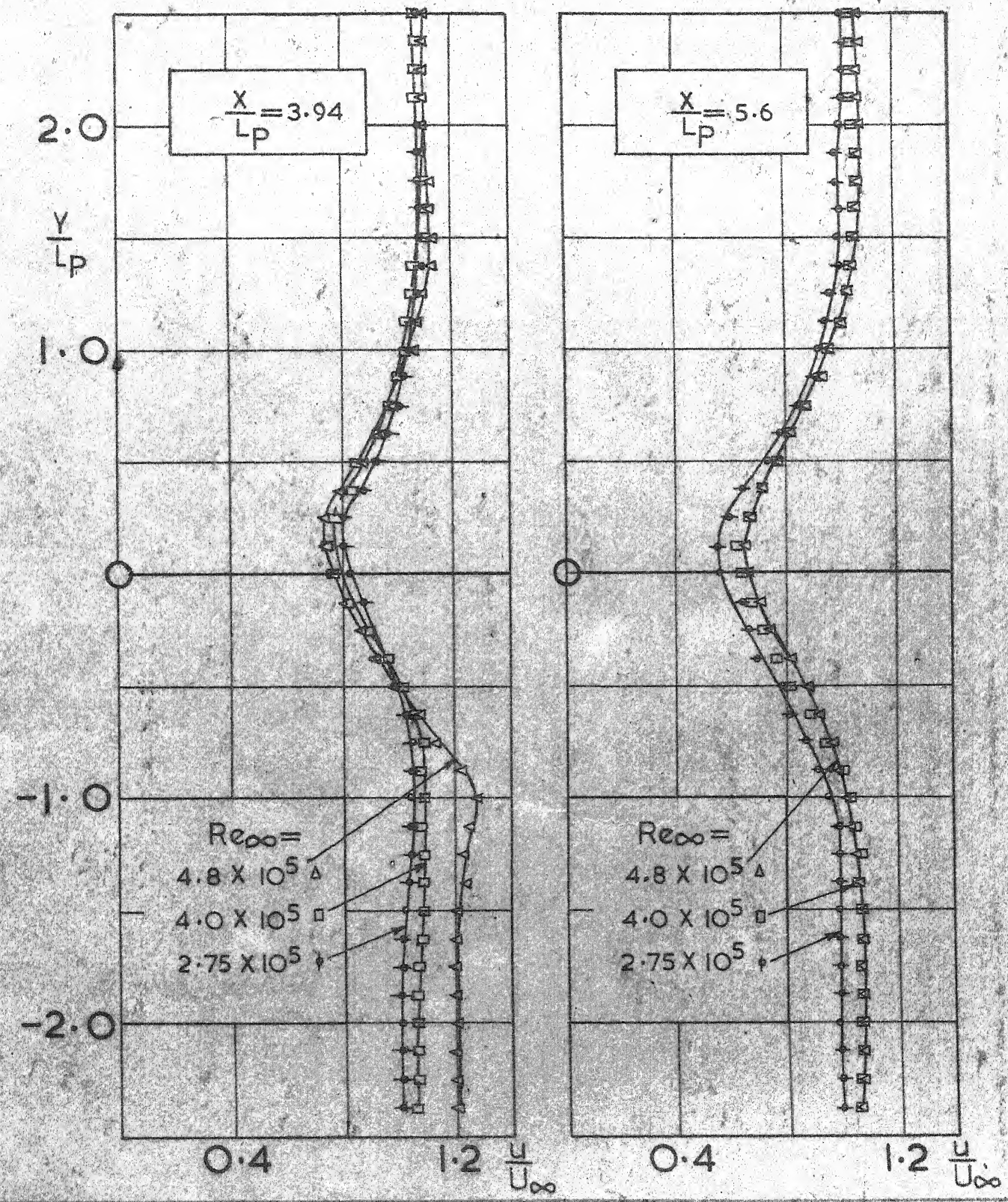

DRAWN: I.S.G. | DATE: | SQN. LDR. I.S. GUPTA | REPORT NO:

WAKE VELOCITY PROFILES FLAT PLATE

FIG·51

$\alpha = 30°$

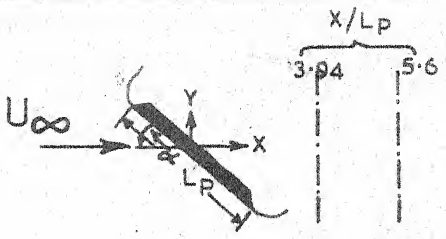

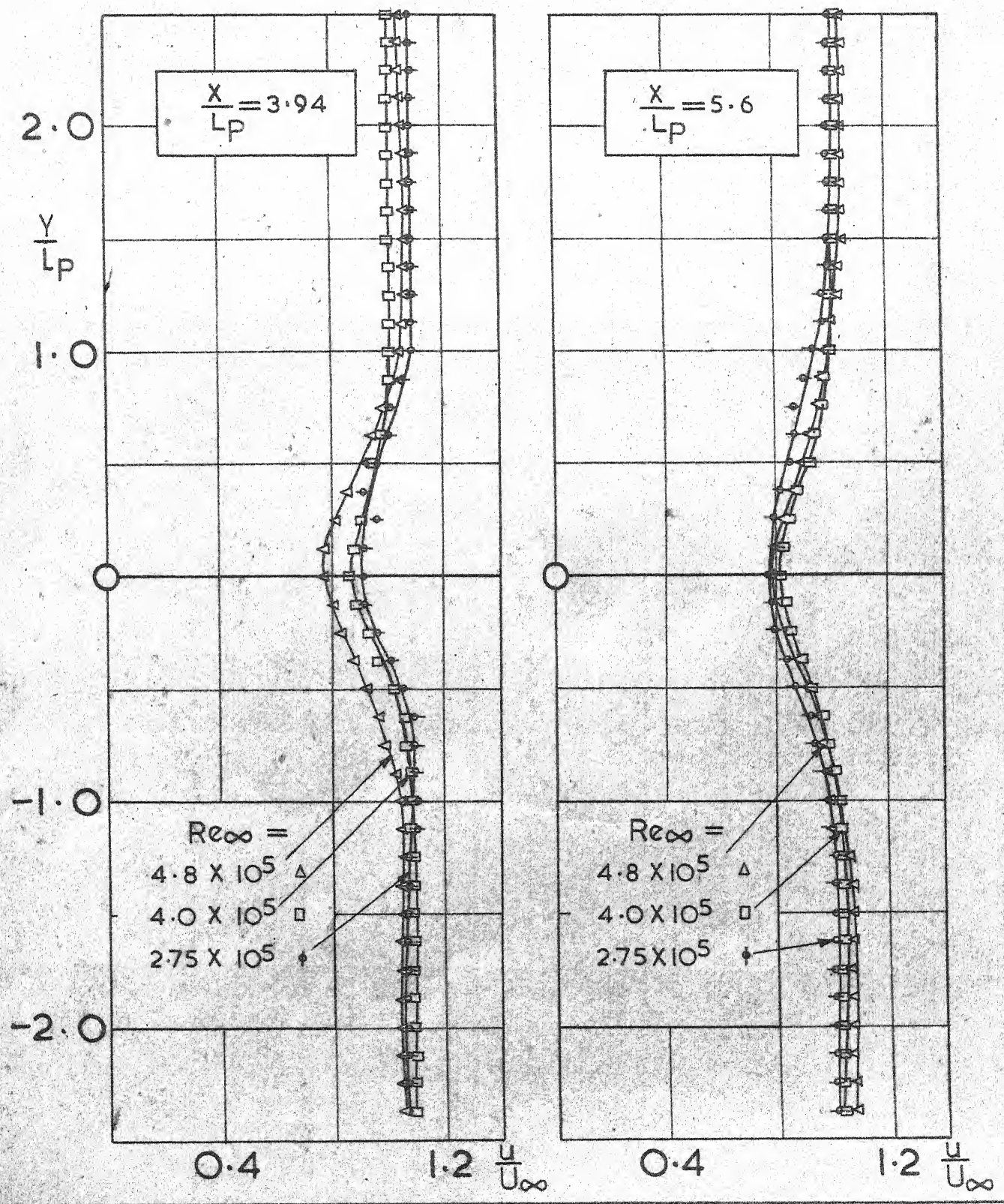

DRAWN: I.S.G | DATE: | SQN. LDR. I.S. GUPTA | REPORT NO:

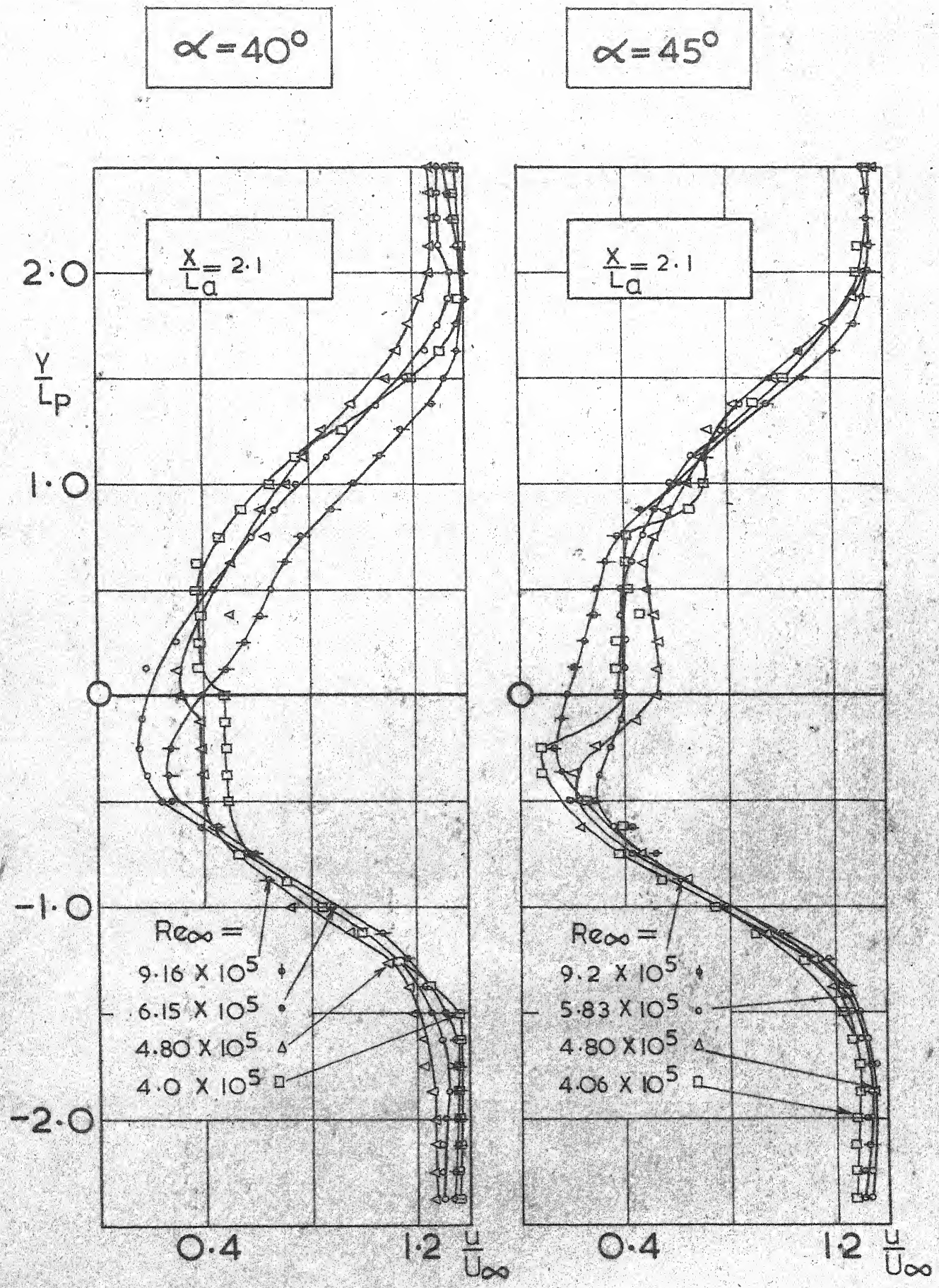
α=40°
α=45°
X/La = 2·1
X/La = 2·1
2·0
1·0
-1·0
-2·0
Y/Lp
Re∞ =
9·16 X 10^5
6·15 X 10^5
4·80 X 10^5
4·0 X 10^5
Re∞ =
9·2 X 10^5
5·83 X 10^5
4·80 X 10^5
4·06 X 10^5
0·4
1·2
u/U∞
0·4
1·2
u/U∞

WAKE VELOCITY PROFILES NACA 6601O WITH SPLITTER PLATE FOREMOST

FIG:53

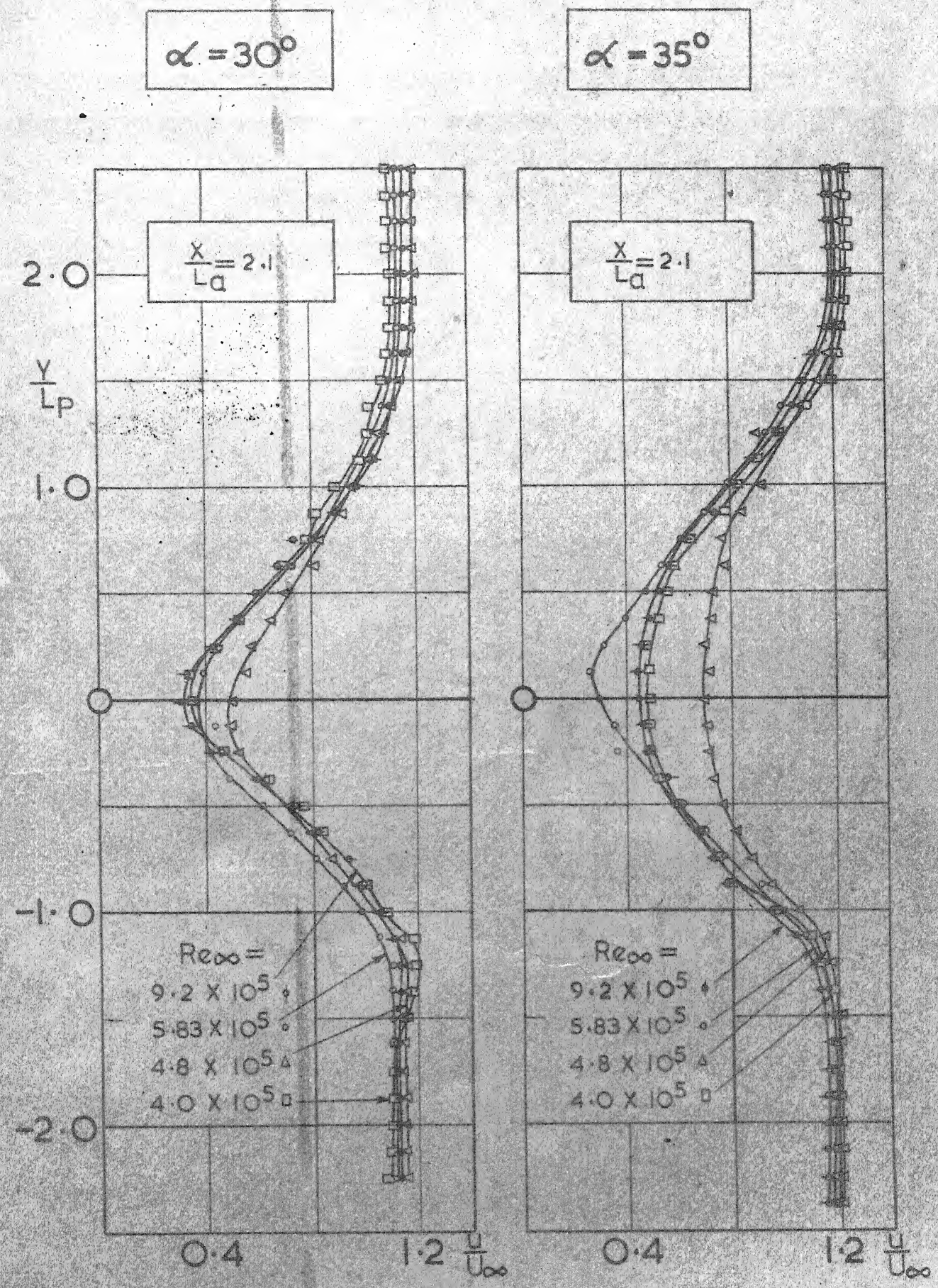

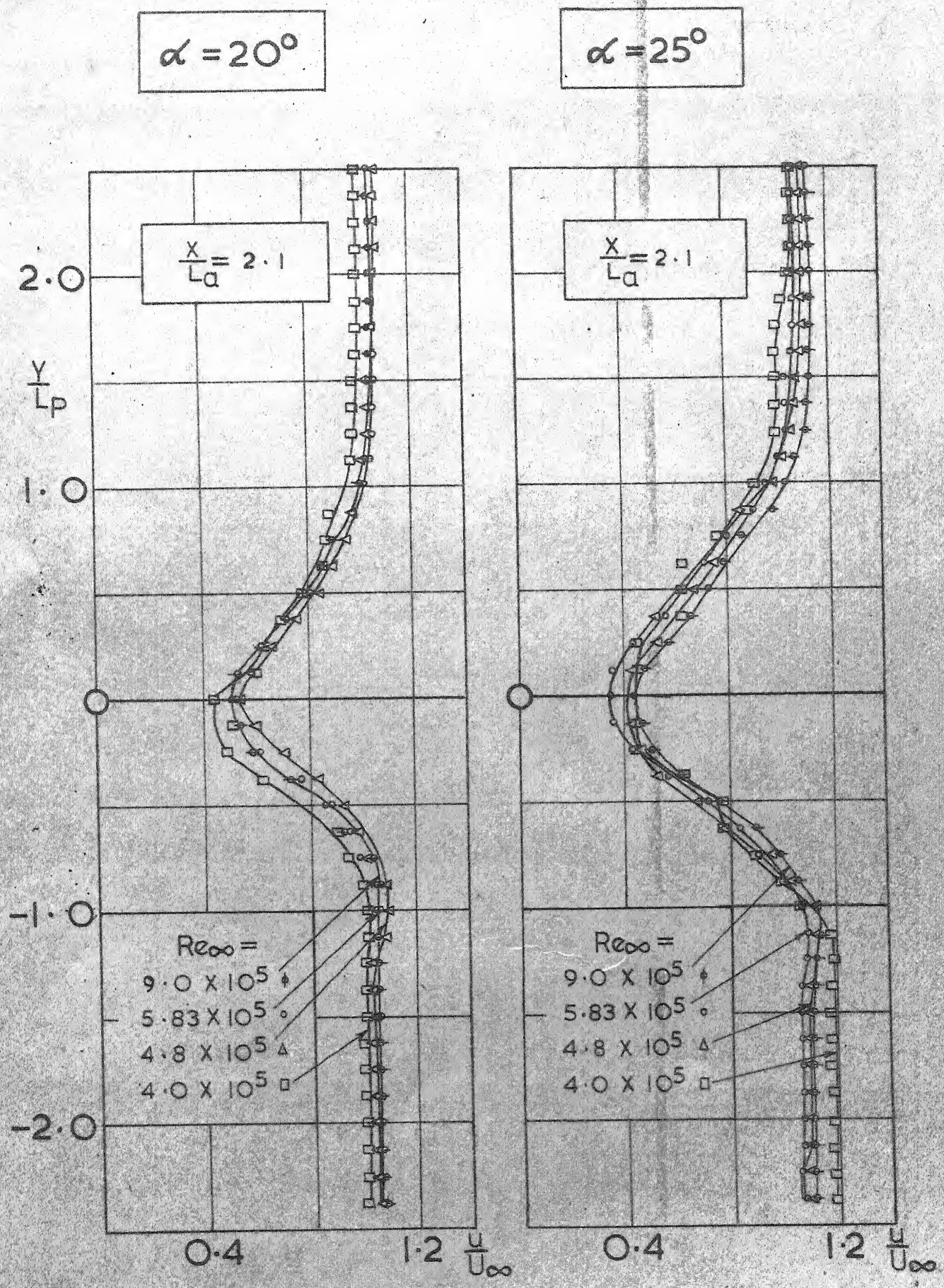
α = 20°
α = 25°
X/La = 2·1
X/La = 2·1
2·0
1·0
-1·0
-2·0
Y/Lp
Re∞ =
9·0 X 10^5
5·83 X 10^5
4·8 X 10^5
4·0 X 10^5
0·4
1·2
u/U∞
Re∞ =
9·0 X 10^5
5·83 X 10^5
4·8 X 10^5
4·0 X 10^5
0·4
1·2
u/U∞

WAKE VELOCITY PROFILES NACA 66010 WITH SPLITTER PLATE REARMOST

FIG. 55

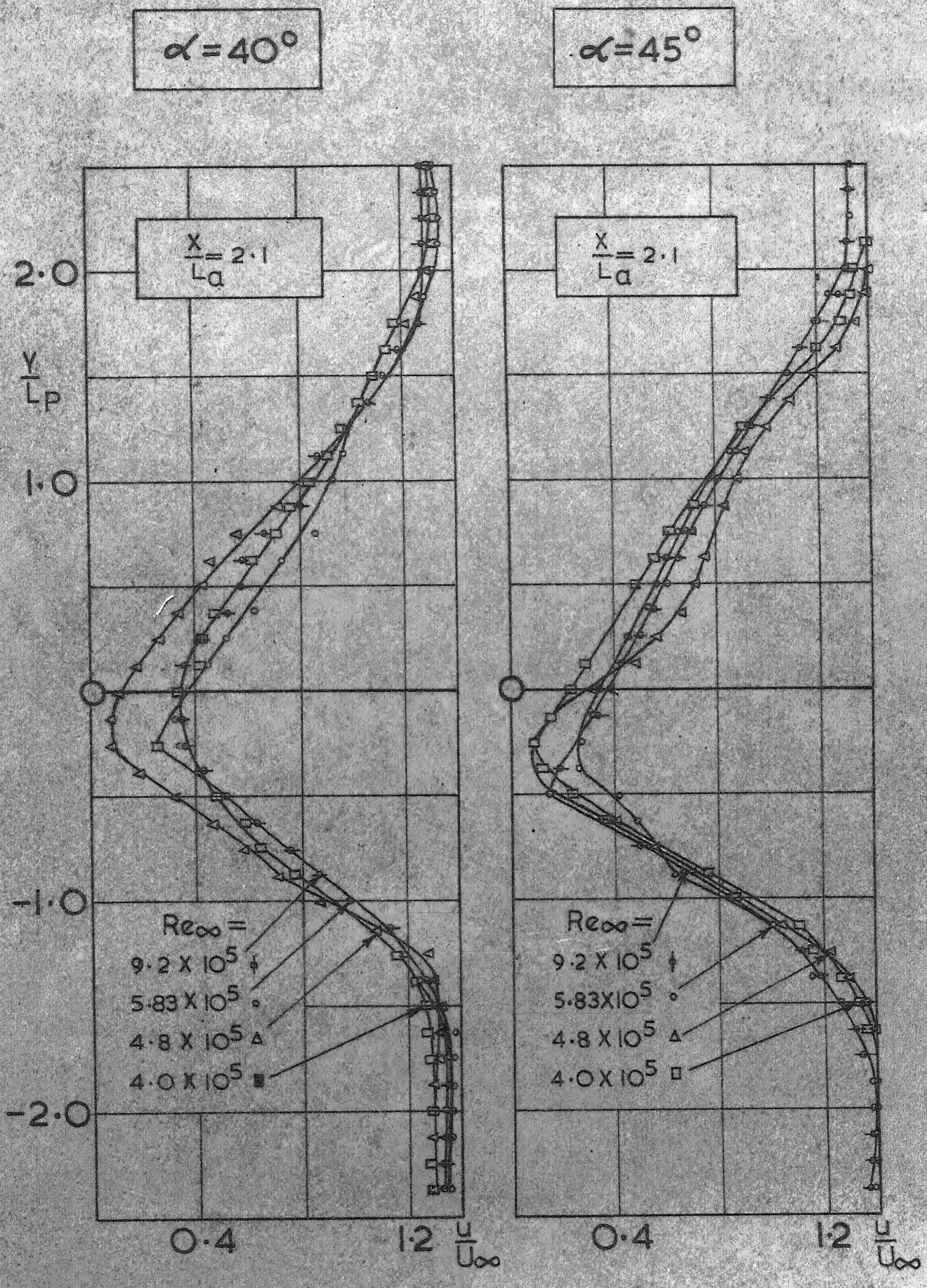

DRAWN: I.S.G.	DATE:	SQN. LDR. I.S. GUPTA	REPORT NO:

WAKE VELOCITY PROFILES NACA 66010 WITH SPLITTER PLATE REARMOST

FIG·56

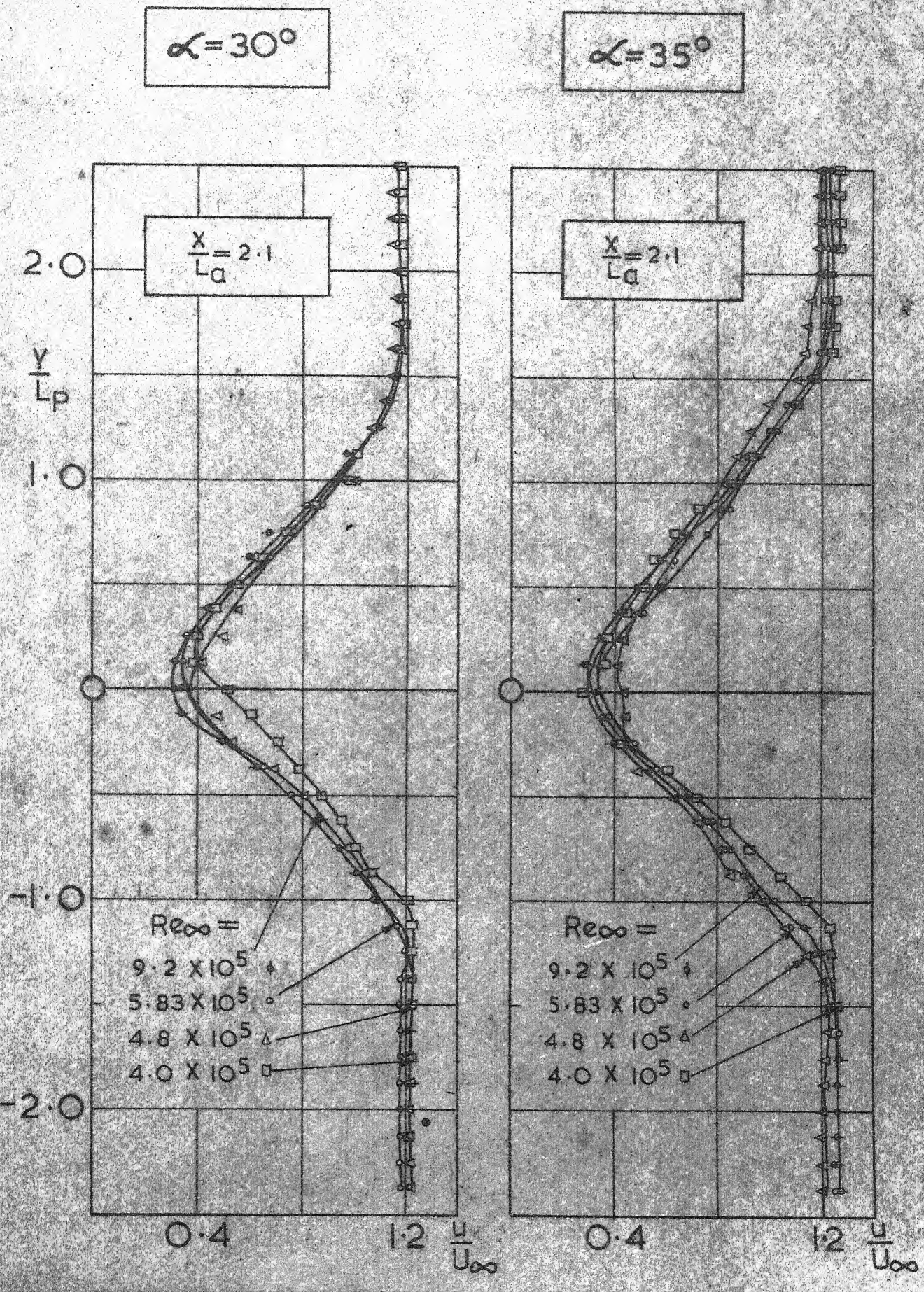

DRAWN: I.S.G. | DATE: | SQN.LDR. I.S. GUPTA | REPORT NO:

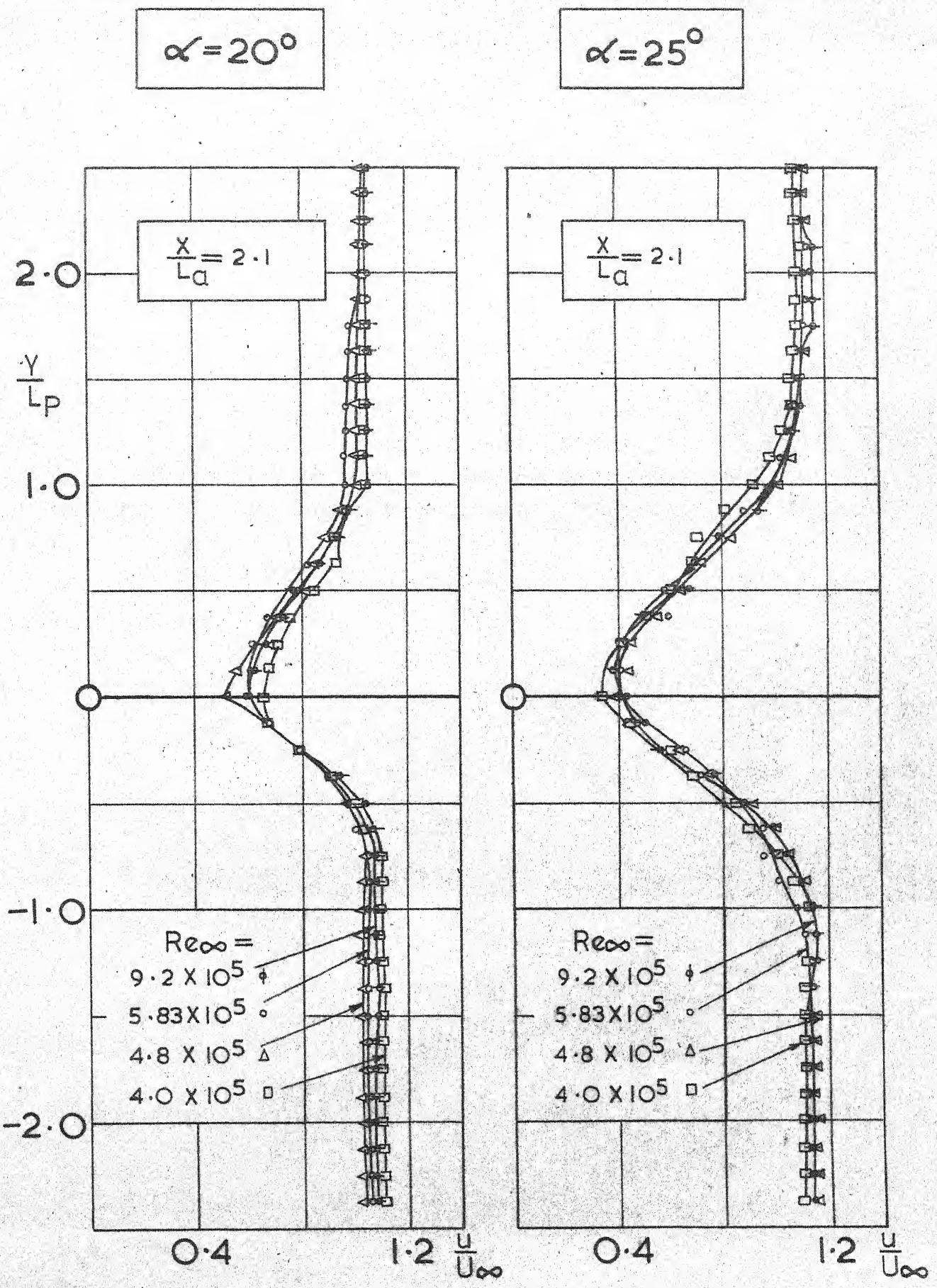
α=20°
α=25°
X/La = 2·1
X/La = 2·1
2·0
Y/Lp
1·0
-1·0
-2·0
Reω =
9·2 X 10^5
5·83X10^5
4·8 X 10^5
4·0 X 10^5
Reω =
9·2 X 10^5
5·83X10^5
4·8 X 10^5
4·0 X 10^5
0·4
1·2
u/Uω
0·4
1·2
u/Uω

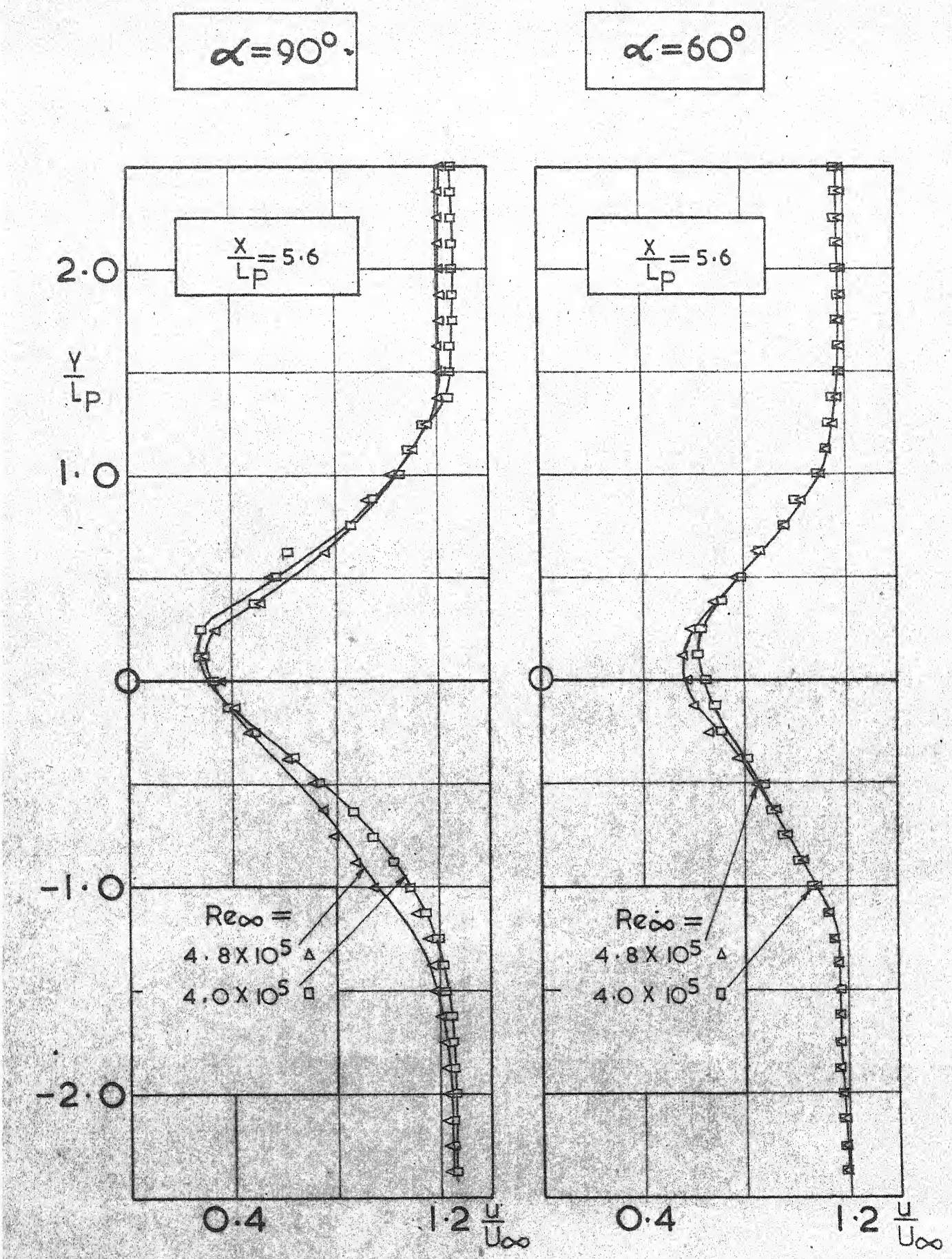

DRAWN: I.S.G. | DATE: | SQN. LDR. I.S.GUPTA | REPORT NO:

WAKE VELOCITY PROFILES FLAT PLATE WITH SPLITTER PLATE FOREMOST

FIG.59

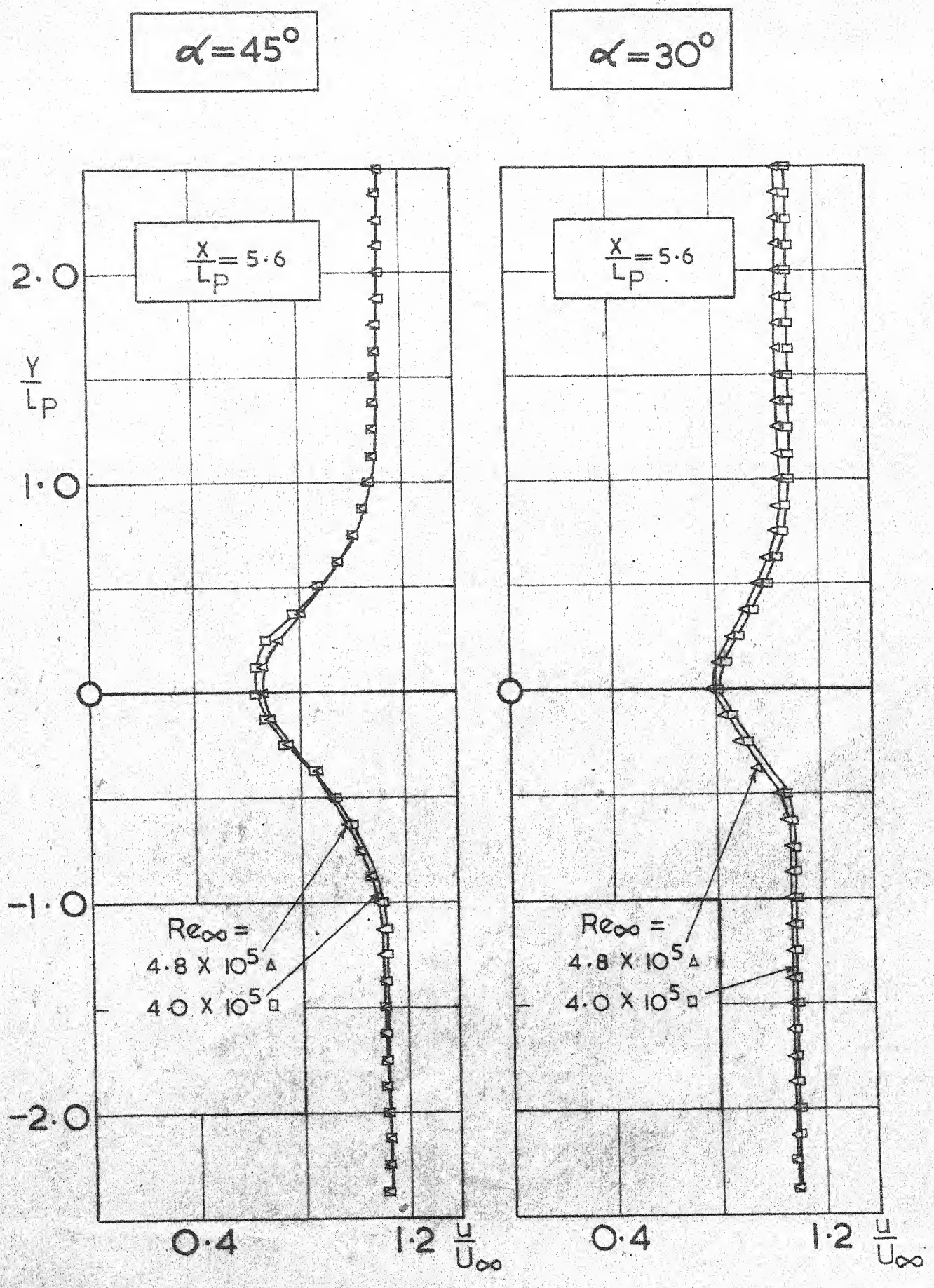

DRAWN: I.S.G. | DATE: | SQN. LDR. I.S. GUPTA | REPORT NO:

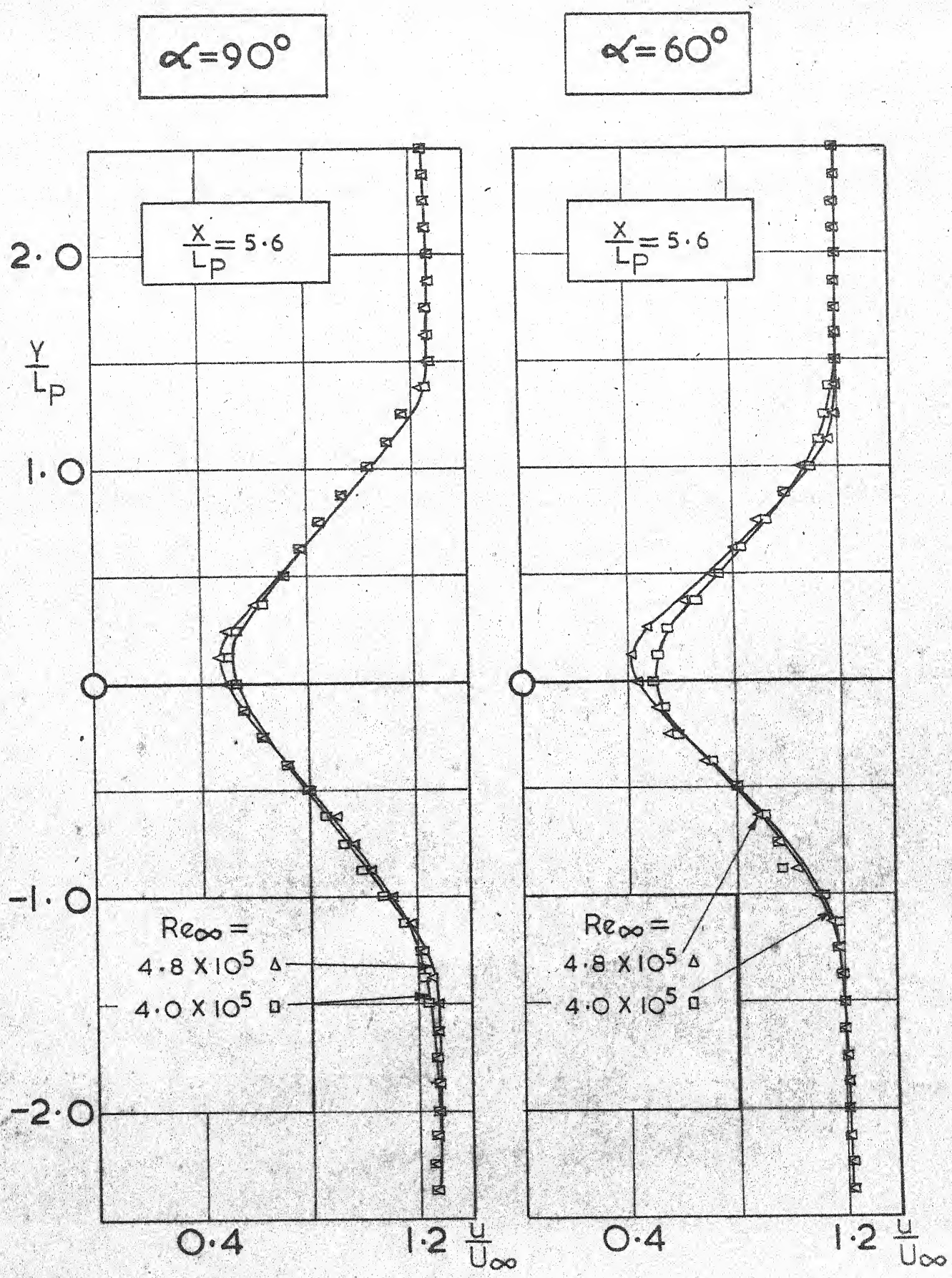

DRAWN: I.S.G. | DATE: | SQN. LDR. I.S. GUPTA | REPORT NO:

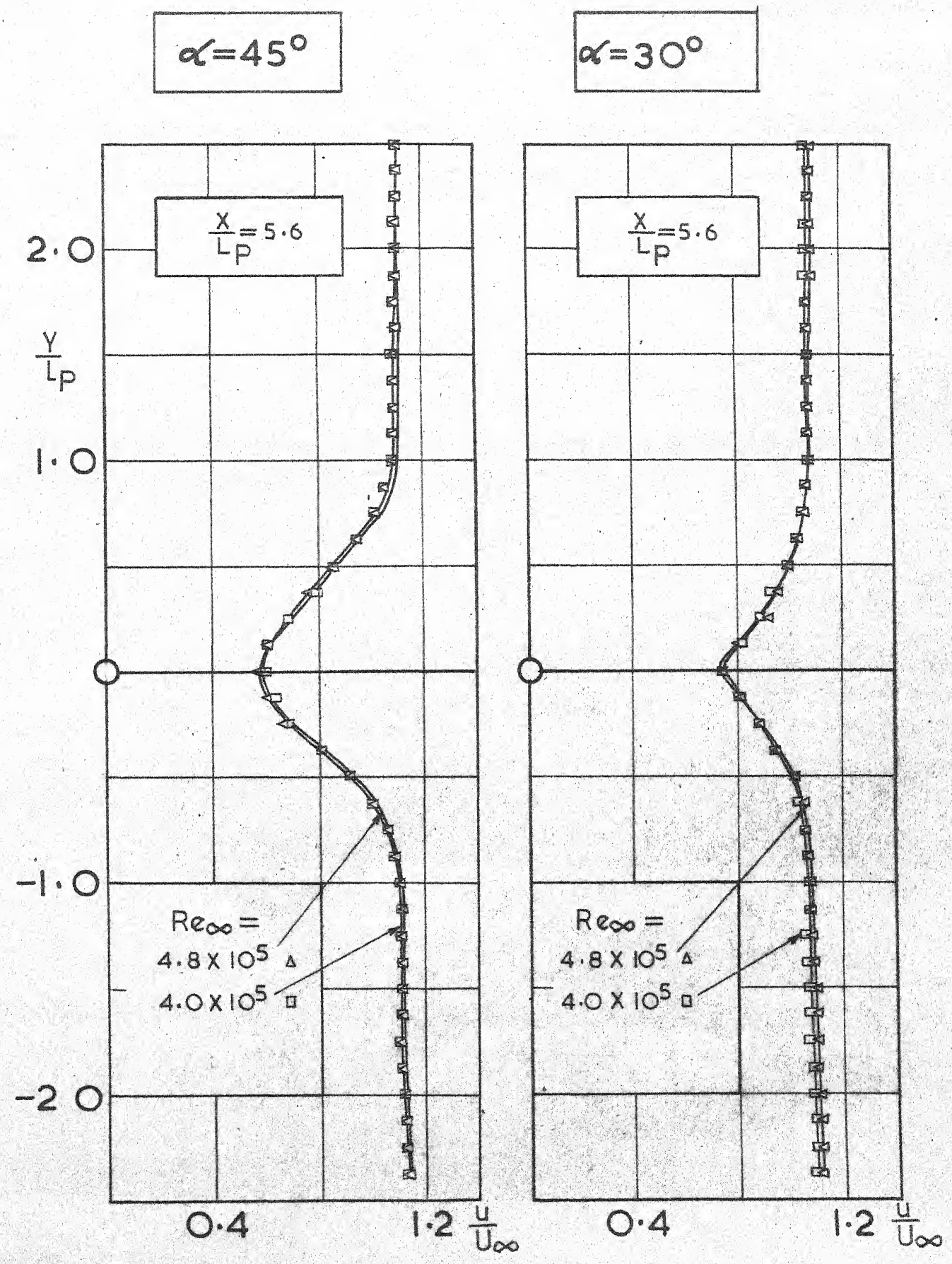
α=45°
α=30°
X/Lp=5.6
X/Lp=5.6
2·0
Y/Lp
1·0
-1·0
-2 0
Re∞ =
4·8 X 10^5 △
4·0 X 10^5 □
Re∞ =
4·8 X 10^5 △
4·0 X 10^5 □
0·4
1·2 U/U∞
0·4
1·2 U/U∞

DEPT OF AERO ENGG	AIRFOIL NACA 66010, BASE PRESSURE VS. ANGLE OF ATTACK (α)	PAGE NO: 87
		FIG·62

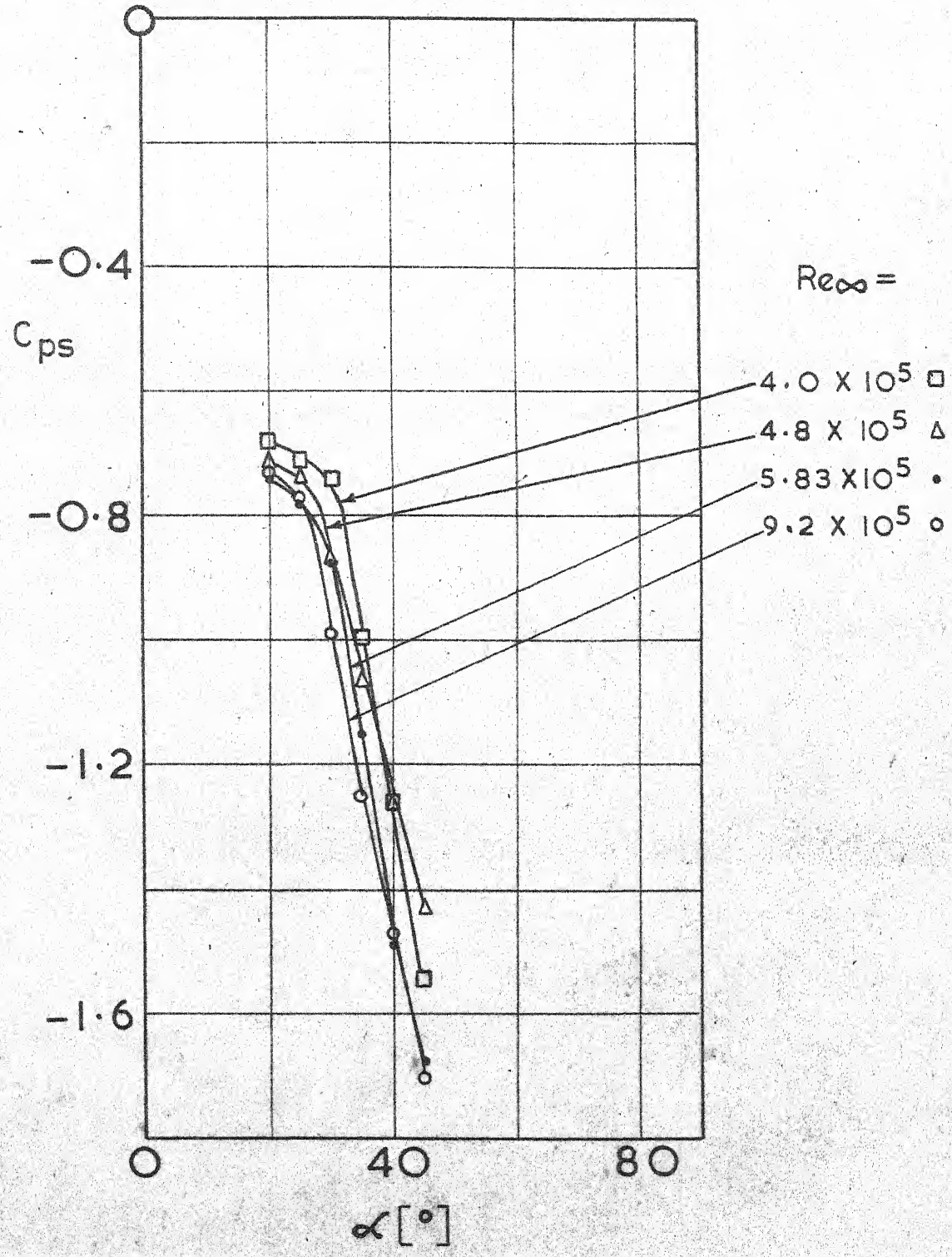

DRAWN: I.S.G.	DATE:	SQN. LDR. I.S.GUPTA	REPORT NO:

FLAT PLATE BASE PRESSURE VS. ANGLE OF ATTACK (α)

FIG·63

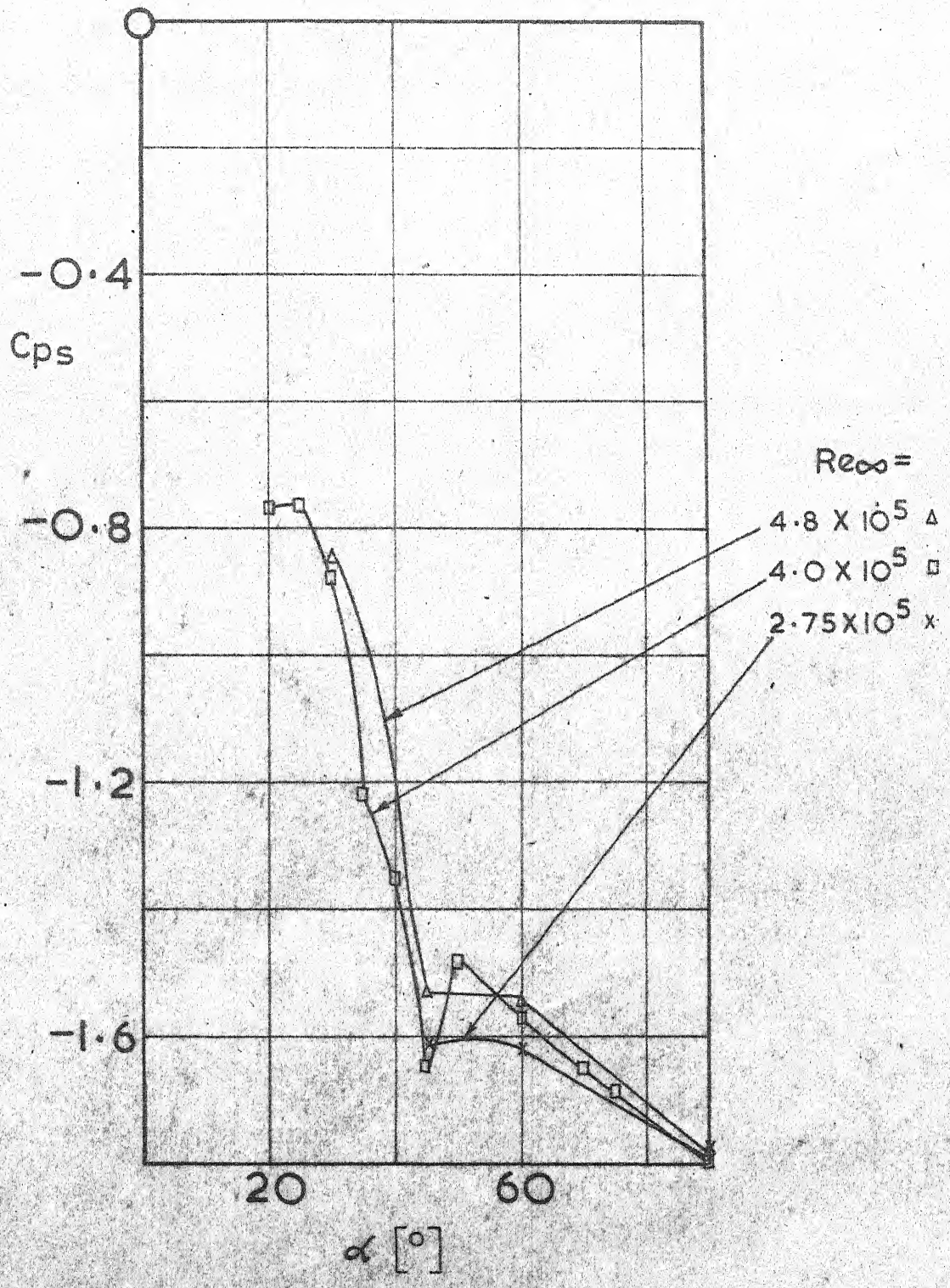

DRAWN: I.S.G.	DATE:	SQN. LDR. I. S. GUPTA	REPORT NO:

AIRFOIL NACA 66010 BASE PRESSURE, EFFECT OF SPLITTER PLATE

FIG·64

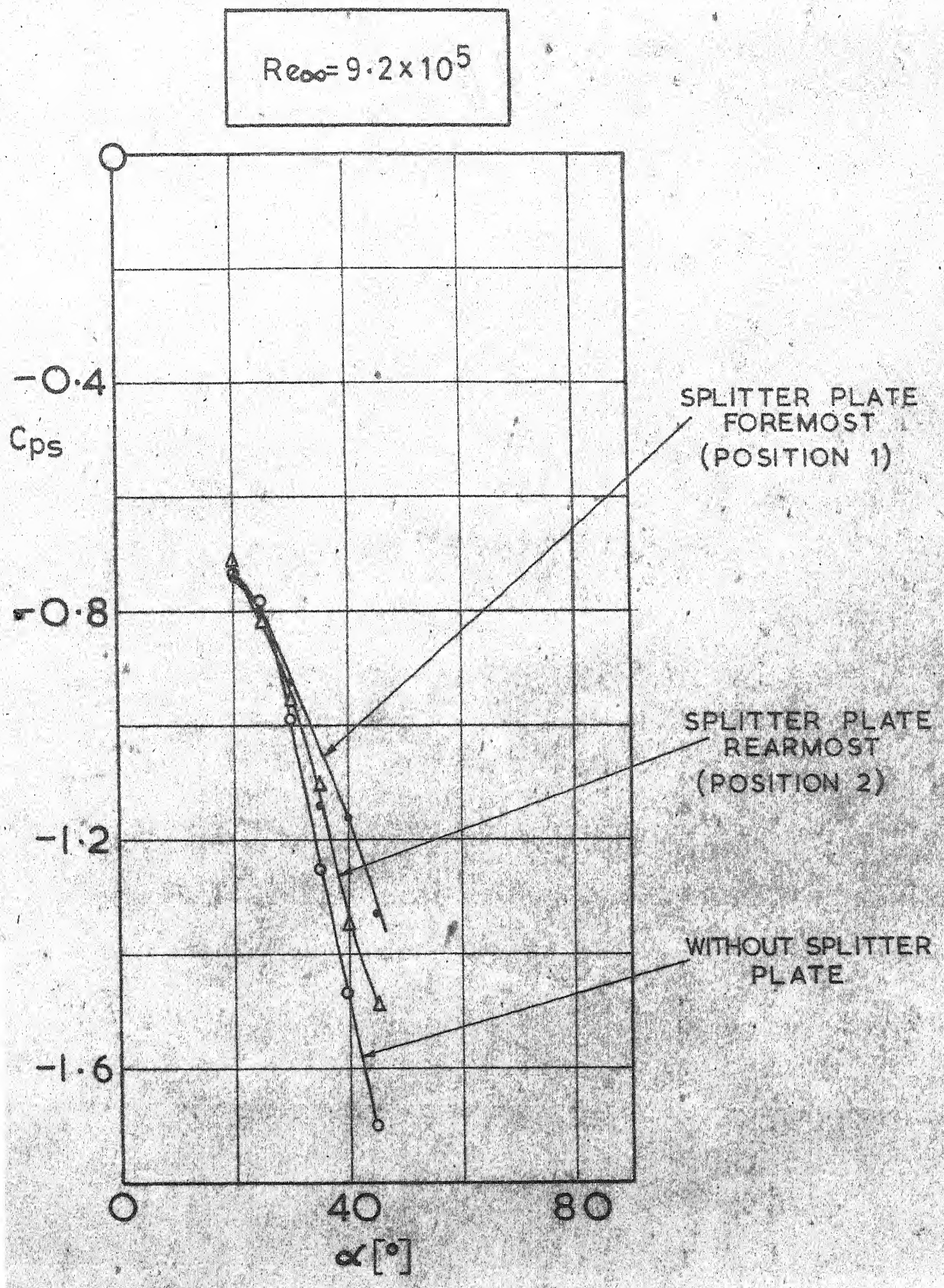

FLAT PLATE BASE PRESSURE, SPLITTER PLATE EFFECT

FIG·65

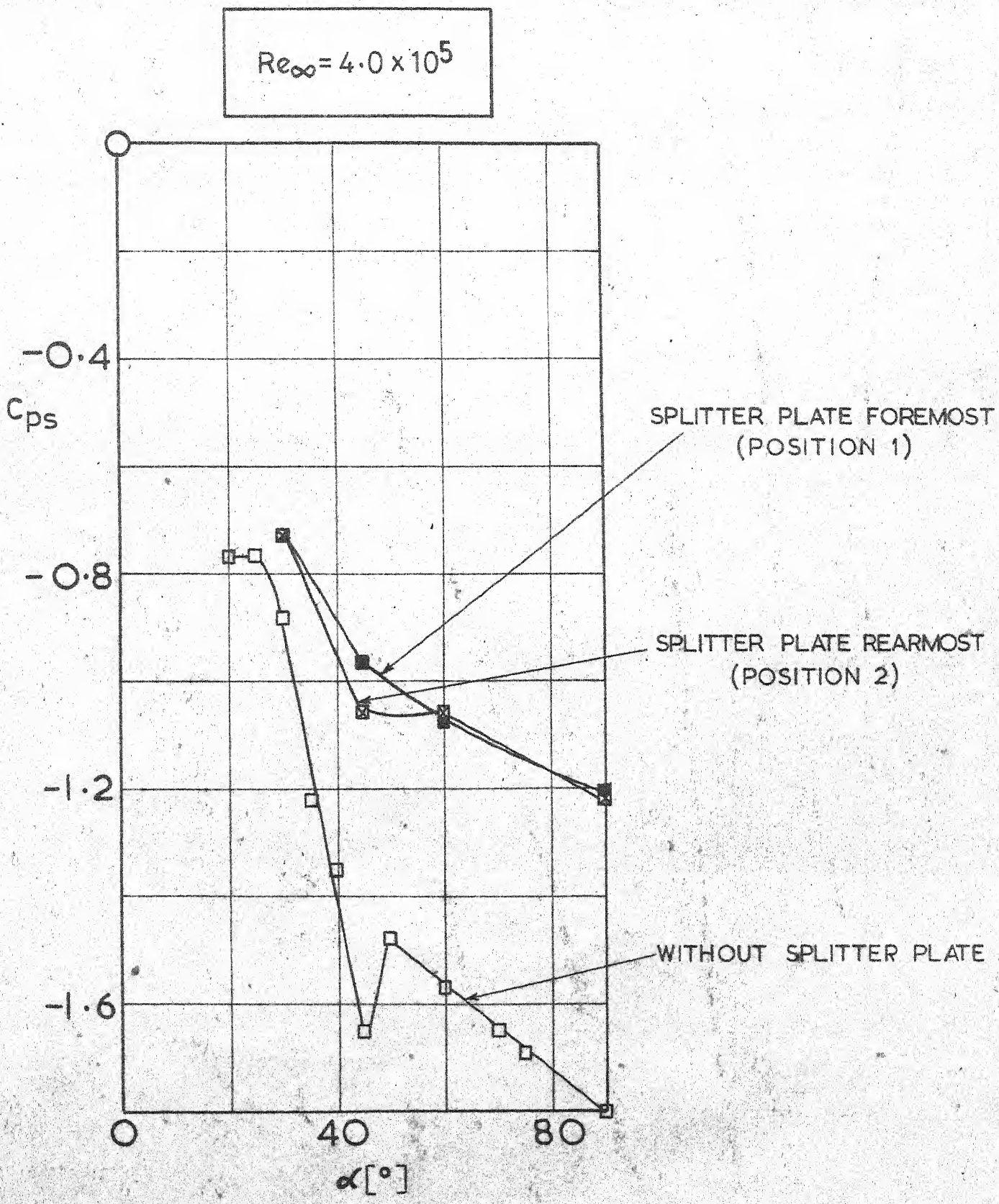

DEPT. OF AERO ENGG	PRESSURE DISTRIBUTION ON SPLITTER PLATE DOWN STREAM OF AIRFOIL NACA 66010 AT $\alpha=20^\circ$	PAGE NO: 91
		FIG·66

$Re_\infty = 4.0 \times 10^5$

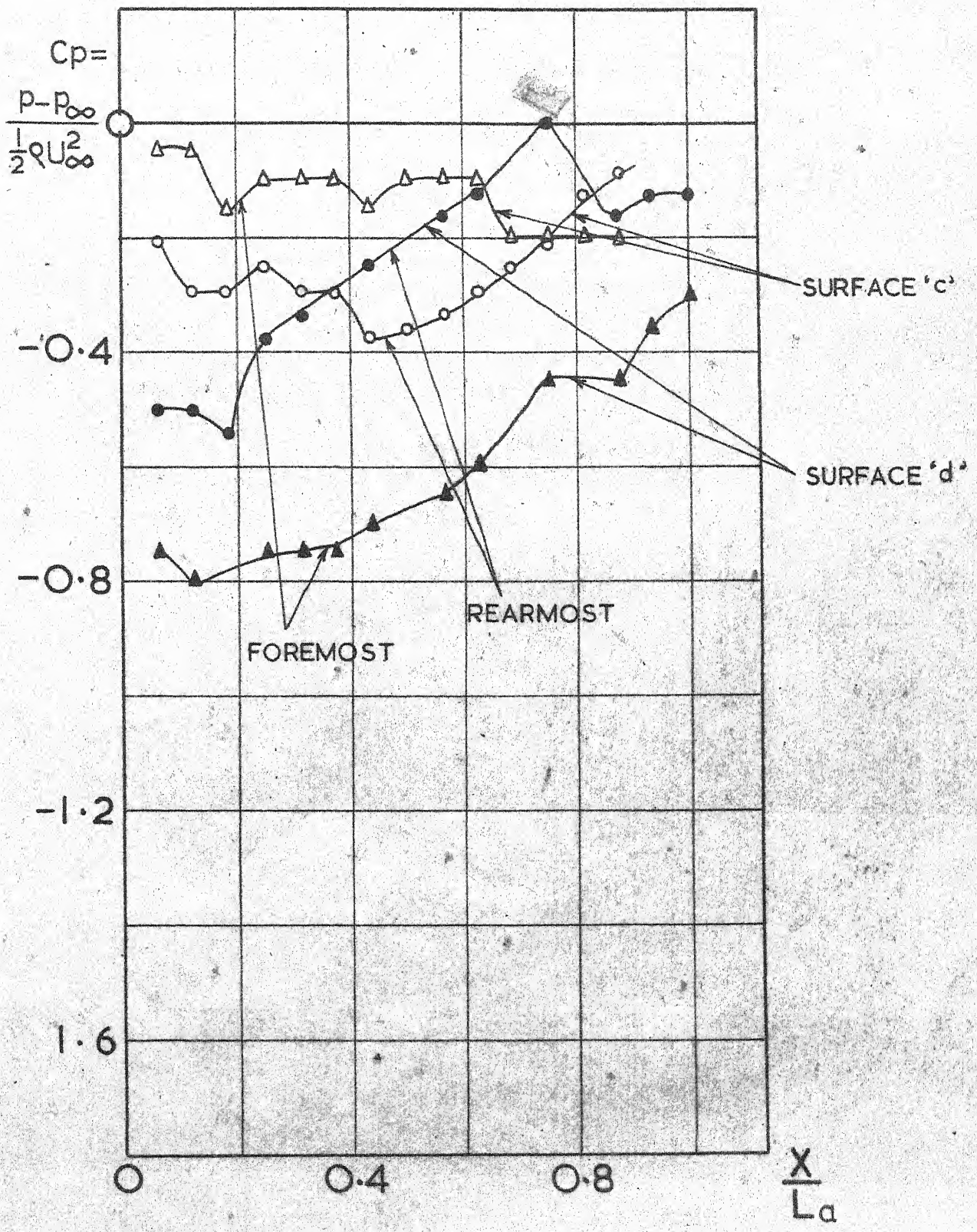

DRAWN: I. S. G.	DATE:	SQN. LDR. I. S. GUPTA	REPORT NO:

DEPT. OF AERO ENGG	PRESSURE DISTRIBUTION ON SPLITTER PLATE DOWN STREAM OF AIRFOIL NACA 66010 AT $\alpha = 45°$	PAGE NO: 92
		FIG·67

$Re_\infty = 9 \cdot 2 \times 10^5$

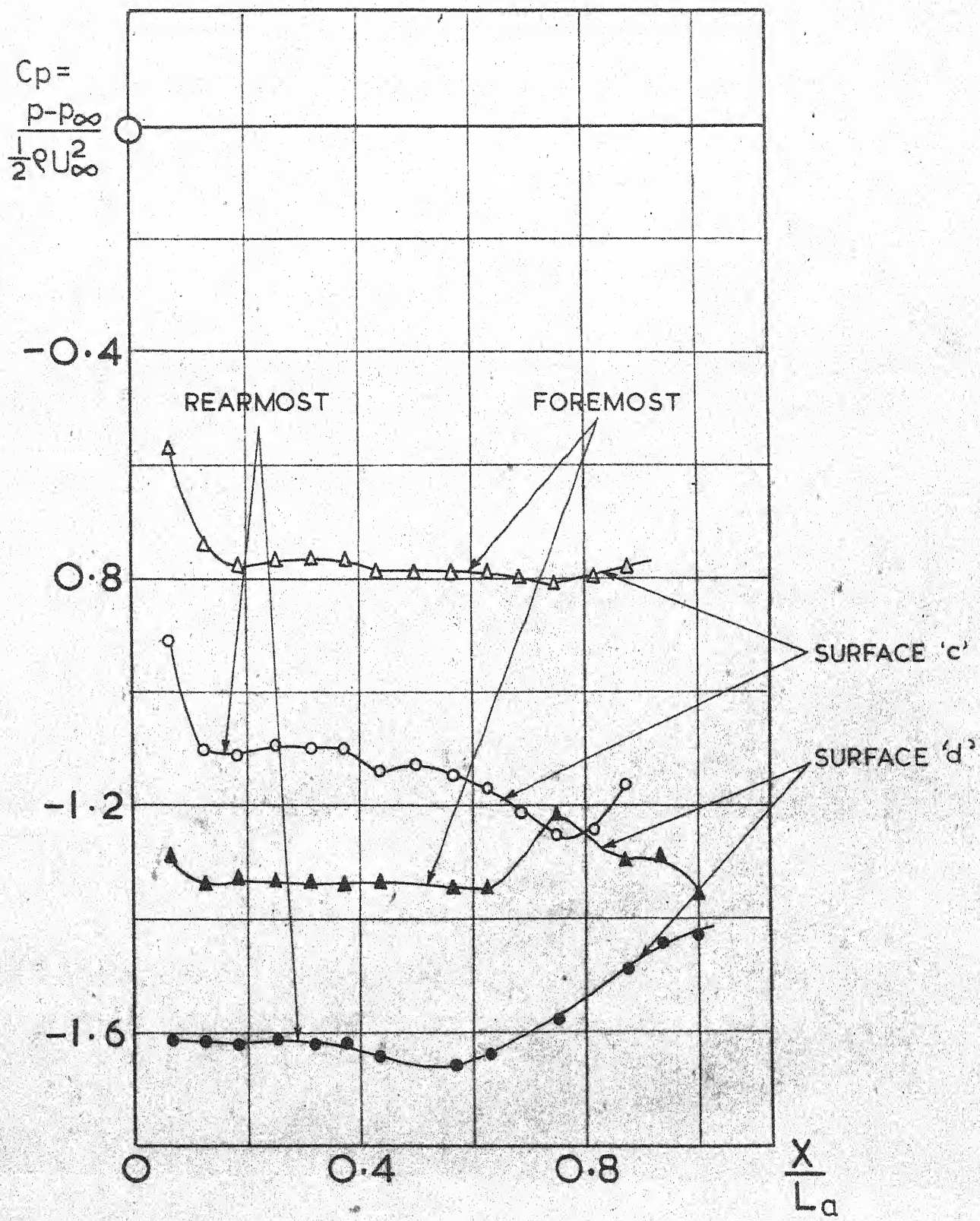

DRAWN: I.S.G.	DATE:	SQN. LDR. I.S.GUPTA	REPORT NO:

DEPT. OF AERO ENGG	PRESSURE DISTRIBUTION ON SPLITTER PLATE DOWN STREAM OF A FLAT PLATE AT $\alpha = 30^0$	PAGE NO: 93
		FIG·68

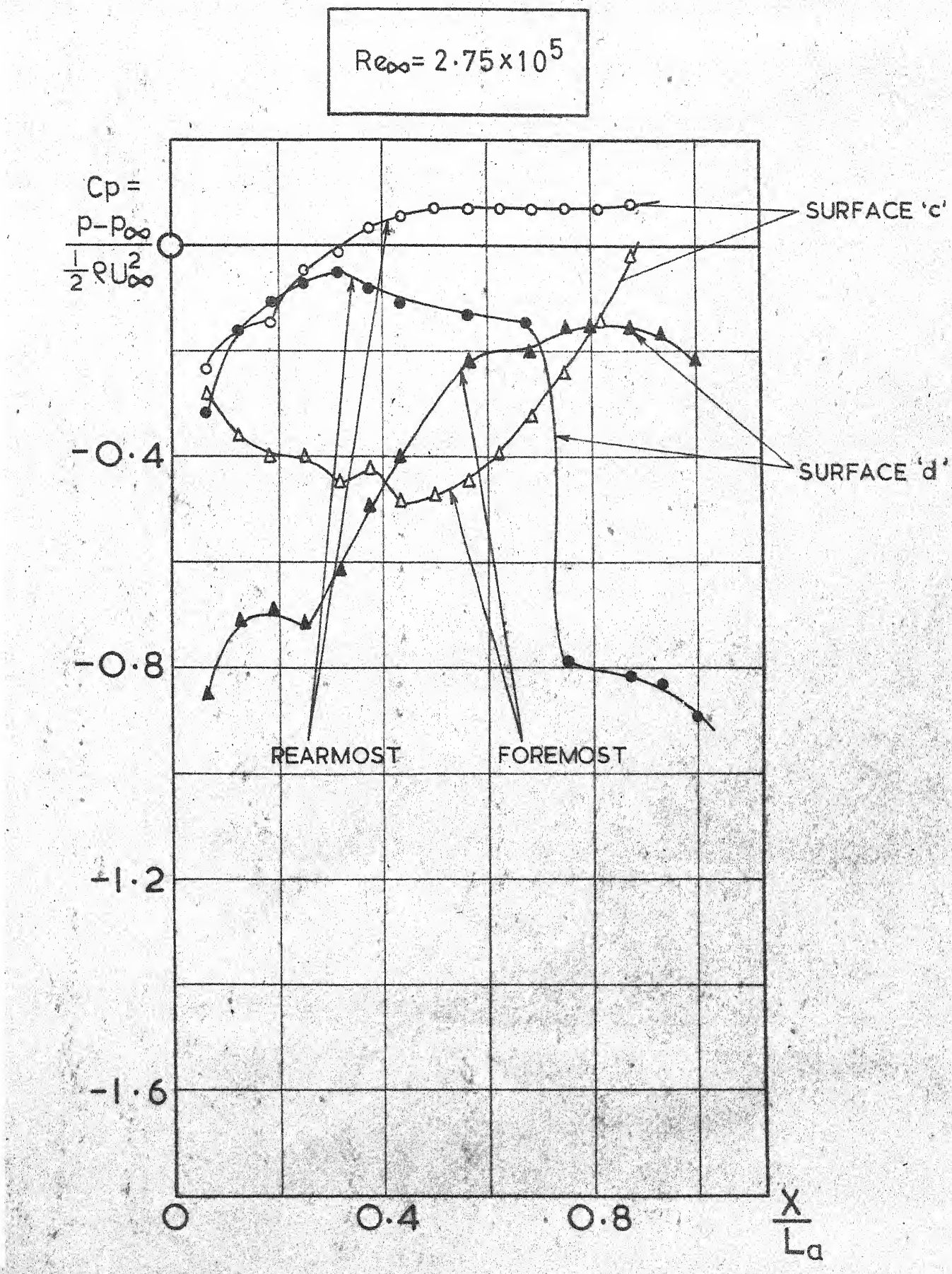

DRAWN: I.S.G.	DATE:	SQN. LDR. I.S.GUPTA	REPORT NO:

DEPT. OF AERO ENGG	PRESSURE DISTRIBUTION ON SPLITTER PLATE DOWN STREAM OF A FLAT PLATE AT $\alpha = 90^\circ$	PAGE NO: 94
		FIG·69

$Re_\infty = 4.0 \times 10^5$

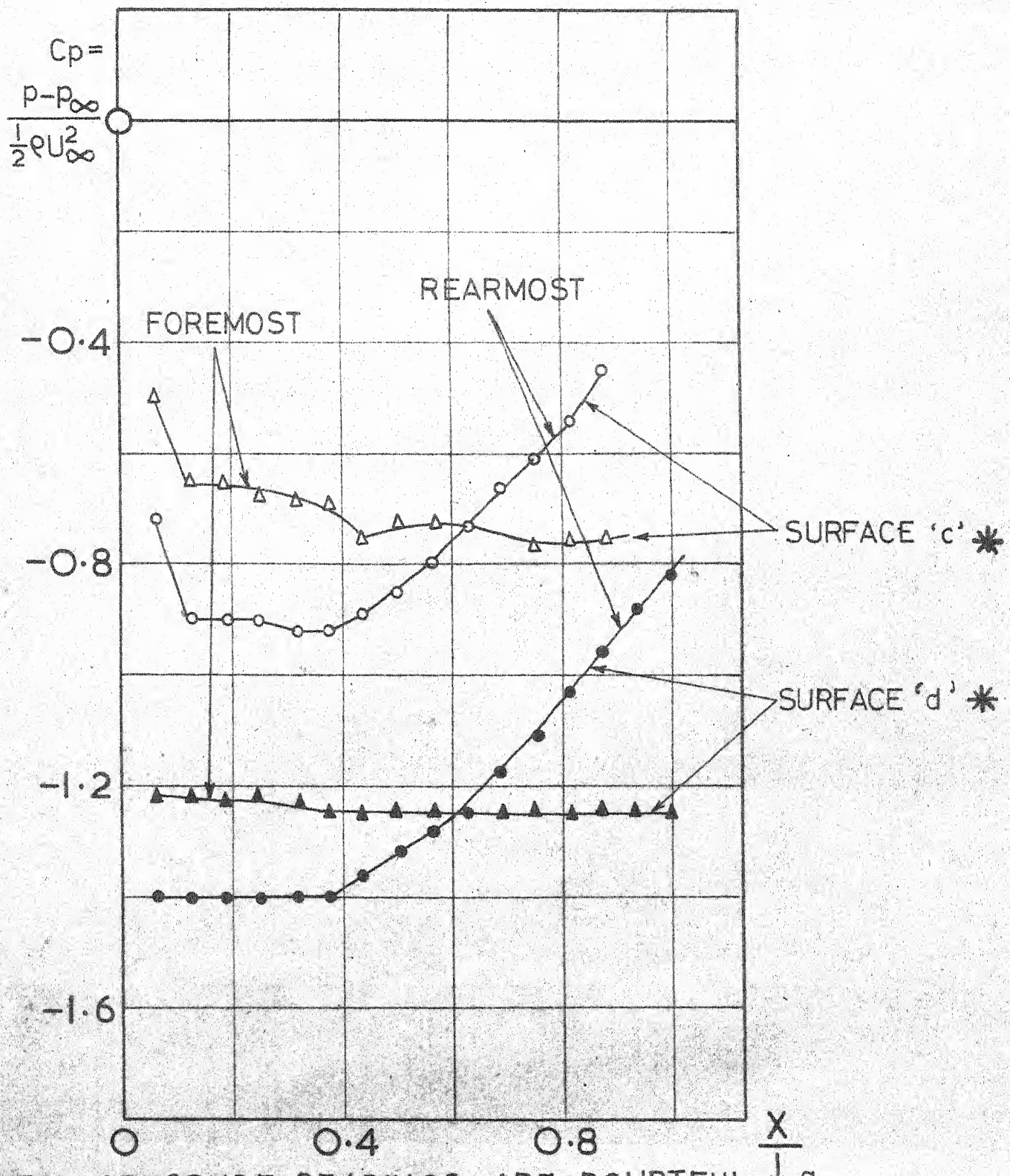

* NOTE:- PRESSURE READINGS ARE DOUBTFUL

DRAWN: I.S.G.	DATE:	SQN. LDR. I.S. GUPTA	REPORT NO:

$\frac{2}{C_{DS}}$ Vs. Res

FIG. 70

$Re_\infty = 4.8 \times 10^5$

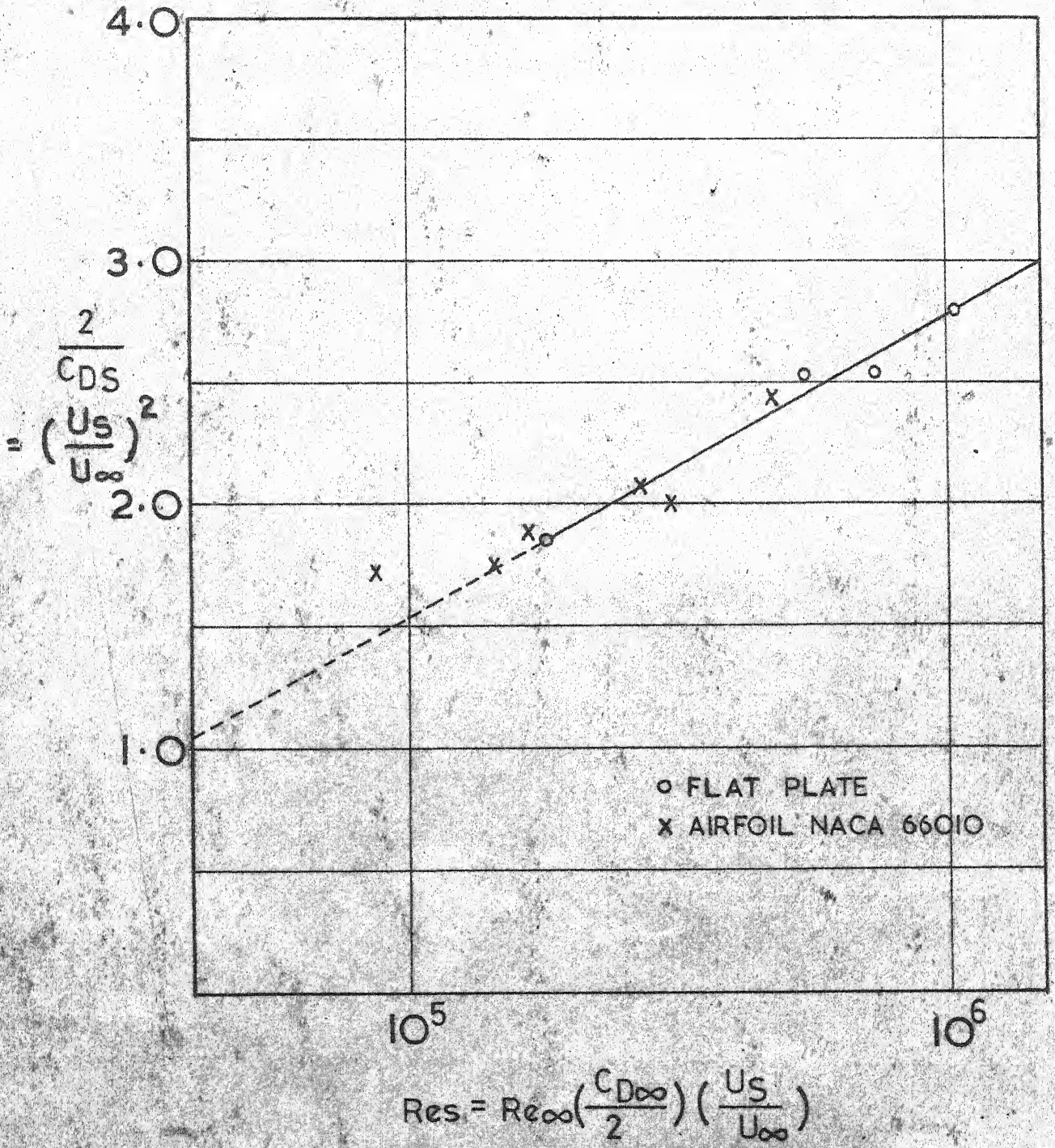

$$Res = Re_\infty \left(\frac{C_{D\infty}}{2}\right)\left(\frac{U_S}{U_\infty}\right)$$

DRAWN: I.S.G.	DATE:	SQN. LDR. I.S.GUPTA	REPORT NO:

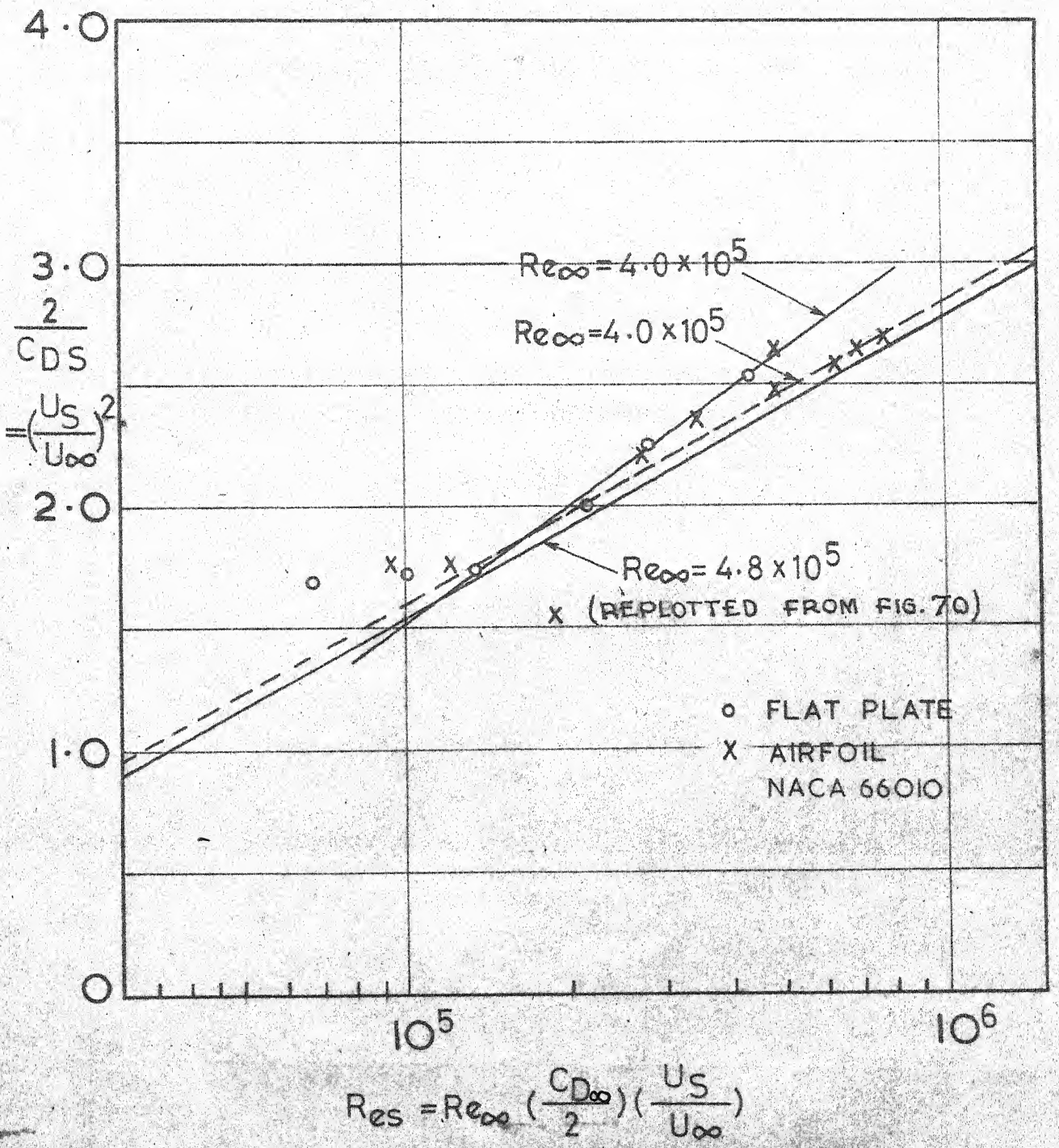
4·0
3·0
2·0
1·0
0
$\frac{2}{C_{DS}} = \left(\frac{U_S}{U_\infty}\right)^2$
$Re_\infty = 4.0 \times 10^5$
$Re_\infty = 4.0 \times 10^5$
$Re_\infty = 4.8 \times 10^5$
x (REPLOTTED FROM FIG. 70)
o FLAT PLATE
X AIRFOIL NACA 66010
10^5
10^6
$Res = Re_\infty \left(\frac{C_{D\infty}}{2}\right)\left(\frac{U_S}{U_\infty}\right)$

$Re_\infty = 4.8 \times 10^5$

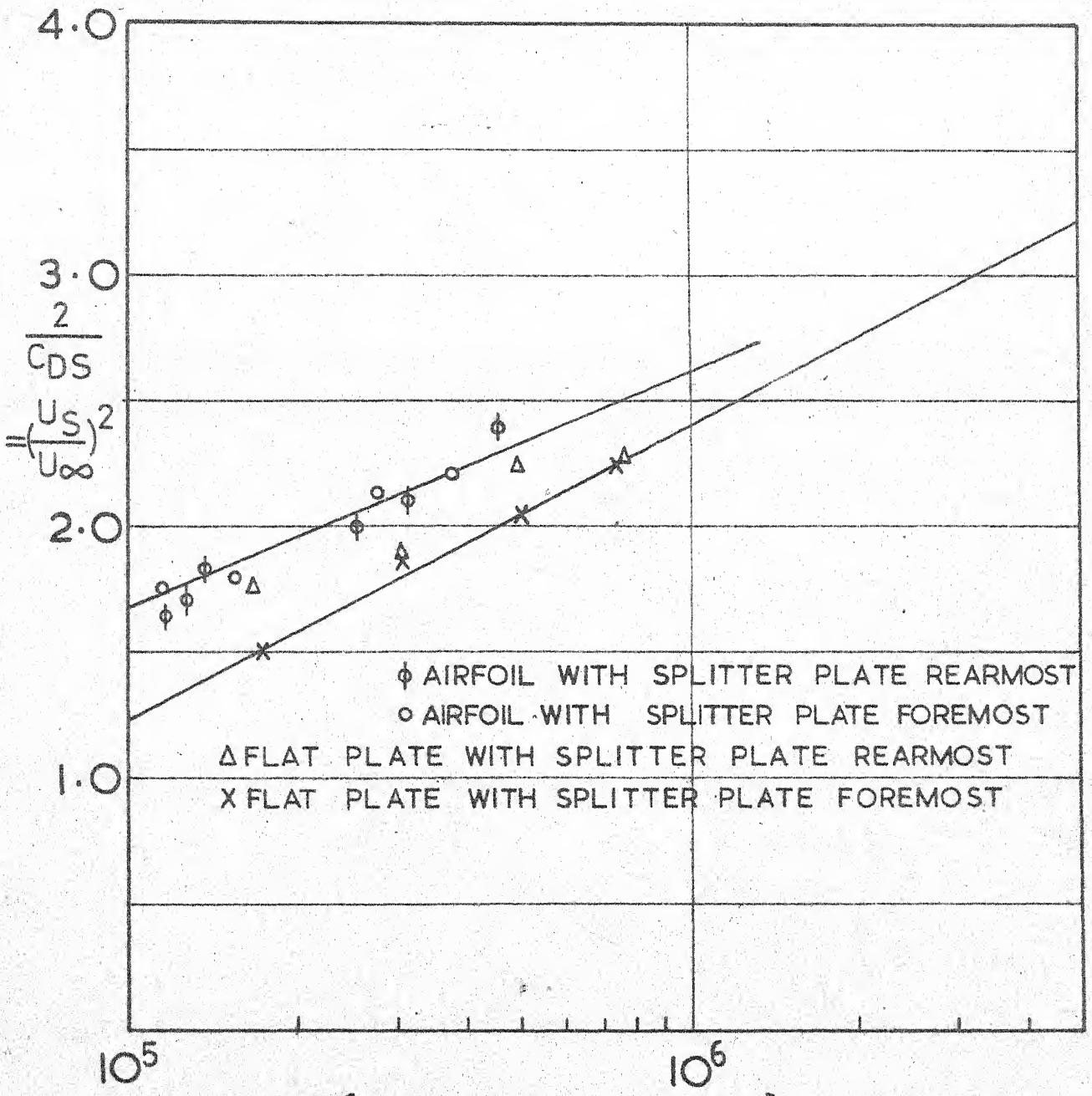

$$\left\{ Res = Re_\infty \left(\frac{C_{D\infty}}{2}\right)\left(\frac{U_S}{U_\infty}\right) \right\}$$